178
100

CHARACTERIZATION AND SCALE-UP OF MICROBUBBLE GENERATION IN COLUMN FLOTATION

by

Van Leslie Davis, Jr.

Thesis submitted to the Faculty of the
Virginia Polytechnic Institute and State University
in partial fulfillment of the requirements for the degree of

MASTER OF SCIENCE

in

Mining and Minerals Engineering

APPROVED:

G. H. Luttrell, Chairman

R. H. Yoon

M. E. Kaimis, Dept. Head

G. T. Adel

April, 1990

Blacksburg, Virginia

CHARACTERIZATION AND SCALE-UP OF MICROBUBBLE GENERATION IN COLUMN FLOTATION

by

Van Leslie Davis, Jr.

Committee Chairman: Dr. Gerald H. Luttrell
Mining and Minerals Engineering

(ABSTRACT)

Recent hydrodynamic studies suggest that small air bubbles can be used to improve the performance of column flotation. Tests carried out at Virginia Tech during the past several years have shown that various types of in-line motionless (or static) mixers can successfully produce microbubbles for column flotation. Unfortunately, few guidelines exist for selecting the proper size and type of motionless mixer for generating microbubbles.

In the present work, the mean bubble size produced by various types of in-line motionless mixers has been experimentally determined over a wide range of operating conditions and generator geometries. Test results indicate that generator performance is described by a series of expressions derived from a dimensional analysis. These expressions demonstrate that bubble diameter is primarily determined by the generator geometry and a dimensionless term known as the Weber number.

Tests have also been conducted to determine the reduction in the performance of centrifugal pumps under

air admitting conditions. A semi-empirical pump model has been utilized which allows the proper size of pump to be selected for microbubble generation. This information should prove useful for the design and operation of microbubble generation circuits on an industrial scale.

Acknowledgments

I would sincerely like to thank everyone at Virginia Tech that I have been associated with during my graduate studies. First, special thanks are to be given to Dr. G. H. Luttrell for serving as my committee chairman and for all of the guidance and support he gave me during the course of my studies. Sincere appreciation is also expressed to Dr. R. H. Yoon and Dr. G. T. Adel for their assistance concerning my work as well as future plans.

Special thanks are given to my fellow graduate students, especially Mike Mankosa, Ricky Honaker, Richard Forrest, Zhenghe Xu, and Hector Rojas for their support and friendship. I also extend thanks to Wayne Slusser and Jerry Rose for their assistance in the construction of much needed equipment and for being friends.

Appreciation is also given to Dr. M. E. Karmis, head of the Department of Mining and Minerals Engineering, the United States Department of Energy (Contract DE-AC22-86PC91274), and the Department of the Interior's Mineral Institutes program administered by the Bureau of Mines (Allotment Grant G1184151) for the financial support that made this work possible.

Finally, the deepest appreciation is expressed to my wife, Ellen, and the rest of my family for their love and support.

TABLE OF CONTENTS

Abstract ii

Acknowledgments iv

Table of Contents v

List of Figures viii

List of Tables xii

1. Introduction 1

    1.1 General 1

    1.2 Research Objectives 5

    1.3 Literature Review 6

        1.3.1 Microbubble Generation 7

        1.3.2 Motionless Mixers 10

        1.3.3 Centrifugal Pump Performance 14

2. Experimental 17

    2.1 Materials 17

        2.1.1 Column Flotation Tests 17

            a) Coal Samples 17

            b) Flotation Reagents 19

        2.1.2 Microbubble Generation Studies 19

    2.2 Test Equipment 19

        2.2.1 Microbubble Column Flotation 19

        2.2.2 Microbubble Generation Studies 23

            a) In-Line Microbubble Generators . . . 23

            b) Microbubble Generation Circuit . . . 24

c) Surface Tension Measurements 29
2.2.3 Centrifugal Pump Performance Studies . 30
2.3 Experimental Procedure 32
2.3.1 Microbubble Column Flotation 32
2.3.2 Microbubble Generation Studies 33
2.3.3 Centrifugal Pump Performance Studies . 34
3. Experimental Results 36
3.1 Microbubble Column Flotation Tests 36
3.1.1 DOE Test Work 36
a) Pittsburgh No. 8 Seam Coal 36
b) Illinois No. 6 Seam Coal 40
c) Upper Freeport Seam Coal 41
3.1.2 Ultraclean Coal Test Work 43
3.1.3 Refuse Coal Test Work 46
a) Shell Mining Company Test Work . . . 46
b) Pittston Coal Test Work 52
3.2 Microbubble Generation Studies 56
3.2.1 Pressure Versus Flow Relationships . . 56
a) Effect of Bubble Size 56
b) Effect of Air Fraction 58
c) Effect of Generator Length 64
d) Effect of Generator Diameter 67
3.2.2 Bubble Diameter Measurements 70
a) Determination of Sample Size 70
b) Effect of Flow Rate 70

c) Effect of Generator Geometry 72
d) Effect of Surface Tension 72
e) Effect of Air Fraction 72
3.3 Centrifugal Pump Performance Studies 76
3.4 Microbubble Size Distributions 78
4. Discussion 84
4.1 Microbubble Column Flotation 84
4.2 Scale-Up of In-Line Microbubble Generators . 86
4.2.1 Pressure Drop 86
4.2.2 Volume Mean Bubble Diameter 90
4.3 Centrifugal Pump Performance Prediction . . . 102
4.3.1 Performance Prediction Model 107
4.3.2 Model Validation 111
4.4 Microbubble Circuit Scale-Up Procedure . . . 112
5. Summary and Conclusions 117
6. Recommendations For Future Work 119
References 121
Appendix I 125
Vita 156

LIST OF FIGURES

Figure 2.1 Schematic diagram of the 2-inch diameter microbubble flotation column 21

Figure 2.2 Schematic diagram of the microbubble column flotation circuit 22

Figure 2.3 Mixing element configuration for the Koflo mixer as depicted by Federighi and Federighi (1985) 25

Figure 2.4 Mixing element configuration for the Kenics mixer 26

Figure 2.5 Circuit arrangement used to study the generation of microbubbles 27

Figure 2.6 Circuit arrangement used for the two-phase pump performance studies . . . 31

Figure 3.1 Recovery versus ash for -150 mesh Coalburg seam coal 50

Figure 3.2 Recovery versus ash for -28 mesh Coalburg seam coal 51

Figure 3.3 Recovery versus ash for -100 mesh Warfield seam coal 53

Figure 3.4 Recovery versus ash for the Middle Fork sample from Pittston's Moss #3 plant . . 55

Figure 3.5 Pressure versus flow for the 7-element Kenics mixer as a function of frother concentration at 10% air 57

Figure 3.6 Pressure versus flow for the Koflo mixer (0.62-inch diameter) as a function of frother concentration at 20% air 59

Figure 3.7 Pressure versus flow for the Koflo mixer (0.82-inch diameter) as a function of frother concentration at 20% air 60

Figure 3.8 Pressure versus flow for the 15-element Kenics mixer at various air fractions using 10^{-3}M Dowfroth 1012 61

Figure 3.9 Pressure versus flow for the Koflo mixer (0.62-inch diameter) at various air fractions using 10^{-3}M Dowfroth 1012 . . . 62

Figure 3.10 Pressure versus flow for the Koflo mixer (0.82-inch diameter) at various air fractions using 10^{-4}M Dowfroth 1012 . . . 63

Figure 3.11 Normalized pressure versus total flow curve for the Koflo mixer (0.62-inch diameter) using 10^{-3}M Dowfroth 1012 . . . 65

Figure 3.12 Normalized pressure versus total flow curve for the 15-element Kenics mixer using 10^{-4}M Dowfroth 1012 66

Figure 3.13 Pressure/length versus total flow for constant diameter Kenics mixers of various lengths 68

Figure 3.14 Effect of generator diameter on the pressure-flow curves for Koflo mixers . . 69

Figure 3.15 Effect of sample size on the volume weighted mean bubble diameter for the Koflo mixer (0.62-inch diameter) 71

Figure 3.16 Effect of total flow rate on volume mean bubble diameter for a 7-element Kenics mixer at 10% air and constant surface tension 73

Figure 3.17 Effect of generator length on volume mean bubble diameter for the Kenics mixer 74

Figure 3.18 Effect of surface tension on volume mean bubble diameter for a 7-element Kenics mixer at 10% air 75

Figure 3.19 Effect of air fraction on volume mean bubble diameter for a 7-element Kenics mixer at various flow rates 77

Figure 3.20 Effect of entrained air on the pressure versus total flow curve for an open face impeller centrifugal pump 79

Figure 3.21 Microbubble size distribution produced by a Koflo mixer (0.62-inch diameter) at 10% air using 10^{-3}M Dowfroth 1012 81

Figure 3.22 Microbubble size distribution produced by a 7-element Kenics mixer at 10% air using 10^{-3}M Dowfroth 1012 82

Figure 3.23 Microbubble size distribution produced by a 15-element Kenics mixer at 10% air using 10^{-3}M Dowfroth 1012 83

Figure 4.1 Mixer constant (K) versus Reynolds number (Re) for various element configurations, air fractions and frother dosages 89

Figure 4.2 Normalized volume mean bubble diameter versus Weber number (We) for various element configurations at 10% air 96

Figure 4.3 Normalized volume mean bubble diameter versus Weber number (We) for various element configurations at 10% air 97

Figure 4.4 Normalized volume mean bubble diameter (corrected) versus Weber number (We) for various element configurations at 10% air 98

Figure 4.5 Normalized volume mean bubble diameter (corrected) versus Weber number (We) for various element configurations at 10% air 99

Figure 4.6 Normalized volume mean bubble diameter versus K for all mixers under various air fractions and operating conditions . . . 101

Figure 4.7 Normalized volume mean bubble diameter versus Weber number for all mixers under various air fractions and operating conditions 103

Figure 4.8 Normalized volume mean bubble diameter versus Weber number for all mixers under various air fractions and operating conditions 104

Figure 4.9 Entrance and exit velocity triangles relative to a centrifugal pump impeller as depicted by Karassik et al. (1976) . . 106

Figure 4.10 Normalized pump performance curves showing hypothetical single- and two-phase curves relative to the theoretical performance curve 108

Figure 4.11 Head loss ratio versus air fraction for various flow coefficients (ψ) for a Teel centrifugal pump (Model 1P797A) 110

Figure 4.12 Normalized performance curves for a Teel centrifugal pump depicting theoretical single-, two- and predicted two-phase performances at 15% air 113

LIST OF TABLES

Table 2.1 Coal samples used in the microbubble column flotation tests 18

Table 3.1 Raw coal sample analyses of coals used in the Department of Energy (DOE) test work 37

Table 3.2 Microbubble column flotation results obtained using the Pittsburgh No. 8 seam coal 39

Table 3.3 Microbubble column flotation results obtained using the Illinois No. 6 seam coal 42

Table 3.4 Microbubble column flotation results obtained using the Upper Freeport seam coal 44

Table 3.5 Effectiveness of microbubble column flotation in producing ultraclean coal . . 47

CHAPTER 1

INTRODUCTION

1.1 General

The processing of fine particles is one of the major challenges in the minerals industries. Since the demand for minerals has increased and many high grade ore deposits have been depleted, larger amounts of ore must be processed. As a result, larger amounts of fine particles are being produced during mining operations (Furstenau, 1980). Also, the processing of fine particles is required due to the existence of ore deposits in which the valuable minerals are finely disseminated (Weiss, 1985).

It is generally accepted that froth flotation is the most effective means for treating fine particles. Froth flotation, patented early in this century, is presently used to upgrade over two billion tons of minerals and coal each year (Leja, 1982). Froth flotation has allowed the exploitation of low grade ore deposits which could not be treated in any other cost effective manner (Wills, 1988).

Froth flotation is a process in which the differences in physico-chemical surface properties of particles are exploited. Mineral surfaces are selectively rendered hydrophobic by the addition of reagents. The hydrophobic particles subsequently attach to air bubbles and are carried to the top of the flotation cell where a

mineralized froth is formed. This froth is then removed from the cell, thereby resulting in concentration of the hydrophobic particles. The hydrophilic portion of the material in the cell is removed as gangue. This method of concentration is known as direct flotation. It should be noted that gangue minerals may be rendered hydrophobic and removed from the cell as concentrate instead of the valuable mineral. This process is known as reverse flotation.

Although froth flotation can be used to upgrade a wide variety of mineral fines, there are limitations on the size range of particles which can be effectively processed. Generally, flotation performance diminishes when particles less than 10 microns in diameter are to be processed (Leja, 1982). Although a number of reasons can be given for the decreased performance at this size, the difficulties can generally be attributed to:

i) poor selectivity associated with the hydraulic entrainment of fine gangue particles, and
ii) low flotation kinetics resulting from a low frequency of bubble-particle collisions.

Therefore, conventional froth flotation techniques must frequently be modified in order to process very fine particles.

One technique for upgrading very fine particles which has met with much success is column flotation. This process, which was originally patented in 1961 by Canadians Boutin and Tremblay, provides for a countercurrent flow of wash water which removes fine gangue particles which would otherwise be entrained and carried into the froth product. As a result, higher product grades can usually be achieved in a single stage of column flotation than a single stage of conventional flotation. It is also believed that flotation columns provide a more favorable environment for the flotation of fine particles due to their quiescent behavior. As a result, column flotation has received much attention in recent years by the mineral and coal industries.

Recent studies conducted at Virginia Tech have shown that small bubbles can be used to substantially improve the performance of column flotation cells (Yoon et. al., 1984; Luttrell, et al., 1988). The improved performance has been attributed to an increase in the probability of bubble-particle collision with decreasing bubble size (Yoon and Luttrell, 1986). In general, the probability of bubble-particle collision has been shown to be roughly proportional to the inverse square of bubble diameter (Yoon and Luttrell, 1986). This concept has been utilized at Virginia Tech in the development of an advanced

flotation process commonly referred to as microbubble column flotation (MCF). Bubbles generated by this technique are sufficiently small so as to have no turbulent wake during free rise. The upper size limit for this characteristic is generally in the 0.3-0.4 millimeter diameter range. The use of microbubbles provides for improved flotation kinetics and the incorporation of microbubbles with column flotation has yielded an effective means of treating fine particle sizes (Yoon, et. al., 1988).

The microbubble column flotation (MCF) process developed at Virginia Tech has been characterized by Weber (1988), who examined many of the key operating parameters associated with the operation of the column. However, the operational and design aspects of the bubble generation circuit were only superficially examined in this study. Therefore, the goal of the present investigation has been to characterize the key variables associated with the design and operation of the bubble generation circuit used in the MCF process. This information is essential in developing design guidelines for scale-up of the MCF process. The present investigation also includes testing of the MCF process on a variety of coal samples with sizes ranging from micronized to -28 mesh.

1.2 Research Objectives

The objectives of the research are as follows:

1. To develop a rapid and accurate method for determining bubble diameter.
2. To characterize the performance of in-line microbubble generators of varying design and configuration.
3. To develop a quantitative scale-up procedure for selecting the proper size in-line generator for a given application.
4. To study centrifugal pump behavior under air admitting conditions, since pumps are key components of microbubble generation circuits.
5. To develop a two-phase pump model for the prediction of centrifugal pump performance under air admitting conditions in order to allow for proper pump selection for a given application.
6. To further evaluate column flotation performance on a wide range of coal samples of various sizes.

Numerous operating parameters were examined in order to characterize the microbubble generation circuit utilized in the microbubble column flotation process. These tests were conducted as a function of operating parameters which included generator geometry, shear element configuration, surfactant dosage and the

volumetric flow rates of air and liquid. Generator performance was monitored in terms of the pressure drop across the generator and the mean size of bubbles produced. Since the performance of the centrifugal pump deteriorates under air admitting conditions, an extensive literature search and two-phase flow test work was also required in order to fully predict the performance of the microbubble generation circuit.

The results of this research effort provide data which have been used to derive expressions which characterize the behavior of microbubble generation circuits. These expressions can be used to scale-up the microbubble generation circuits used in the microbubble column flotation process. This work should complete the last step toward allowing for industrial applications of microbubble column flotation technology in mineral and coal processing plants.

1.3 Literature Review

The flotation column can be considered as a long vertical tube in which the downward flow of feed material encounters air bubbles rising from the bottom of the cell. The hydrophobic particles become attached to air bubbles and are removed from the top of the column as a froth product, while hydrophilic particles remain in the slurry

and eventually exit via the bottom of the cell. A flow of countercurrent wash water aids in the removal of entrained particles from the froth product. The bubble generation system of the column is of critical importance. In many cases, the large bubbles produced by conventional sparging systems result in low flotation kinetics and a loss of recovery (Luttrell, et. al., 1988). Because of the importance of bubble generation in determining column performance, the microbubble generation circuit of the microbubble column flotation process is the major factor examined in this investigation.

1.3.1 Microbubble Generation

There are numerous methods which can be used to generate air bubbles for froth flotation. A number of methods also exist which have the capability to produce microbubbles.

The sparging of air through porous media is one of the more commonly used methods for generating bubbles for use in flotation columns (Mathieu, 1972). The spargers are normally mounted inside the column at various levels. Unfortunately, traditional porous spargers have been characterized by a wide range of operational problems. Bubble size control is limited and the flotation column must be removed from service for maintenance and repair of the sparging units (USBM, 1988). It should also be noted

that sparging units are also subject to obstruction and plugging, since it is nearly impossible to obtain completely uncontaminated compressed air in industrial environments.

Aspirators may also be used to generate microbubbles for flotation processes (Sebba, 1971; Deister, 1988). Aspiration involves forcing liquid through a venturi where gas is allowed to enter the stream under a high shear rate. This method has been successful in generating microbubbles and it is not necessary to remove the flotation column from service to perform maintenance. However, this type of sparger requires that fresh solutions of make-up frother be injected into the flotation column. This situation can reduce the effective residence time in a flotation cell and result in downstream dewatering problems. Also, the surface tension of the make-up water must be relatively low, generally in the order of less than 50 dynes/cm (Deister, 1988).

Another popular method of generating bubbles for column flotation is to use a high shear device consisting of a chamber filled with a packing material (Suggs, 1987; USBM, 1988). The packing material may be glass beads, wire mesh, stainless steel shavings, or any other suitable materials (Suggs, 1987). The United States Bureau of Mines has met with success in using a packed tube device

for the generation of microbubbles. This type of bubble generator is mounted externally, as in the aspiration systems, allowing for ease of maintenance. However, fresh make-up solution is required to prevent plugging of the packed bed. Fairly high air pressures (e.g., 60-90 psi) are also required for effective gas dispersion.

Microbubbles may also be generated by mechanical means that involve spinning disks or impellers to provide the shear necessary to cause bubble formation. This method is used extensively in conventional flotation cells, but has not been applied to column flotation technology in a widespread manner. The major disadvantages for this technique involve complex design and turbulence which may be induced by the mechanical agitation. Turbulent conditions are generally avoided in column flotation, since a quiescent environment allows for more efficient bubble loading due to a decrease in bubble-particle detachment (Bogdanov and Emelyanov, 1980).

The method for generating microbubbles employed in the Virginia Tech microbubble column flotation process involves the use of a centrifugal pump and external in-line microbubble generators. These generators are similar in design to the motionless or static mixers commonly utilized in the polymer industries. The centrifugal pump is used to circulate a portion of the flotation pulp from

the bottom of the flotation column. This provides the liquid in which the microbubbles are dispersed. Upon leaving the outlet side of the centrifugal pump, the solution is aerated and frother solution is added. The frother solution lowers the surface tension to aid in microbubble generation and provides a frothing agent for the flotation process. This entire mixture is then forced through the in-line microbubble generator where the air is sheared into microbubbles and the entire suspension is injected into the bottom of the flotation column. This process has several advantages which include:

i) improved maintenance since the generators can be mounted externally,

ii) maximization of cell residence time since the need for fresh make-up solution is eliminated, and

iii) the elimination of generator obstruction and plugging problems.

1.3.2 Motionless Mixers

Motionless mixers are used widely in numerous process industries. There are approximately 30 different designs and configurations of these units, but all are designed for in-line continuous mixing and processing. The main area of application of static mixing units is the continuous mixing of mutually soluble fluids of differing

viscosity (Pahl and Muschelknautz, 1982). This single area of application covers a broad range of processes in many industries.

Motionless mixers are being used successfully in the area of viscous polymer processing. They are being used to intimately mix various ingredients into polymer streams. These devices are particularly attractive to this area, since many plugging problems and incomplete mixing problems associated with more conventional mixing methods have been eliminated. The ultimate result is products of more uniform quality (Chen and Macdonald, 1973). Due to designs with no moving parts and continuous flow capabilities, static mixing technology has resulted in lower operating costs, improved quality and higher yield and throughput for polymer process systems (Mutsakis, Streiff and Schneider, 1986).

Static mixing units are being used effectively in the field of dispersive mixing. In this area of motionless mixer application two immiscible fluids are subjected to shear forces inside the mixing device resulting in drops of one phase being dispersed in the other (Chen, 1974; Mutsakis, Streiff and Schneider, 1986). The preparation of oil-water emulsions and other homogenizing processes have benefited from static mixing technology. It should also be noted that dispersed phase droplet size

distributions cover a relatively narrow size range and the average droplet size is easily controlled.

Motionless mixers have also found uses as chemical reactors in many process industries. In these applications, feed materials undergo chemical and physico-chemical changes. Most unit operations of this type involve mixing, since the reactants must be intimately interspersed (Bor, 1971). Since short resident times are required in many process applications and the stoichiometry of chemical reactions is enhanced by rapid intimate contact of dispersed fluid particles with the continuous phase of the product stream, static mixers are of particular use as devices for the rapid onset of chemical reactions (Oldshue, 1983).

Another important area of application for static mixing technology is in the area of continuous aeration. Motionless mixers are used to provide bubble beds for various downstream process stages in the chemical and food process industries. For example, static mixers are used in the chemical industry as devices for dissolving various gases in water streams and detergent slurries (Grosz-Roll, Battig and Moser, 1982). Motionless mixers are also being used as aerators in water and wastewater treatment operations. In this industry the devices are generally submerged in containment areas and used for oxygenation,

reagent mixing, and solids suspension (Mutsakis and Rader, 1986; Chen and Gilbert, 1976; Gilbert and Libby, 1977).

Numerous methods exist for determining the size, number and performance characteristics of static mixing devices. The mixing characteristics of various motionless mixers have been quantified by defining terms such as the intensity of segregation (Chen, 1974), using statistical methods to judge mixture homogeneity (Streiff, 1979; Williams, 1984; Pahl and Muschelknautz, 1982), and defining stream mixing indexes (Wilkinson and Cliff, 1977). The pressure drop across a static mixing device has been quantified by utilization of the Darcy-Weisbach equation for head loss in a pipe and an empirically determined multiplier that is a function of mixer geometry (Oldshue, 1983; Boss and Czastkiewicz, 1982; Pahl and Muschelknautz, 1982; Wilkinson and Cliff, 1977; Chen, 1974).

A method for approximating the number of elements required in any type of static mixer has been devised based on the utilization of a nomograph containing information on Reynolds number, velocity, specific gravity and viscosity (WE & M Reference Handbook, 1985). Dispersive mixing in static mixing units has been quantified by a droplet size/Weber number relationship (Oldshue, 1983) and by a similar relationship involving

viscosity effects and shear forces (Mutsakis, Streiff, and Schneider, 1986). The selection of the size and number of static mixing devices required for aeration processes has been empirically based on oxygen transfer efficiency, biological oxygen demand, and the amount of material to be treated (Gilbert and Libby, 1977; Chemineer, 1986). Unfortunately, the explicit use of static mixing devices for microbubble generation is a relatively new area which has not previously been studied. As a result, operational data and scale-up procedures, especially for mineral processing systems, is essentially nonexistent.

1.3.3 Centrifugal Pump Performance

Centrifugal pump performance under two-phase, or air admitting, flow conditions is of critical importance, since pump capacity is adversely affected by the introduction of air. The ability to predict centrifugal pump performance during two-phase flow is of special interest to the nuclear power industry in the event of a loss of coolant accident. Under these conditions, reactor coolant pumps are subjected to two-phase flow conditions and performance prediction is important for safety analysis (Kim, 1984; Furuya, 1984; Kim, 1983; Mikielewicz, et. al., 1978; Rohatgi, 1978; Patel and Runstadler, 1978). The performance of centrifugal pumps under air admitting conditions is also of importance to the petroleum

industry, since submersible pumps for deep oil wells must sometimes handle oil in which a substantial amount gas is contained (Furuya, 1984).

Numerous models for the prediction of centrifugal pump performance under two-phase flow conditions have been proposed. Many of the performance prediction models are purely empirical in form. The empirical models involve approaching the problem from outside the pump and are expressed in terms of correlations obtained by curve fitting methods (Kim, 1983). Some of the two-phase pump models are based more on first principles and are approached in an analytical manner. These analytical models are generally based an a set of governing differential equations and are based on theoretical flow conditions inside the pump (Rohatgi, 1978). Perhaps the most applicable two-phase centrifugal pump models are semi-empirical in nature. These models generally relate theoretical pump performance to actual two-phase performance characteristics and allow for performance prediction from single phase information supplied by the manufacturer (Mikielewicz, et. al., 1978). Semi-empirical models are generally much easier to apply, since the need for the simultaneous solution of complex differential equations is eliminated.

The effect of entrained air on the performance

characteristics and the prediction of performance degradation on centrifugal pumps is of importance to this investigation, since entrained air is present in the fluid used as a medium for microbubble generation. Centrifugal pumps tend to experience significant head degradation when the air content of the pumped fluid reaches values greater than 5% to 10% (Kim and Duffey, 1985). In most applications related to microbubble generation, the amount of entrained air in the fluid entering a centrifugal pump will generally reach the range in which performance characteristics are affected.

CHAPTER 2

EXPERIMENTAL

2.1 Materials

2.1.1 Column Flotation Tests

a) Coal Samples

Various coal samples were tested in the microbubble column flotation cell. The samples were obtained from several coal companies and the size classes when tested varied from micronized to -28 mesh. Samples included coal from refuse streams (i.e., hydrocyclone overflow), dense media cleaning processes and run-of-mine plant feed. The characteristics of the coal samples examined in the present work are listed in Table 2.1.

All coal samples that were not in slurry form were subjected to the following preparation and storage procedures. The samples were passed through laboratory jaw and roll crushers to obtain a -6 mm top size. They were then riffled into representative samples of approximately 1500 grams each and sealed in airtight plastic containers. Finally, the samples were stored in a freezer at approximately 20^{o}C to minimize surface oxidation. Coal samples that were received in slurry form (e.g., cyclone overflow or refuse pond samples) were processed immediately after receipt in order to prevent alteration of the surfaces by oxidation.

Table 2.1 Coal samples used in the microbubble column flotation tests.

Coal	Supplier	Type	Feed Ash (%)
Elkhorn #3	United Coal	R-O-M	12.0
Elkhorn #3	United Coal	Processed	1.1
Pittsburgh	DOE/PETC	R-O-M	18.1
Illinois #6	DOE/PETC	R-O-M	12.9
Upper Freeport	DOE/PETC	R-O-M	13.6
Coalburg	Tug Valley	Refuse	53.4
Warfield	Tug Valley	Refuse	46.6
Middle Fork	Pittston Coal	Refuse	43.8

b) Flotation Reagents

The flotation reagent package and dosages varied with each coal sample and size processed. Dowfroth M-1012 was used as the flotation frother for microbubble generation in all tests. The collectors used for coal particles were either kerosene or No. 2 diesel fuel. In some experiments, dispersants such as sodium silicate and pH modifiers such as sodium hydroxide were used during flotation testing. The specific reagent package and dosages will be reported with each individual test in this report.

2.1.2 Microbubble Generation Studies

The only reagent employed in the microbubble generation studies was a flotation frother. The specific frother used in this investigation was Dowfroth M-1012, a polyproplyene glycol blend. This reagent was chosen because of past experience which indicated that very stable microbubble suspensions could be produced at relative low dosages using this surfactant.

2.2 Test Equipment

2.2.1 Microbubble Column Flotation

The microbubble flotation column used in the flotation studies was constructed of Plexi-glas tubing with an inner diameter of 2 inches. The Plexi-glas

sections comprising the column were 18-inches long and threaded on the ends so as to allow the length to be altered. Each section was equipped with a stopcock in order to allow for sample removal from various levels within the flotation device. The in-line microbubble generator was inserted into the cell at the bottom and sealed in place with o-rings. This allowed the bubble generator to be easily removed for cleaning and inspection. Countercurrent wash water and flotation feed were introduced at the top of the cell, concentrate was removed from the top, and tailings were removed from the bottom. A schematic diagram of the microbubble column flotation cell is shown in Figure 2.1.

The entire microbubble column flotation circuit is shown in Figure 2.2. A peristaltic pump was used to introduce the feed slurry into the top of the cell from the feed slurry sump. Countercurrent wash water was added by means of a spider-type distributor. A centrifugal pump was used to pull tailings pulp from the bottom of the cell in order to provide a medium for the generation of microbubbles. Upon leaving the centrifugal pump, air was injected into the recirculated tailings pulp from a small tee. Frother solution was added continuously to the recirculated stream using a small peristaltic pump. After aeration and the addition of frother solution, the

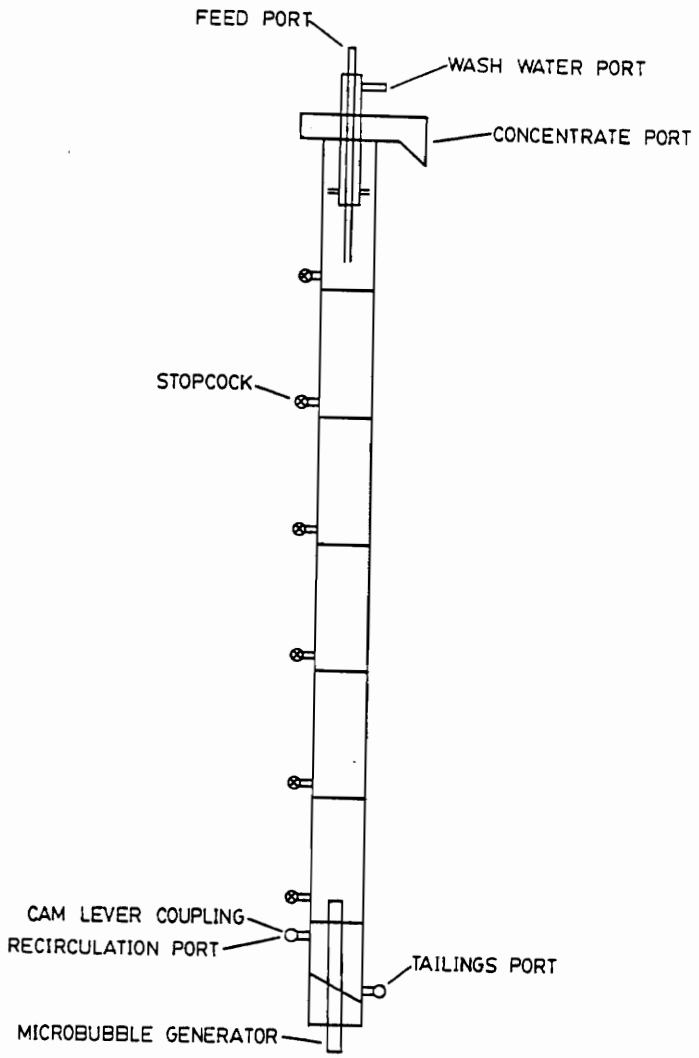

Figure 2.1 Schematic diagram of the 2-inch diameter microbubble flotation column.

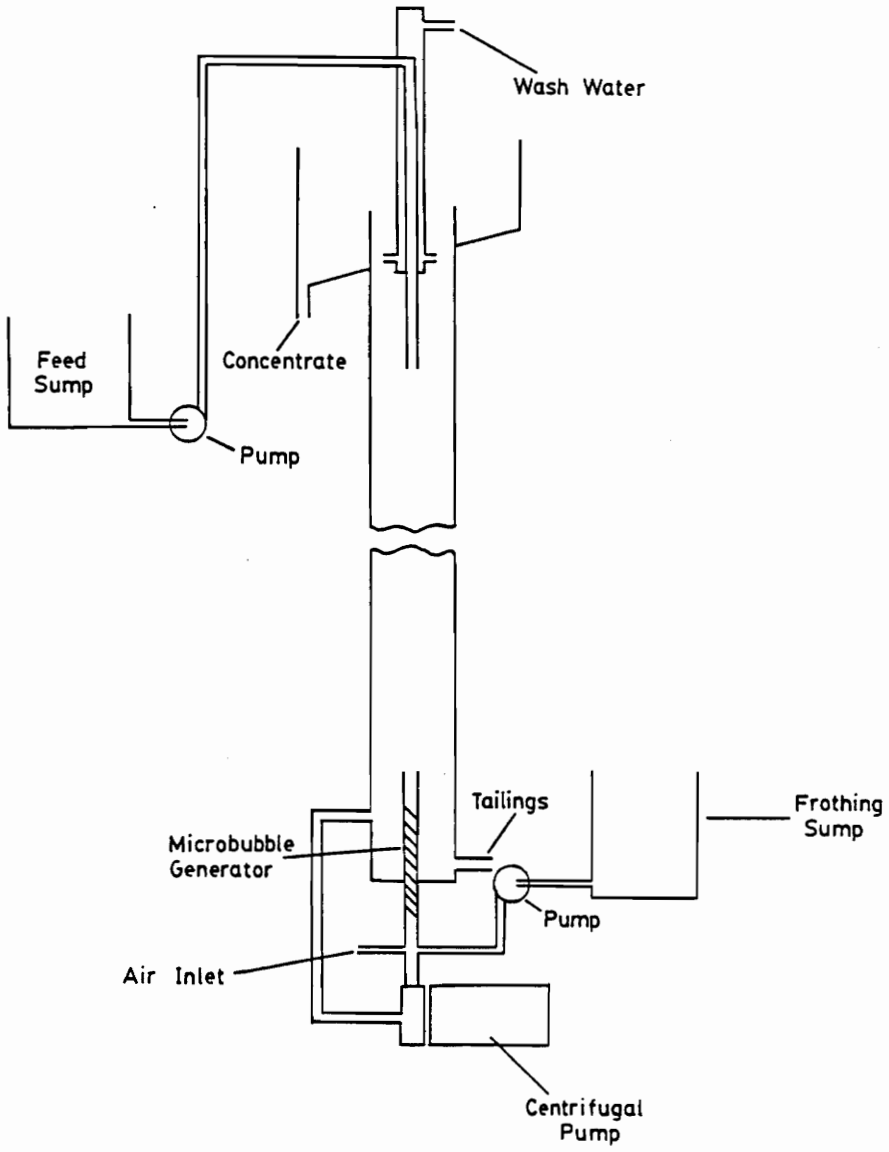

Figure 2.2 Schematic diagram of the microbubble column flotation circuit.

suspension was forced under pressure through the in-line microbubble generator located at the bottom of the cell. The microbubbles generated by this process flowed upward into the column where they encountered the downward flow of feed slurry. Hydrophobic particles contained in the slurry became attached to the microbubbles and were lifted to the top of the column, while hydrophilic particles flowed out the bottom of the column as reject material. The continuous operation of the column allowed the process to be operated under conditions which simulated the performance of an industrial-scale microbubble flotation column.

2.2.2 Microbubble Generation Studies

a) In-Line Microbubble Generators

Two different types of in-line microbubble generators were used in the microbubble generation studies. Motionless mixers of the Koflo and Kenics element configurations were investigated. Each type of static mixing device consisted of an elongated tube which contained various mixing element configurations.

The Koflo mixing element design consists of a chain of metal segments each of which contains two components with a sinuous cross-section between opposite ends. The two components are connected along the center of the tube

with the two components axially staggered with respect to each other (Federighi, 1985). A schematic diagram of the Koflo element configuration is shown in Figure 2.3.

The Kenics static mixer is constructed of a number of elements of alternating left- and right-hand helices. The elements are positioned such that the leading edge of one element is perpendicular to the trailing edge of the adjacent component. The twist of each element is 180^{o} (Wilkinson and Cliff, 1977). A schematic diagram of the Kenics element configuration is shown in Figure 2.4.

b) Microbubble Generation Circuit

A schematic diagram of the system used to determine bubble size and characterize the in-line microbubble generators is shown in Figure 2.5. The basic circuit consisted of a centrifugal pump, ball value, interchangeable in-line microbubble generator and large collection and storage sumps. The equipment used to determine bubble size included a transparent viewing cell, low-power microscope, a Panasonic "noiseless" freeze frame videocassette recorder equipped with a black and white video monitor. Other instrumentation used in the circuit included a turbine water flow meter with a chronograph display, two pressure gauges, and an air flow meter.

Microbubbles were generated by using the centrifugal pump to force surfactant solution from the intake sump

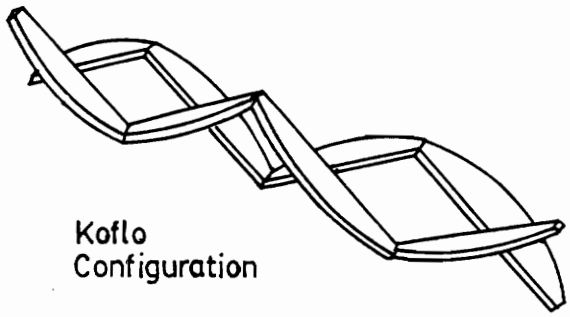

Figure 2.3 Mixing element configuration for the Koflo in-line mixer as depicted by Federighi and Federighi (1985).

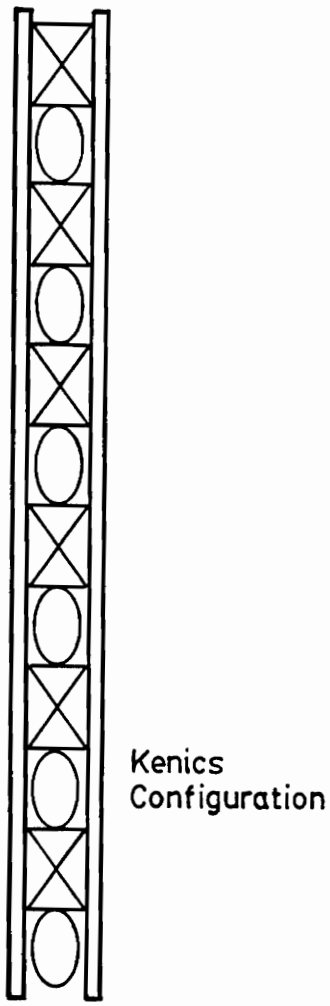

Figure 2.4 Mixing element configuration for the Kenics in-line mixer.

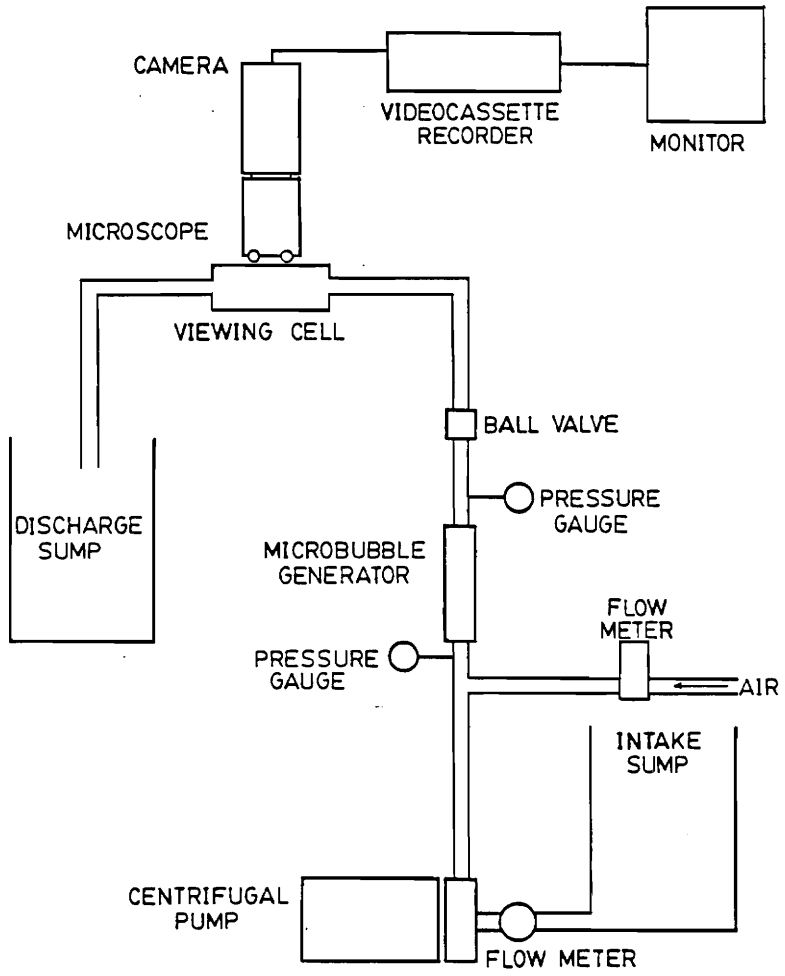

Figure 2.5 Circuit arrangement used to study the generation of microbubbles.

through an in-line generator. Air was injected under pressure directly ahead of the generator. The suspension then passed through a viewing cell constructed of glass and Plexi-glas of the same cross sectional area as the hoses containing the fluid. The microbubble suspension was then emptied into a separate discharge sump in order to prevent the recirculation of bubbles.

Operating conditions were monitored and controlled by the instrumentation installed within the circuit. Pressure drop across a generator was determined by simple diaphram-type pressure gauges. The volumetric flow of liquid was determined by an in-line electronic flow meter in the pumping circuit. The calibration of the flow meter was checked by direct measurement at the discharge entering the second collection sum. Air flow rate was monitored and regulated by an air flow meter/valve combination. When necessary, a ball value installed on the low pressure side of the microbubble generator was closed momentarily to stop the flow of the microbubble suspension to improve the viewing of the microbubbles.

Microbubble size was determined using the following procedure. During a test, the microbubble suspension flow was momentarily stopped by closing the ball valve. At the same time, the flow of microbubbles through the glass viewing cell was being recorded via the microscope mounted

camera connected to the videocassette recorder. Mean bubble size was determined by directly measuring the diameters of the bubbles from the video screen during tape playback using an appropriate scale factor. From this procedure, it was determined that images of at least 150 bubbles had to be recorded in order to obtain a reasonable estimate of the average bubble size. It should be noted that bubble diameters were weighted by volume in order to allow for better representation of air volume used for microbubble generation.

The bubble measurement system used in the present work offers several advantages over many of other methods commonly used for bubble sizing. First, the entire stream of the microbubble suspension is viewed so that sampling biases are minimized. Also, the process can be performed fairly rapidly since the need for still photography and subsequent data analysis are eliminated. Finally, a large amount of data such as flow, air fraction, and pressure drop as well as bubble diameter may be collected from a single test run of the circuit.

c) Surface Tension Measurements

The final information needed from a microbubble generation study was the interfacial tension of the water/surfactant solution. This value along with

volumetric flow and pressure drop was needed for the scale-up equations. The surface tension was measured using a Fisher Surface Tensiomat. This unit makes use of the Denouye Ring method for determining surface tension. Analysis procedures for this technique are well documented in the literature.

2.2.3 Centrifugal Pump Performance Studies

A schematic diagram of the circuit used for evaluating centrifugal pump performance under two-phase flow conditions is shown in Figure 2.6. Two separate pumping systems were required in order to obtain the desired pump performance data. The first system, which consisted of an in-line mixer and centrifugal pump, was used to produce microbubbles. This procedure allowed the generation of an air-water mixture with an air fraction and bubble size which could be easily varied to a predetermined value and then held constant for testing. Once these values were set, pump performance was established for the second pump. The operating performance of the pump was determined by taking readings from the pressure gauges on each side of the pump and by measuring the corresponding volumetric liquid flow rate from the pump. This procedure allowed for performance of the pump to be established under two-phase conditions as a function of bubble size and air fraction.

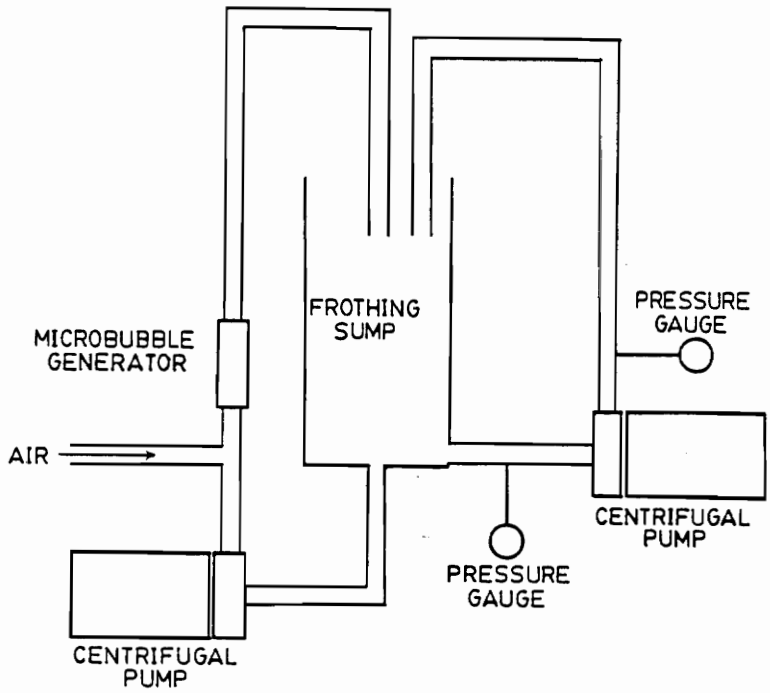

Figure 2.6 Circuit arrangement used in the two-phase pump performance studies.

The amount of air contained in the suspension was determined by removing a sample from the bottom of the sump and allowing it to flow continuously into the bottom of a 100 ml graduated cylinder. The cylinder was then allowed to set undisturbed until all of the air had escaped from the liquid. This allowed for calculation of the amount of air in the suspension by measuring the amount of liquid left in the graduated cylinder after all of the entrained air had escaped. The measurements made during these tests allowed for the construction of performance characteristic curves for the pump under two-phase flow conditions.

2.3 Experimental Procedure

2.3.1 Microbubble Column Flotation

Coal samples that were to be micronized before flotation testing were removed from the freezer and passed through a laboratory scale hammer mill in order to obtain a mean size of approximately 65 microns. The samples were then ground to a mean particle size of approximately 5 microns in a Szegvari attrition mill containing stainless steel balls of 1/8-inch diameter. In a few of the tests, grinding media of 1/4-inch diameter were used. The attrition grinding was done at 30% solids by weight. The coal samples were then diluted to 5% solids by weight and

placed in a feed sump for conditioning with kerosene before being fed into the column flotation cell. Coal samples that were not micronized before flotation testing were passed through the laboratory hammer mill and then slurried without additional grinding. Samples that were obtained in slurry form were processed as received after appropriate conditioning with collector in the feed sump.

Once flotation testing began, the coal was fed continuously into the column using a peristaltic pump. A peristaltic pump was also used to continuously add frother solution into the bubble generation circuit. After the flotation column was allowed to come to steady-state conditions, product and tailings samples were collected at the same time. This normally required a period equivalent to 2-3 times the slurry retention time. Feed samples were obtained directly from the feed sump. The samples were then dewatered in a vacuum filter and dried and ashed according to standard procedures specified by ASTM.

2.3.2 Microbubble Generation Studies

The tests on in-line microbubble generators were conducted such that all the data needed for characterization and scale-up for a given set of operating conditions could be collected from a single test run.

The first step of the test procedure was to prepare the surfactant solution and pour it into the storage sump.

A representative sample was taken from the sump and the surface tension was measured. The centrifugal pump was then started and aeration begun with the videocassette recorder in operation. After steady-state conditions were achieved, pressure drop across the generator was determined from the pressure gauges. Volumetric liquid flow measurements were then made by cutting samples at the discharge point. The ball valve that was installed in the circuit was then closed repeatedly for a few seconds each time. By momentarily stopping the flow, clear images of the microbubble suspension were recorded.

The volume weighted mean diameter of the microbubbles generated were then determined by direct measurement from the video monitor screen. This procedure was repeated for various values of air fraction, surface tension, and volumetric liquid flow rate for each generator size and configuration tested. Flow rates were varied by altering pump speed and air fraction was kept constant for a given test run by utilization of the air and liquid flow meters. Surface tension was varied by the addition of Dowfroth M-1012 flotation frother.

2.3.3 Centrifugal Pump Performance Studies

Centrifugal pump performance studies under two-phase flow conditions were conducted by utilization of the

equipment shown in Figure 2.6. A predetermined air fraction was maintained in the air-water suspension contained within the frothing sump by recirculating fluid from the sump, aerating it, and forcing it through an in-line microbubble generator by means of a centrifugal pump. This suspension was then used to evaluate the performance characteristics of a centrifugal pump by measuring volumetric flows at given pump heads. The head to be overcome by the pump being tested was varied by restricting the flow from the discharge line. Volumetric flows were measured by cutting samples at the pump discharge point.

The air fraction for a given test run was determined by allowing the air-water suspension to flow from the bottom of the frothing sump into the bottom of a specially designed 100 ml graduated cylinder. The suspension was allowed to flow into the graduated cylinder until it began to spill over the top. The flow was then interrupted and all of the air allowed to escape from the graduated cylinder. The void space in the cylinder divided by total volume was then taken as the air fraction of the suspension.

CHAPTER 3

EXPERIMENTAL RESULTS

3.1 Microbubble Column Flotation Tests

3.1.1 DOE Test Work

A series of microbubble column flotation tests was performed on several coal samples provided by the United States Department of Energy (DOE). The tests were conducted as part of an inter-laboratory program set up to compare advanced froth flotation processes currently under development. The coals used in the "round-robin" testing included the samples from the Pittsburgh No. 8, Illinois No. 6 and Upper Freeport coal seams. A raw coal sample analysis of each coal is given in Table 3.1. Previous test work has shown that these coals are difficult to upgrade by conventional techniques.

After each test run, samples of the product, reject and feed were collected and sent to the DOE for analysis. All of the tests were performed in a microbubble flotation column having a diameter of 2 inches and a height of 60 inches.

a) Pittsburgh No. 8 Seam Coal

The sample of Pittsburgh No. 8 seam coal was obtained by DOE from Belmont County, Ohio. A representative sample of this coal was sent to Virginia Tech in an air-tight

Table 3.1 Raw coal sample analysis of coals used in the Department of Energy tests at 100% passing 10 mesh.

Coal Sample	Ash (%)	Total Sulfur (%)	Pyritic Sulfur (%)
Pittsburgh	18.1	4.79	3.06
Illinois No. 6	12.9	4.01	2.40
Upper Freeport	13.6	2.02	1.46

container filled with inert gas. The sample was prepared for storage using the procedure described in Section 2.1.1. Prior to flotation, the sample was diluted to 30% solids and then pulverized in a Szegvari attritor using 1/8-inch diameter stainless steel media. The attrition grinding resulted in a volume mean particle diameter of 9 microns (Killmeyer, Hucko, and Jacobsen, 1988). Prior to flotation, the ground sample was diluted to 5% solids by weight.

No collector was added during the flotation tests conducted with the Pittsburgh seam coal. All other operating conditions and reagents were similar to those employed for the other microbubble column flotation tests. Dowfroth M-1012 frother was added at a dosage of 3.72 lb/ton to the microbubble generation circuit. Air was introduced into the cell under a pressure of 20 psi at a rate of 1.4 liters/min. Countercurrent wash water was added 3 inches below the top of flotation column overflow lip at a flow rate of 0.5 liters/min. The feed was introduced into the cell at a point 20 inches from the top of the cell at a rate of 4.8 grams/min of solids. The froth height was maintained at 24 inches during the entire series of tests.

The results of the microbubble column flotation test work are shown in Table 3.2. As shown, the microbubble

Table 3.2 Microbubble column flotation results obtained using the Pittsburgh No. 8 seam coal.

Stream	Yield (%)	Ash (%)	Sulfur (%)	Combustible Recovery (%)
Product	74.97	3.54	3.26	86.82
Reject	25.03	61.71	9.37	13.18
Feed	100.00	18.10	4.79	100.00

flotation column was able to reduce the product ash content by more than 80% (i.e., 18.1% to 3.5%) and the sulfur by more than 30% (i.e., 4.79% to 3.26%). This level of rejection was possible while still maintaining a combustible recovery greater than 85%. These results are very good in light of the difficult nature of this coal.

b) Illinois No. 6 Seam Coal

The sample of Illinois No. 6 seam coal from Randolph County, Illinois, was prepared by the procedure outlined in section 2.1.1. The sample was subjected to attrition grinding in the Szegvari stirred ball mill at 30% solids to produce a product with a volume mean diameter of 11 microns (Killmeyer, Hucko, and Jacobsen, 1988). The sample was diluted to 5% solids with tap water prior to flotation.

The flotation reagent additions and column operating parameters were similar to those for the Pittsburgh No. 8 seam coal. The flotation sample was prepared by adding 1 lb/ton of kerosene collector into an agitated feed sump followed by conditioning for 5 minutes. Because of the fine size and poor floatability of this particular sample, a relatively high dosage of 11.8 lb/ton of Dowfroth M-1012 was required in order to obtain acceptable results. The flow rates of air and countercurrent wash water were maintained at 1.3 and 0.5 liters/min, respectively. The

countercurrent wash water was added at a point 3 inches below the top of the cell and the froth height was held at 24 inches. The sample was fed into the column at a point 19 inches below the top of the cell at a solids rate of 2.1 grams/min.

Table 3.3 summarizes the flotation results obtained with the Illinois No. 6 seam coal. As shown, the ash content of the product was reduced from 12.9% to 3.3% (a 74% reduction) while maintaining a combustible recovery of over 85%. The product sulfur was decreased from 4.01% to 2.75% Once again, this result was very encouraging in light of the difficult nature of this coal.

c) Upper Freeport Seam Coal

The Upper Freeport coal sample, which came from Indiana County, Pennsylvania, was also prepared by the method described in section 2.1.1. The coal was ground in a Szegvari attritor charged with 1/4-inch diameter stainless steel balls. The attrition grinding resulted in a volume mean particle diameter of 13 microns (Killmeyer, Hucko, and Jacobsen, 1988).

The sample was diluted to 5% solids and conditioned with 1.5 lb/ton of kerosene collector. The conditioned slurry was fed to the cell at a solids rate of 2.7 grams/min. Dowfroth M-1012 was added continuously at a

Table 3.3 Microbubble column flotation results obtained using the Illinois No. 6 seam coal.

Stream	Yield (%)	Ash (%)	Sulfur (%)	Combustible Recovery (%)
Product	77.67	3.30	2.75	85.59
Reject	22.33	42.71	8.39	14.41
Feed	100.00	12.10	4.01	100.00

dosage of 6.63 lb/ton. The air and wash water flow rates were held constant at 1.2 liters/min and 0.5 liters/min, respectively. The wash water was added at a point 4 inches below the cell lip and the feed slurry was added 20 inches below the top of the flotation column. The froth height was maintained at 24 inches.

The microbubble column flotation test results obtained using for the Upper Freeport coal are shown in Table 3.4. With this particular sample, respectable reductions in both ash (approximately 63%) and sulfur (approximately 36%) were obtained while maintaining a combustible recovery of more than 97%. The very good rejection of ash and sulfur, combined with the negligible loss of recovery, makes this sample an attractive candidate for processing by the microbubble column flotation process.

3.1.2 Ultraclean Coal Test Work

At the request of an industrial research organization, the microbubble column flotation process was used to produce several pounds of ultraclean coal containing less than 0.8% ash. Coal from the Elkhorn No. 3 seam that had been cleaned in a dense medium process at a specific gravity of 1.3 was used as the feed material. The ash content of the feed coal was approximately 1.1%.

The ultraclean coal was produced in a 2-inch diameter

Table 3.4 Microbubble column flotation results obtained using the Upper Freeport seam coal.

Stream	Yield (%)	Ash (%)	Sulfur (%)	Combustible Recovery (%)
Product	89.35	5.02	1.30	97.13
Reject	10.65	85.58	8.06	2.87
Feed	100.00	13.60	2.02	100.00

column that was 91 inches in height. The sample was prepared by the method described in section 2.1.1 and then subjected to attrition grinding in order to obtain a 5 micron mean size feed. It should also be noted that the column used for this series of tests was equipped with a one-way plate that prevented mixing between the flotation pulp and the bubble generation circuit. This procedure was utilized in an attempt to reduce frother consumption by minimizing the adsorption of frother on the surfaces of the finely pulverized coal.

The flotation test procedure used in the production of the ultraclean coal was very similar to that conducted for other finely pulverized coal samples. The feed slurry was diluted to 5% solids and then introduced into the column at a solids flow rate of 5.1 grams/min. Countercurrent wash water was added 4 inches from the top of the cell at a flow rate of 0.5 liters/min. Compressed air was added to the column at a rate of 1.0 liters/min. The slurry feed point was located 20 inches from the top of the cell and the froth height was maintained at 24 inches. The reagent package included a kerosene collector which was added at a dosage of 2 lb/ton. Dowfroth M-1012 was added at a dosage of 4.3 lb/ton.

Test results obtained with this low-ash coal sample demonstrated that a clean coal product containing less

than 0.5% ash could be produced with recoveries in excess of 95%. In order to determine the reproducibility of this result, several samples were taken of product and reject streams throughout an extended production run. Samples were taken at 30-minute intervals during the test. The results for one production run are shown in Table 3.5. This data shows that the microbubble column flotation process is capable of producing an ultraclean coal product at a high level of recovery for an extended period of time.

3.1.3 Refuse Coal Test Work

Microbubble column flotation tests were performed on reject samples obtained from two different coal companies. The reject samples were taken from the classifying cyclone overflow produced at the various plant sites. The samples were considered to be difficult to upgrade by traditional methods due to their fine particle size, low solids content (2-5% solids) and high ash content (>40%). Both of these organizations were interested in the possible implementation of microbubble column flotation for their processing operations.

a) Shell Mining Company Test Work

Three samples of refuse were obtained from two different preparation plants owned and operated by the

Table 3.5 Ultraclean coal production results.

Operating Time (min.)	Product Ash (%)	Combustible Recovery (%)
30	0.43	93.53
60	0.47	97.39
90	0.51	97.64
120	0.45	98.62

Shell Mining Corporation. Two of the samples were obtained from the Coalburg seam coal that were being processed at the company's Marrowbone plant. The first sample was 100% passing 28 mesh and the other was 100% passing 150 mesh. The third sample was Warfield coal from the Wolf Creek plant. This feed sample was 100% passing 100 mesh.

Coalburg Sample : The -150 mesh Coalburg sample was processed using a 2-inch diameter column that was 65 inches in height. A wide range of operating conditions was examined during the test runs. The sample was received in slurry form at approximately 2% solids by weight. The sample was conditioned with 0.5 lb/ton of kerosene before being fed into the cell. Feed rates were varied between 9 and 18 grams/min. Countercurrent wash water addition rates were varied from 0.5 to 0.6 liters/min and was added at a point located 5 inches from the top of the cell. Frother additions were varied from 2.0 lb/ton to 3.0 lb/ton. The aeration rate was held at 1.0 liters/min. The height of the froth zone was maintained at 24 inches. The feed was introduced into the cell at a point located 20 inches from the top during all tests.

The -28 mesh sample of Coalburg seam coal from the Marrowbone plant was received in slurry form at

approximately 2% solids by weight. This sample was processed using the same cell geometry as used during the testing of the -150 mesh sample. Solids feed rates were varied from 8 gms/min to as much as 33 gms/min. Countercurrent wash water additions were kept between 0.3 and 0.5 liters/min. Kerosene dosage was kept at 1 lb/ton and frother additions varied from 1.5 to 4.25 lb/ton. The location of the feed point and froth depth were kept the same as that employed in the -150 mesh sample test work. The countercurrent wash water addition point was located 6 inches from the top of the cell.

As shown in Figure 3.1, the -150 mesh Coalburg seam coal responded very well to treatment by the microbubble column flotation process. In the best case, the ash content of the product was reduced from over 54% to just over 12%. Very high recoveries were obtained for nearly all of the test conditions examined.

The recovery versus ash curve for the -28 mesh sample is shown in Figure 3.2. These results also appear promising and indicate that recoveries greater than 80% can be obtained while reducing the ash content by over 60%.

Warfield Sample : The -100 mesh Warfield coal sample from the Wolf Creek preparation plant was obtained in slurry form at approximately 5.5% solids by weight.

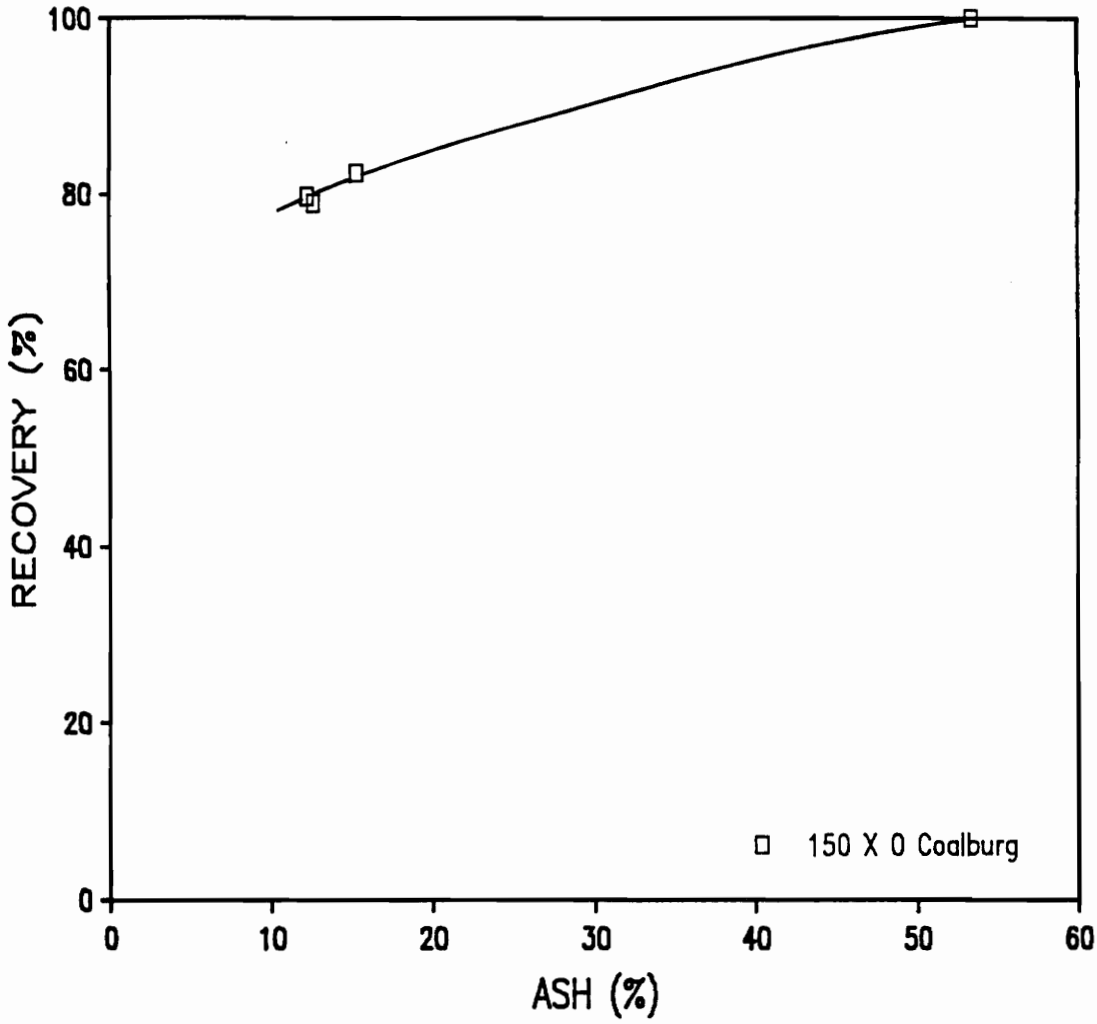

Figure 3.1 Recovery versus ash for -150 mesh Coalburg seam coal.

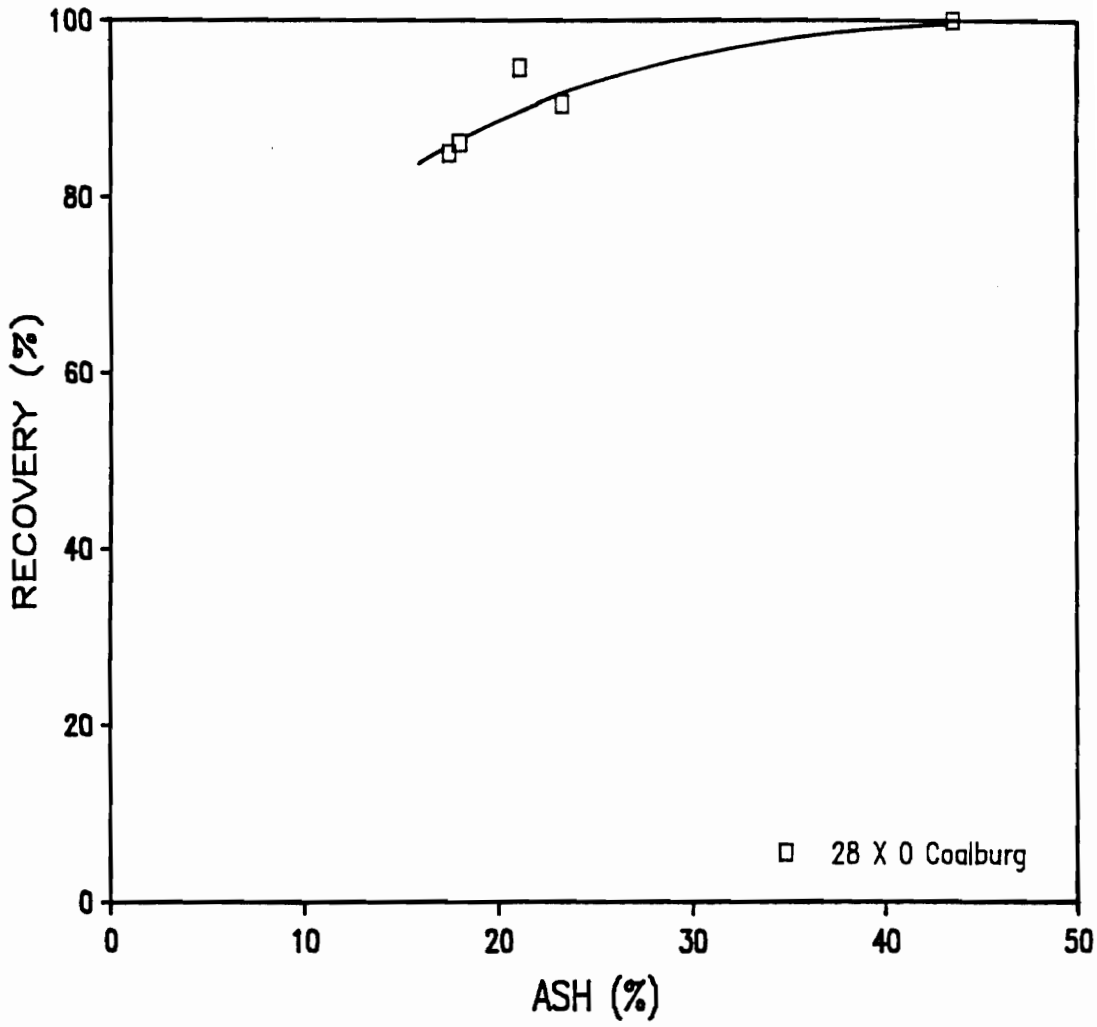

Figure 3.2 Recovery versus ash for -28 mesh Coalburg seam coal.

This sample was also processed over a wide range of operating conditions using the same flotation column used for the other samples examined in this study. A kerosene collector was added at a dosage of 0.25 lb/ton. Feed rates were varied from 8.3 to 74.6 gms/min. Compressed air was added at flow rates which varied between 1.0 and 1.2 liters/min. Frother dosages were varied from 1.38 lb/ton to 3.32 lb/ton. Countercurrent wash water was added at a point 5 inches below the top of the cell at a rate of 0.5 liters/min in all tests. Feed was introduced at a point 20 inches from the top of the cell and froth depth was maintained at 24 inches.

As shown in Figure 3.3, a clean coal product containing less than 5% ash could be produced from this coal seam using the microbubble column flotation process. Combustible recoveries in excess of 80% were obtained under these operating conditions. This sample appears to be a very promising candidate for further test work with the microbubble column flotation process.

b) Pittston Coal Test Work

A series of microbubble column flotation tests was conducted on Middle Fork coal refuse from Pittston Coal Company's Moss No. 3 preparation plant. A sieve analysis of the coal is as follows:

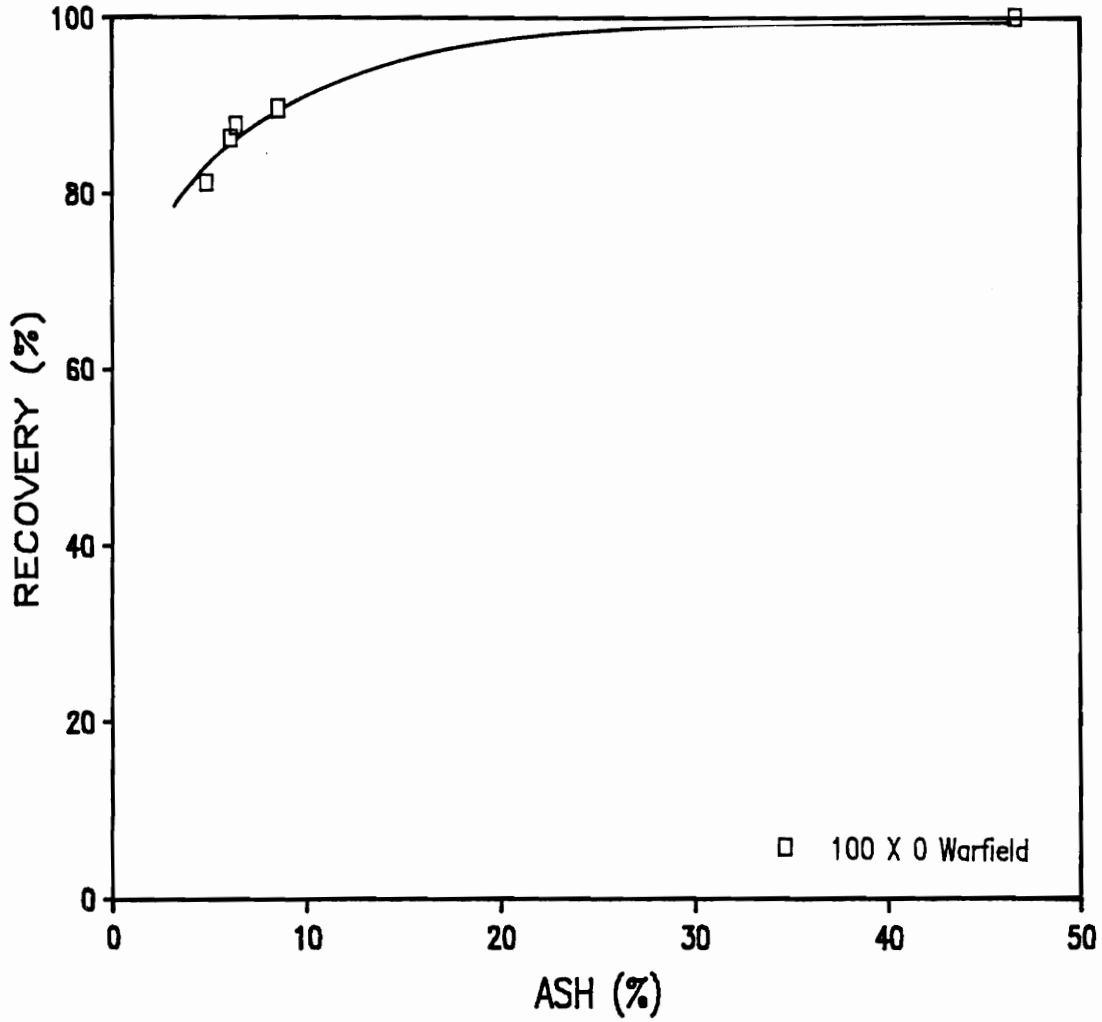

Figure 3.3 Recovery versus ash for -100 mesh Warfield seam coal.

100%	-28 mesh
90%	-100 mesh
65%	-325 mesh.

The sample was received in slurry form at approximately 10% solids by weight. The coal was introduced into the column as received after conditioning with a fuel oil collector.

The tests were conducted in a 2-inch diameter microbubble column flotation cell that was 60 inches in height. Dowfroth M-1012 flotation frother was used in the microbubble generation circuit with dosages varying between 0.3 and 8.5 lb/ton. No. 2 diesel fuel at a dosage of 0.40 lb/ton was used as a collector in all of the tests. Countercurrent wash water was introduced at a point 4 inches below the top of the cell at a rate of 0.5 liters/min in all tests. Solids feed rates varied from 53.4 to 117.2 grams/min. The feed point was located 20 inches from the top of the cell and the froth depth was maintained at 20 inches for all tests. Aeration rates were were varied between 0.75 and 2.0 liters/min during the test work.

The results of the microbubble column flotation test work obtained with this particular coal sample are shown in Figure 3.4. The data illustrate that the column was capable of producing a clean coal product of less than 6% ash at combustible recoveries greater than 60%. The tests

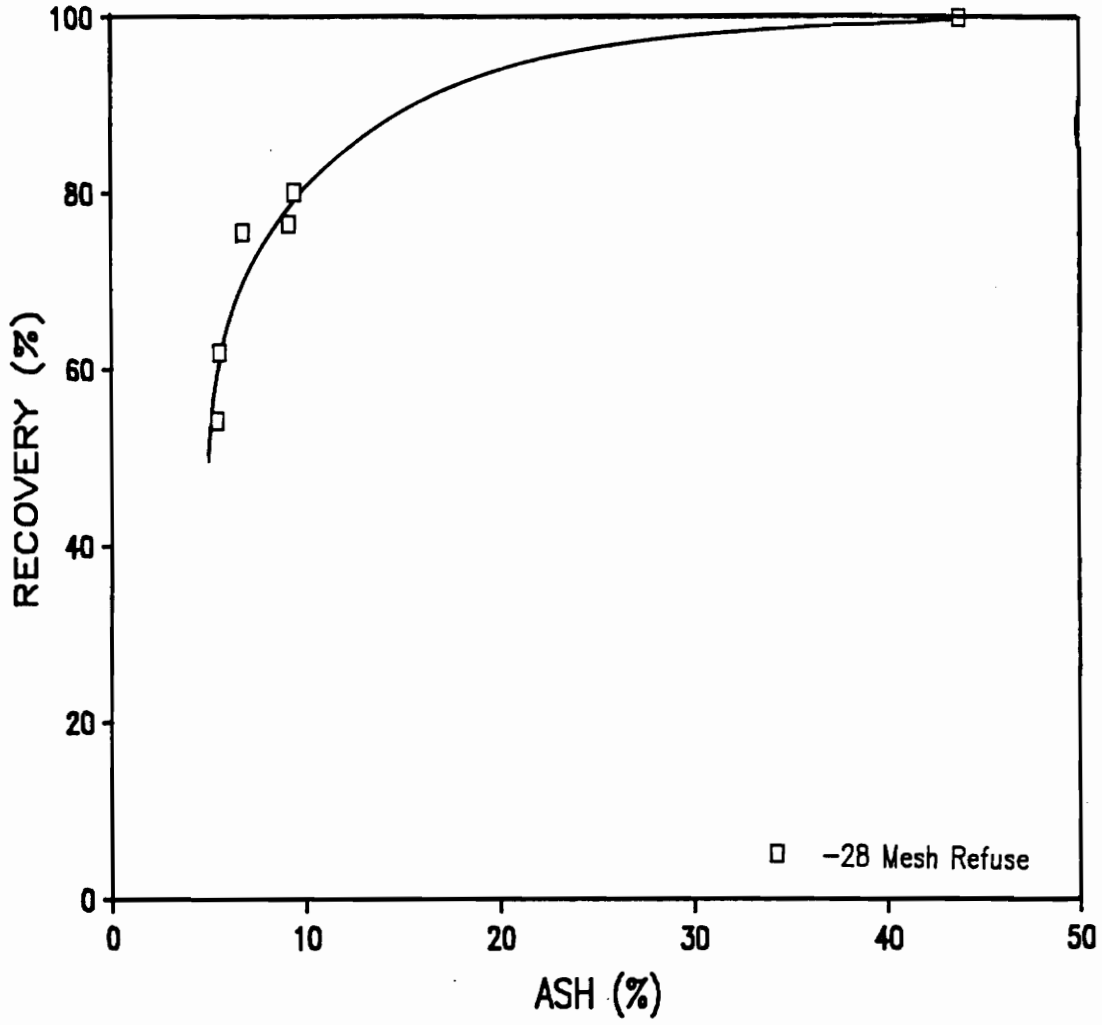

Figure 3.4 Recovery versus ash for the Middle Fork sample from Pittston's Moss No. 3 plant.

clearly demonstrate that a marketable coal can be produced from this material despite the fact that it is presently being discarded as refuse.

3.2 Microbubble Generation Studies

The equipment shown in Figure 2.5 was utilized to collect data to characterize and scale-up various types of in-line microbubble generators, i.e., motionless mixers. The first set of tests was conducted using a generator having a Kenics element configuration. The inside diameter of each of the Kenics generators was 0.44 inches. The elements in the Kenics type generators were 0.75 inches in length and units equipped with 7-, 15-, and 22-elements were studied. Koflo-type generators with inside diameters of 0.62 and 0.82 inches and lengths of 5 and 7 inches, respectively, were also tested.

3.2.1 Pressure Versus Flow Relationships

a) Effect of Bubble Size

The first step in the characterization of in-line microbubble generators was to determine the effect of bubble size on pressure and flow characteristics. Bubble sizes were varied by changing surfactant concentration and volumetric flow rate through the generator.

The data shown in Figure 3.5 shows that changing bubble size has little effect on the pressure-flow

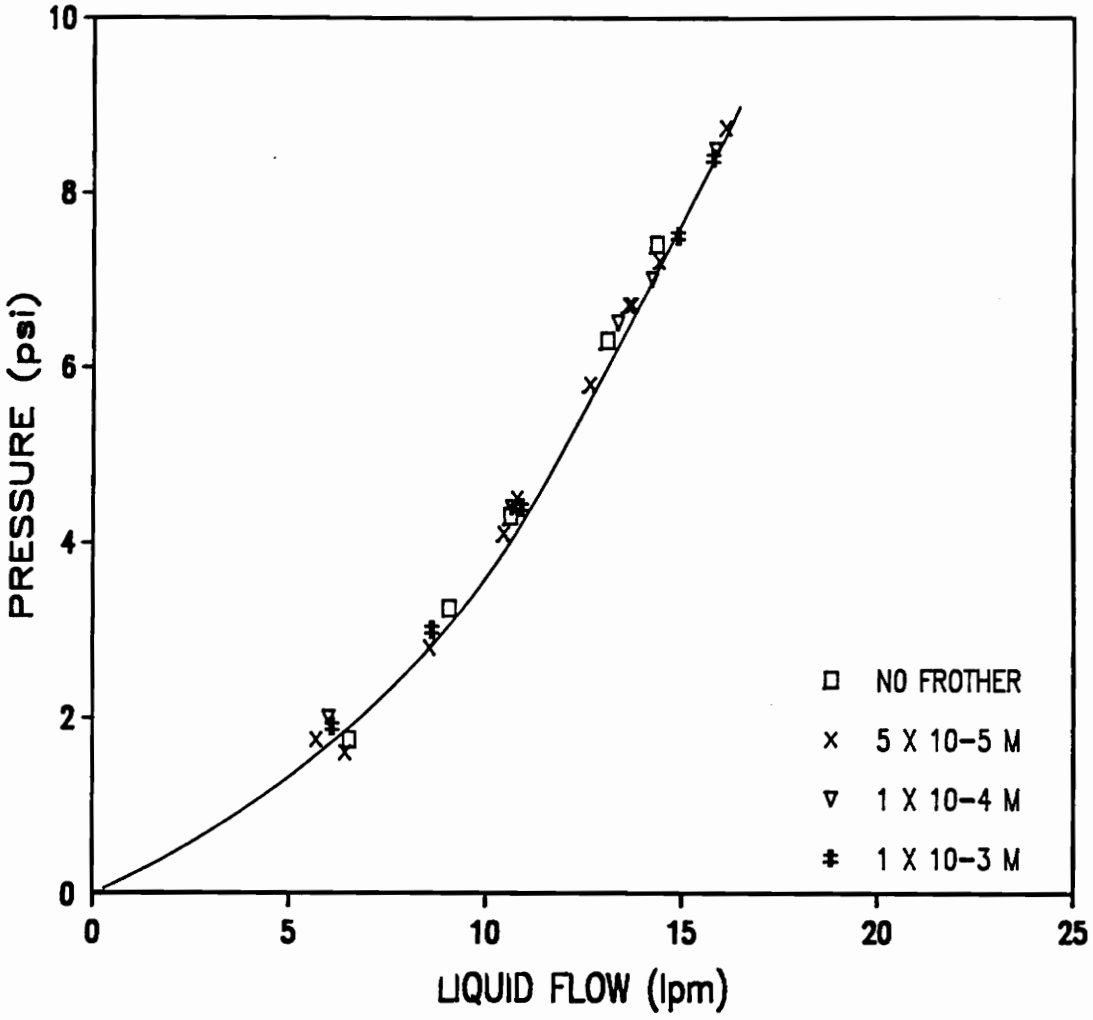

Figure 3.5 Pressure versus flow for the 7-element Kenics mixer as a function of frother concentration at 10% air.

relationship for the Kenics-type generator. Similar results have also been obtained for the two other Koflo generators examined in the present work (Figures 3.6 and 3.7). As will be shown in later sections of this work, this characteristics hold true provided that the element configuration, generator geometry and air fraction of the microbubble suspension remains unchanged.

b) Effect of Air Fraction

In order to determine the effect of air fraction of the microbubble suspension on the performance of the in-line microbubble generators, a series of tests was performed under conditions in which the air hold-up of the bubble suspension was varied. The fractional air content was controlled by adjusting the ratio of the air and liquid flow rates. The results of these experiments are shown in Figures 3.8, 3.9, and 3.10 for the three different Kenics-type generators examined in the present work.

The test data obtained with various Kenics generators indicate that the fractional air content of a microbubble suspension does affect the pressure versus liquid flow characteristic curve. As expected, a higher applied pressure was required at higher air fractions in order to maintain a given volumetric liquid flow through the generator. The same types of trends are found regardless

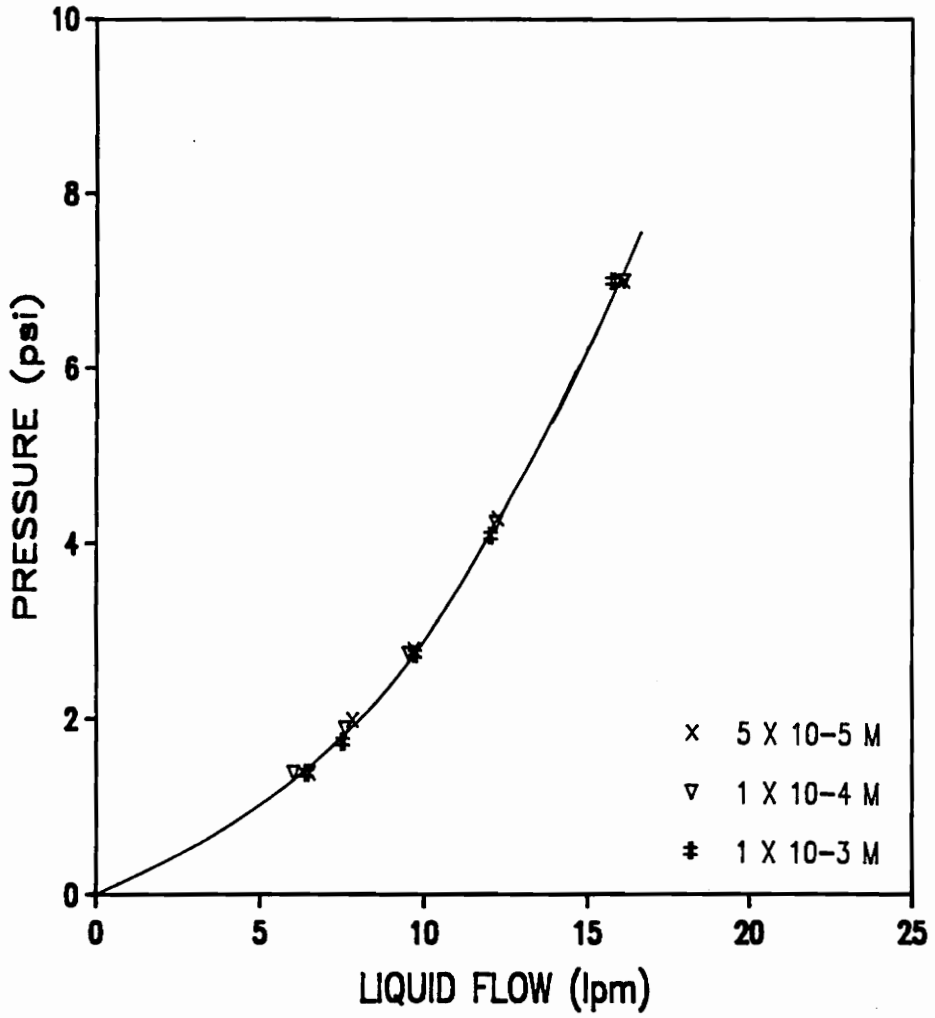

Figure 3.6 Pressure versus flow for the Koflo mixer (0.62-inch diameter) as a function of frother concentration at 20% air.

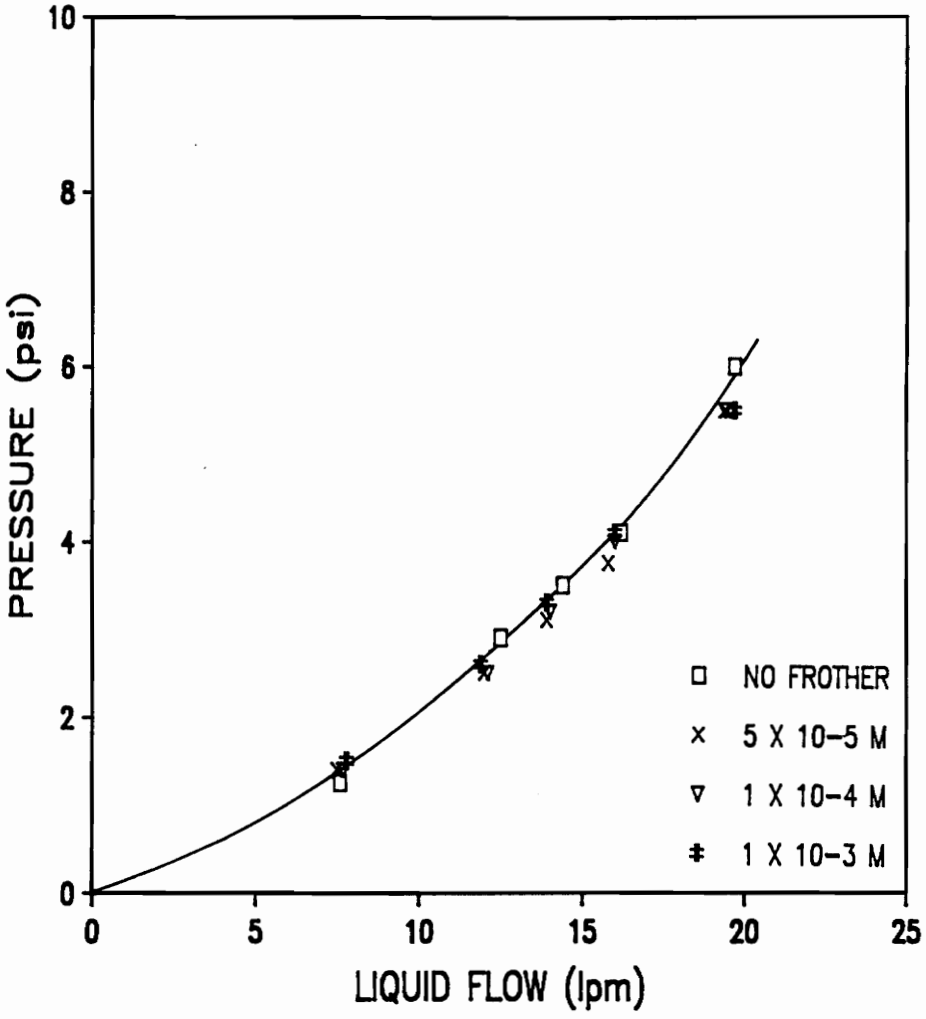

Figure 3.7 Pressure versus flow for the Koflo mixer (0.82-inch diameter) as a function of frother concentration at 20% air.

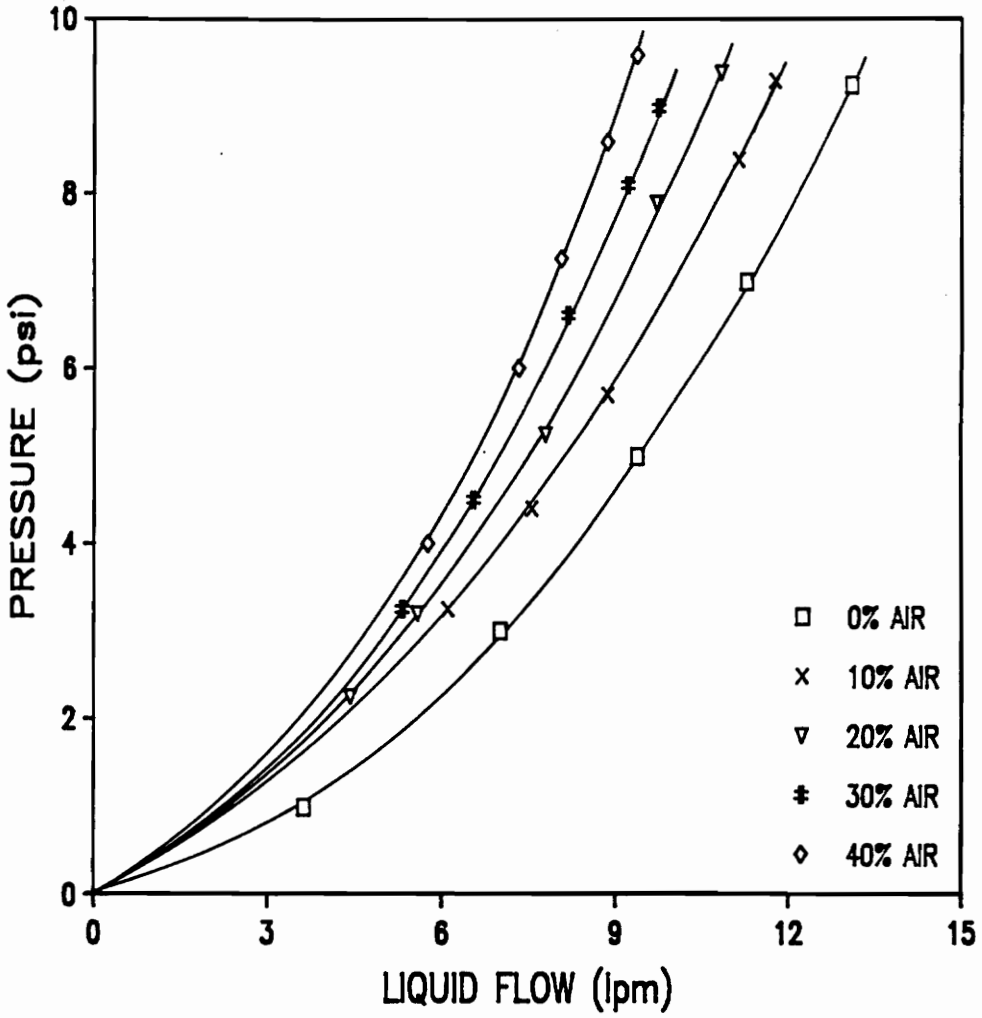

Figure 3.8 Pressure versus flow for the 15-element Kenics mixer at various air fractions using 10^{-3}M Dowfroth 1012.

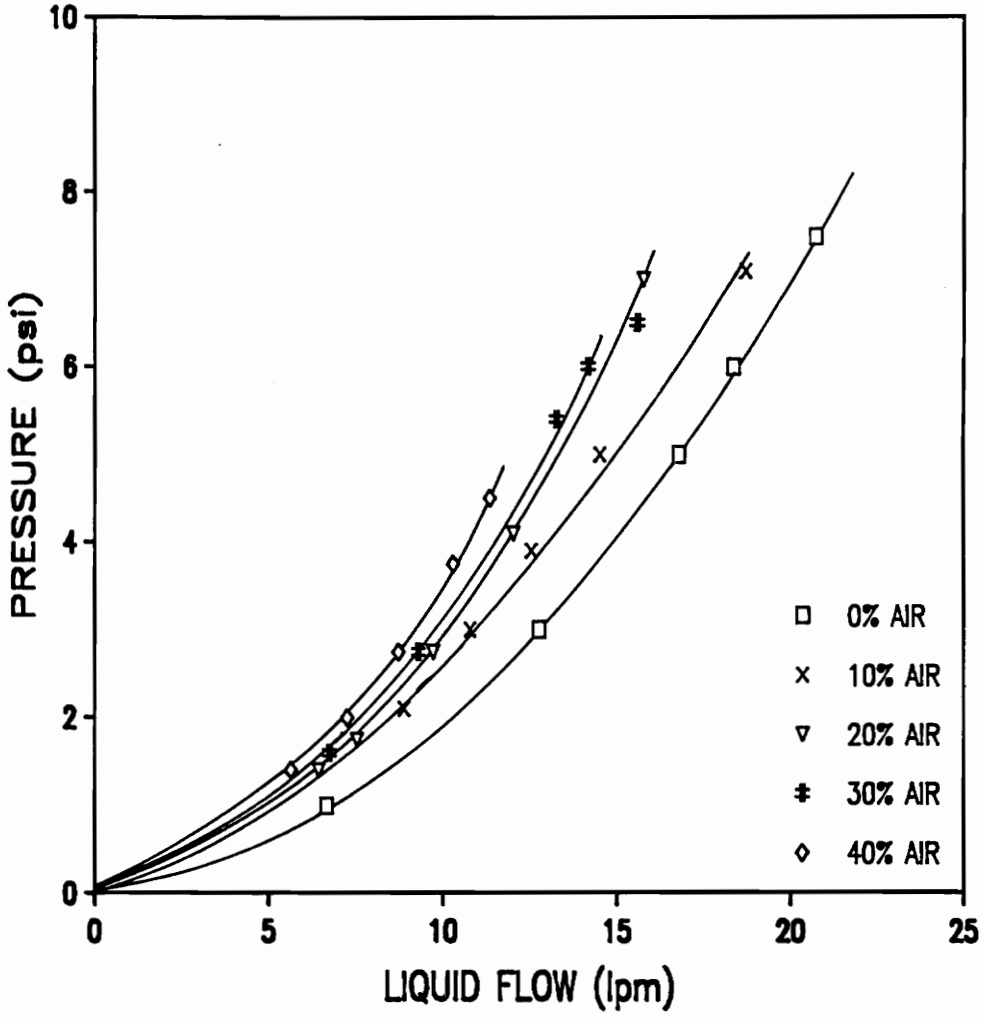

Figure 3.9 Pressure versus flow for the Koflo mixer (0.62-inch diameter) at various air fractions using 10^{-3}M Dowfroth 1012.

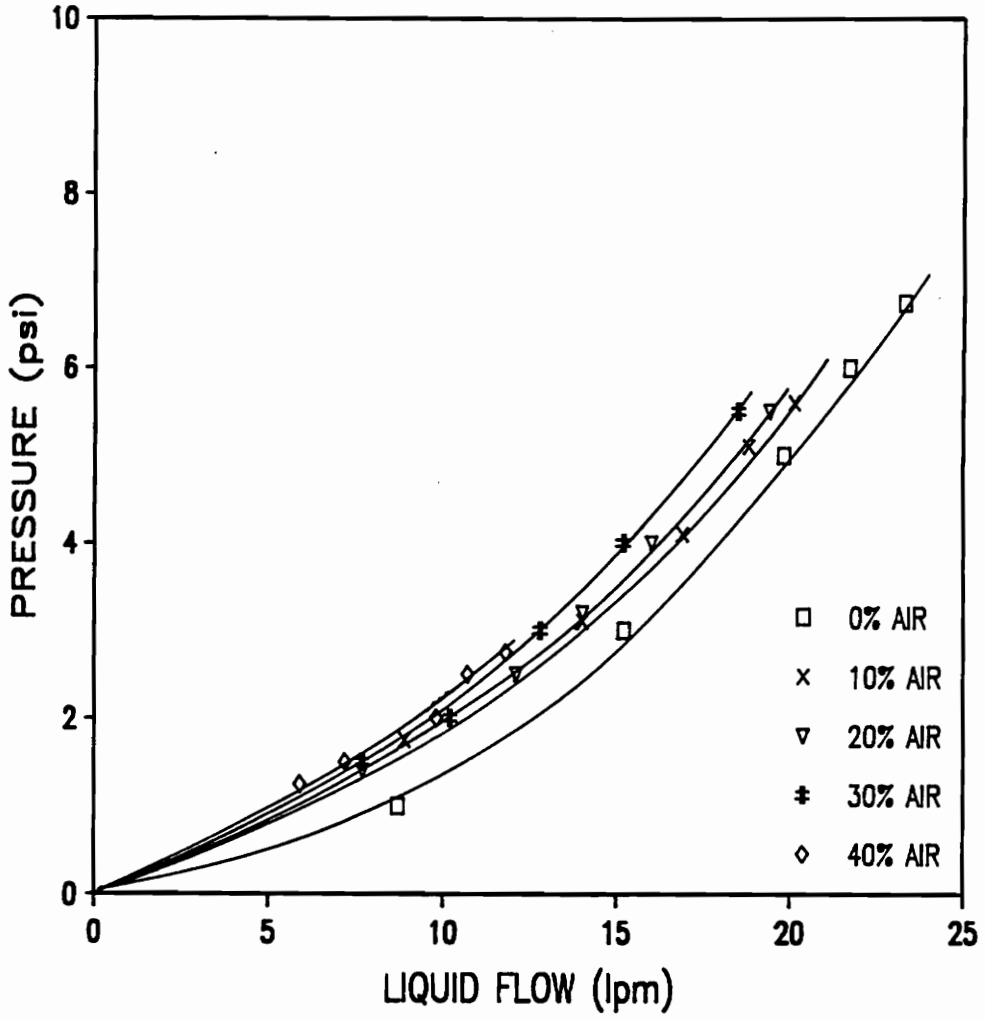

Figure 3.10 Pressure versus flow for the Koflo mixer (0.82-inch diameter) at various air fractions using 10^{-4}M Dowfroth 1012.

of generator diameter, length or element configuration.

By inspection, it was discovered that the pressure versus flow curves for a given generator configuration could be normalized by simply plotting pressure versus the combined volumetric flow rate of gas and liquid. This effect is shown for the Kenics and Koflo element configurations in Figures 3.11 and 3.12. It should be noted that these relationships hold true only under "non-slugging" operating conditions. The generator is operating in "slugging" conditions when the amount of air being passed through the unit is more than can be sufficiently dispersed into the liquid medium. Therefore, it is important that generators be operated under "non-slugging" conditions.

c) Effect of Generator Length

Pressure versus total flow characteristic curves are found to shift for constant diameter generators of varying lengths, i.e., a longer generator requires more applied pressure than a shorter unit to obtain the same volumetric flow. However, one should expect to be able to normalize this data by plotting pressure per unit of generator length versus total volumetric flow. The pressure per unit length versus total flow relationship is shown in Figure 3.13 for constant diameter Kenics-type generators

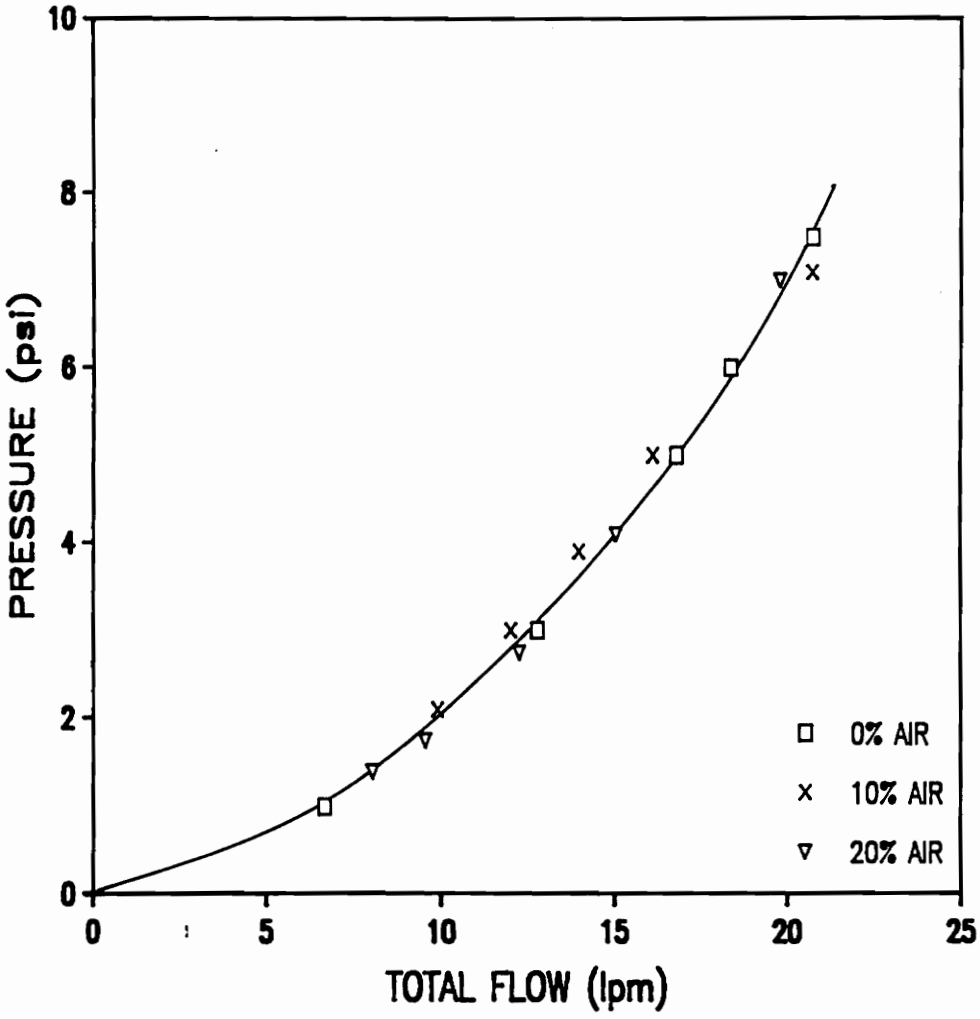

Figure 3.11 Normalized pressure versus total flow curve for the Koflo mixer (0.62-inch diameter) using 10^{-3}M Dowfroth 1012.

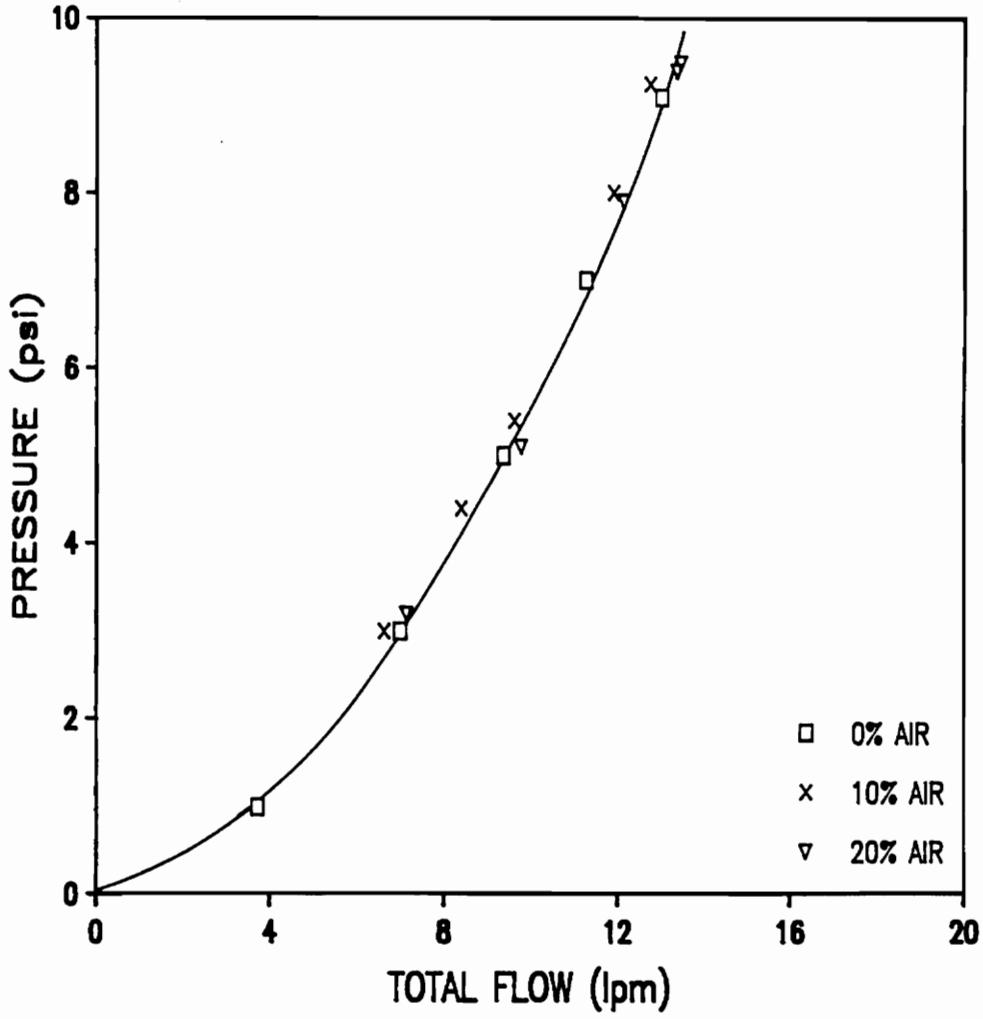

Figure 3.12 Normalized pressure versus total flow curve for the 15-element Kenics mixer using 10^{-4}M Dowfroth 1012.

having 7, 15 and 22 mixing elements. This normalization was required in order to allow for comparison of diameter effects, since generators of equal length and varying diameter were not available during the course of this study. It should be noted that the data comprising the curve depicted in Figure 3.13 were collected under various operating conditions, such as different values for air fraction and surfactant concentration (i.e., varying surface tension). It should also be noted that pressures in Figure 3.13 were expressed in units of inches of water for graphing purposes.

d) Effect of Generator Diameter

The effect of changing the diameter of the Koflo-type generator is shown in Figure 3.14. As expected, the smaller diameter generator requires higher pressure than the larger diameter unit to achieve the same volumetric fluid flow. These tests were conducted on Koflo-type mixers of varying length and diameter, but as mentioned previously the length variation was accounted for by dividing pressure by the respective length of each motionless mixing device. The inside diameters of the Koflo generators tested in the present work were 0.62 and 0.82 inches.

For reference sake, the pressure-flow characteristic curves are shown in Appendix I for all generators and

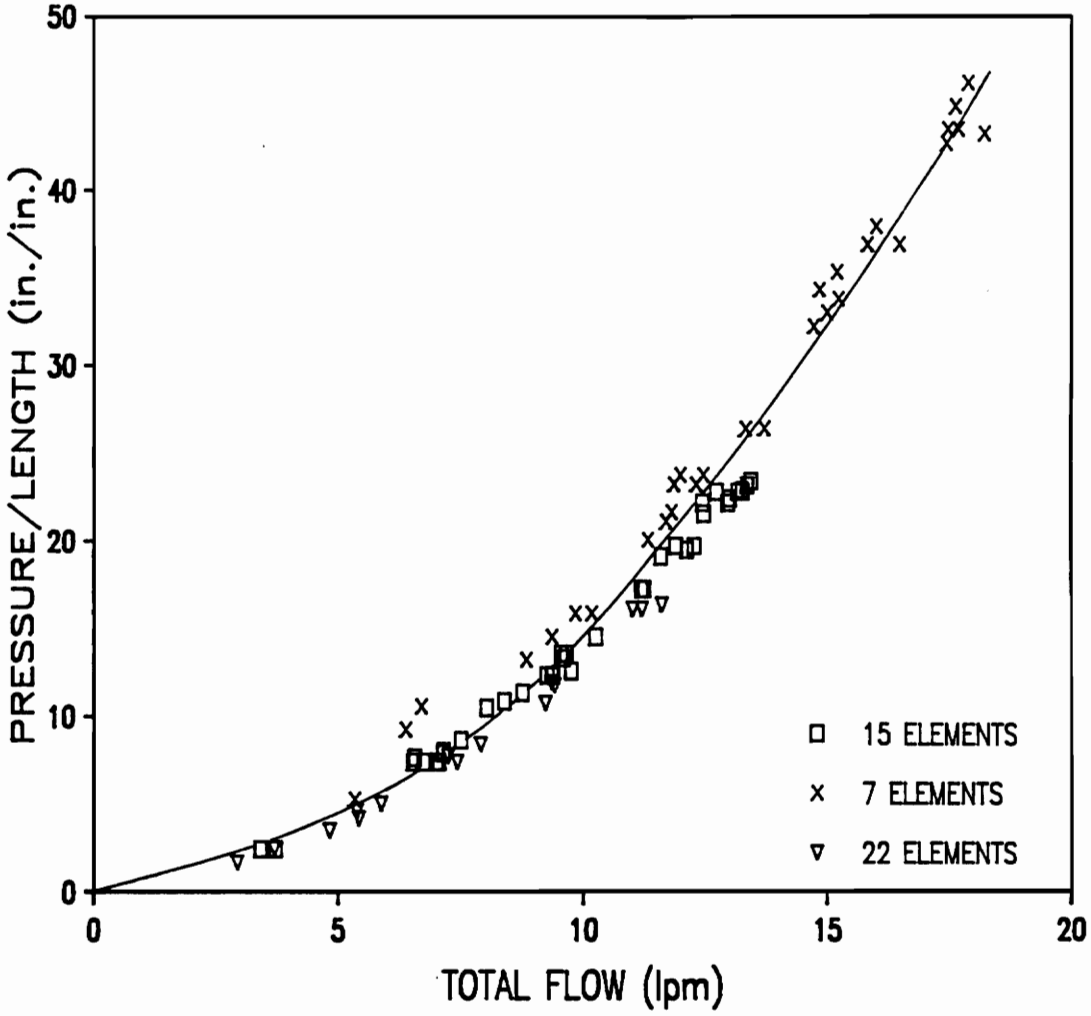

Figure 3.13 Pressure/length versus total flow for constant diameter Kenics mixers of various lengths.

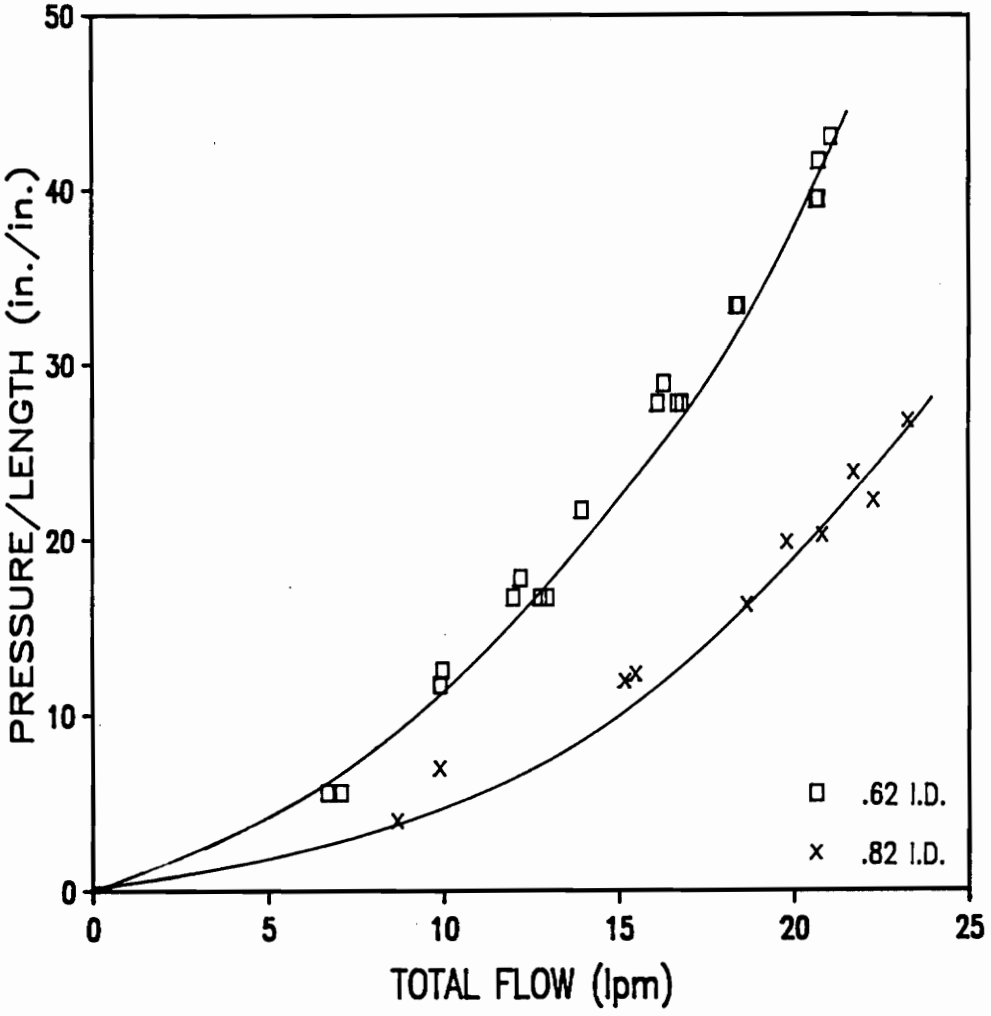

Figure 3.14 Effect of generator diameter on the pressure-flow curves for Koflo mixers.

tests conducted during the present work.

3.2.2 Bubble Diameter Measurements

Images of microbubbles generated by the various in-line motionless mixing devices were recorded during each test run using the video recording system shown previously in Figure 2.5. The volume weighted mean diameters of the microbubbles were determined along with operating parameters such as pressure, volumetric rate of flow and surface tension.

a) Determination of Sample Size

In order to determine the minimum number of bubbles that had to be counted in order to obtain a reasonably accurate measure of the bubble size, an average bubble size was calculated and plotted as a function of sample size. This information was determined from a test on a 0.62 inch diameter Koflo type generator which was 5 inches in length. As is shown in Figure 3.15, a sample size of approximately 90 was required to minimize the variability in the calculated average size. Therefore, a minimum of 130 microbubbles was counted and measured for a given test run.

b) Effect of Flow Rate

The effect of changing volumetric rate of flow of gas

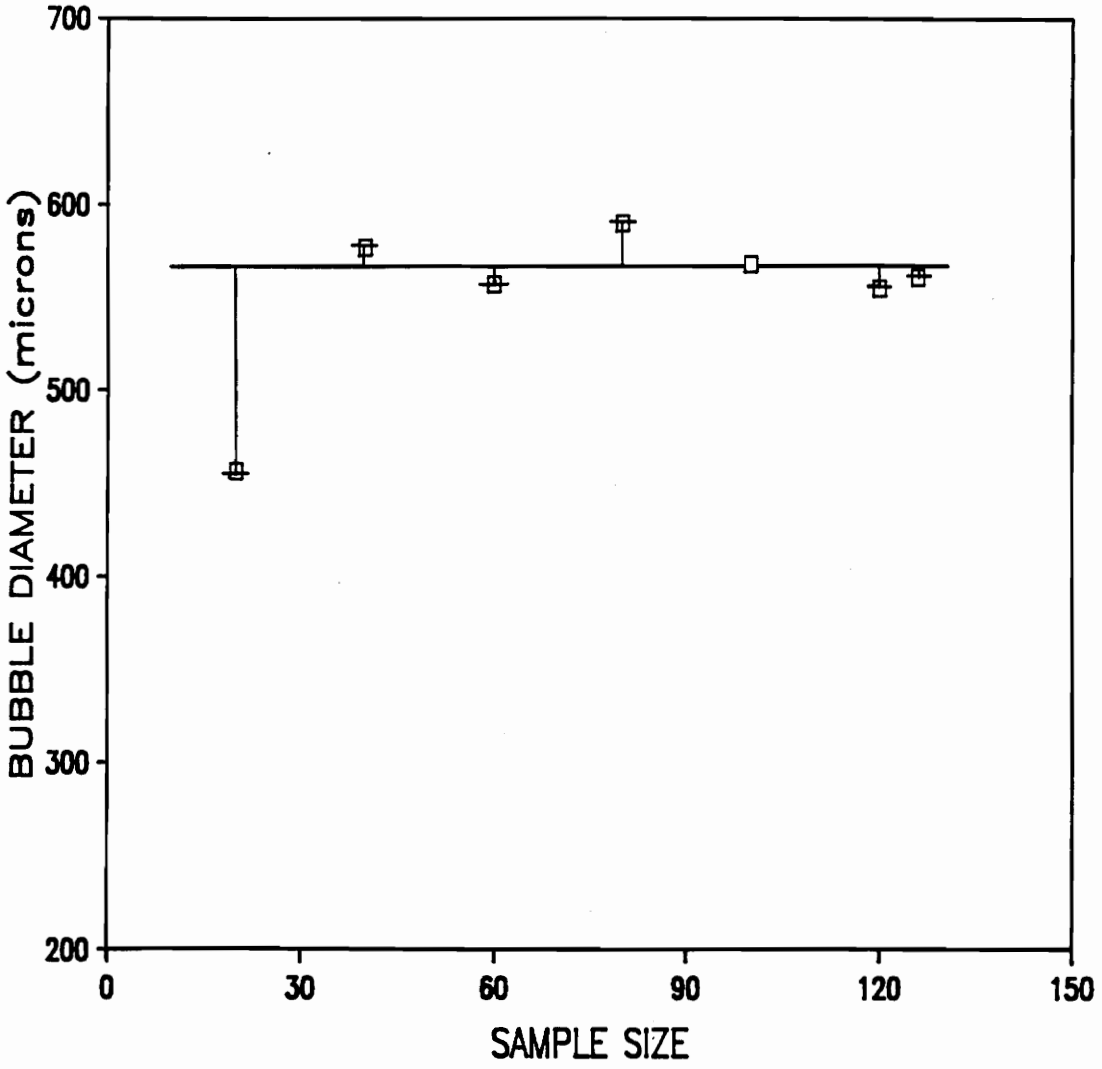

Figure 3.15 Effect of sample size on the volume weighted mean bubble diameter for the Koflo mixer (0.62-inch diameter).

and liquid through a given generator is shown in Figure 3.16. The volume weighted mean bubble diameter increases as volumetric flow rate decreases. This trend should be expected since the force which tends to shear the gas phase diminishes with decreasing fluid velocity.

c) Effect of Generator Geometry

The effect of generator length on volume weighted mean bubble diameter is shown in Figure 3.17. As shown, the longer generator (15 element) produces finer bubbles than the 7-element unit for a given flow rate. This is reasonable, since the gas phase is subjected to more shear forces in the longer generator.

d) Effect of Surface Tension

The effect of varying surface tension (surfactant concentration) on volume weighted mean bubble diameter is illustrated in Figure 3.18. As shown, the diameter of bubbles generated in a 7-element mixer decreases with surface tension for a given volumetric rate of flow. The bubbles should be torn apart easier for a given set of operating conditions as interfacial tension decreases, since surface tension forces must be overcome in order to disperse the gas phase within the liquid medium.

e) Effect of Air Fraction

The effect of air fraction on volume mean bubble

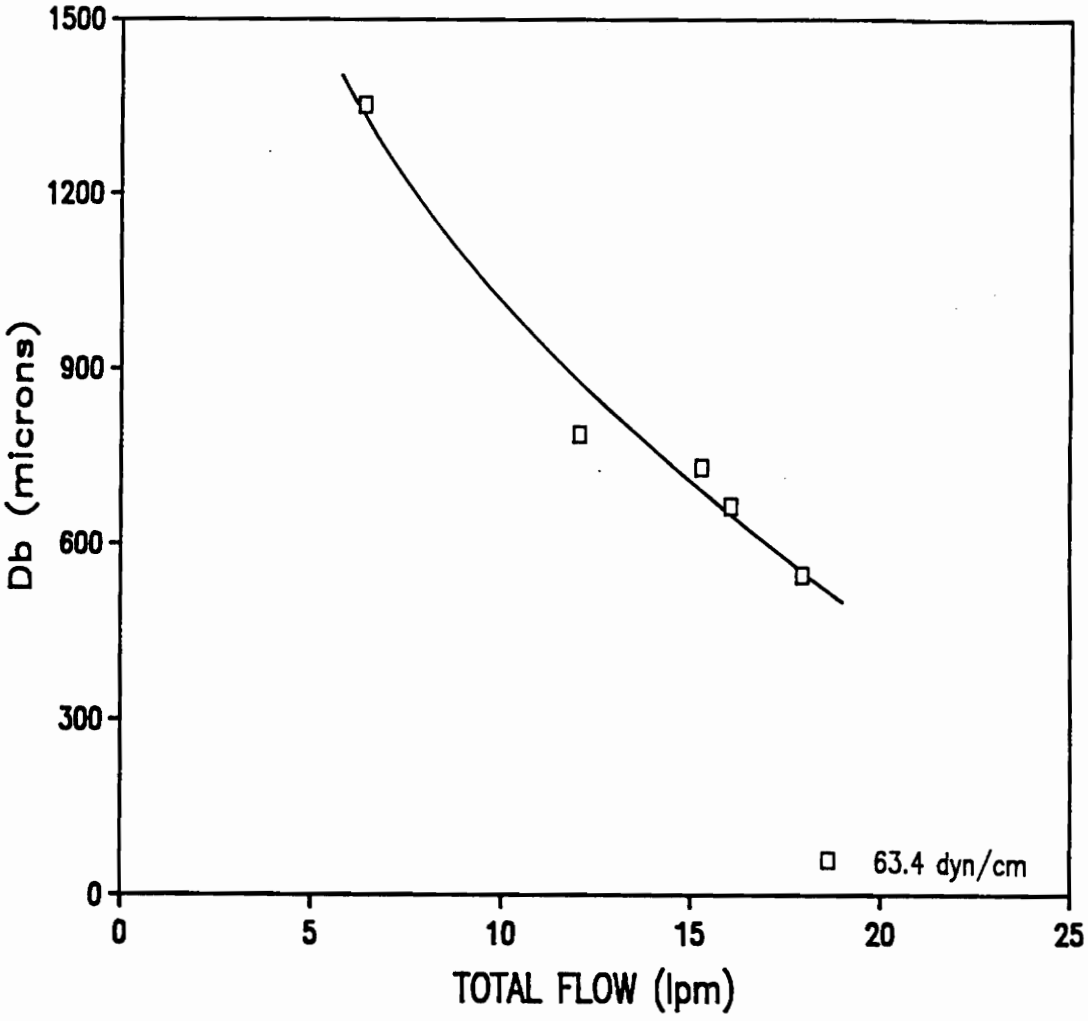

Figure 3.16 Effect of total flow rate on volume mean bubble diameter for a 7-element Kenics mixer at 10% air and constant surface tension.

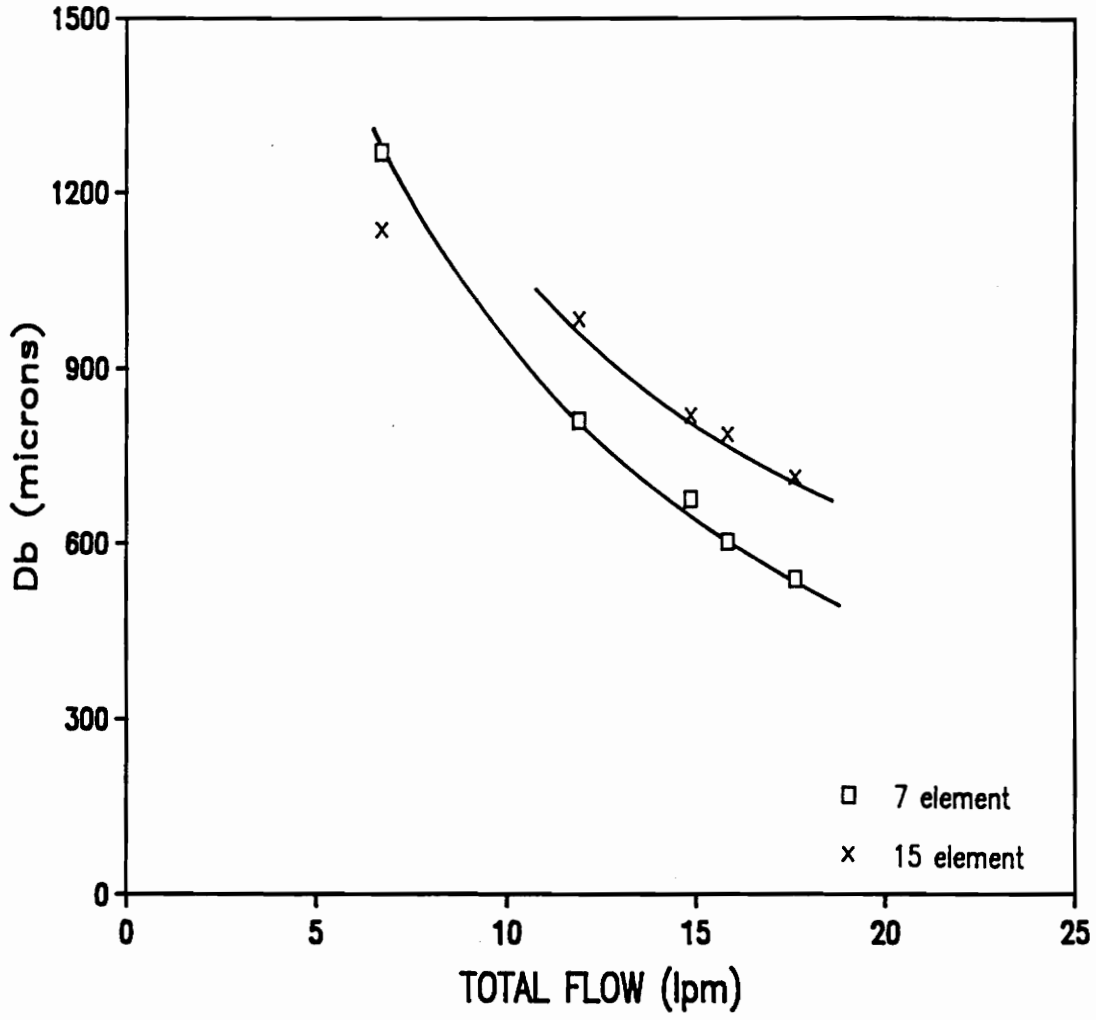

Figure 3.17 Effect of generator length on volume mean bubble diameter for the Kenics mixer.

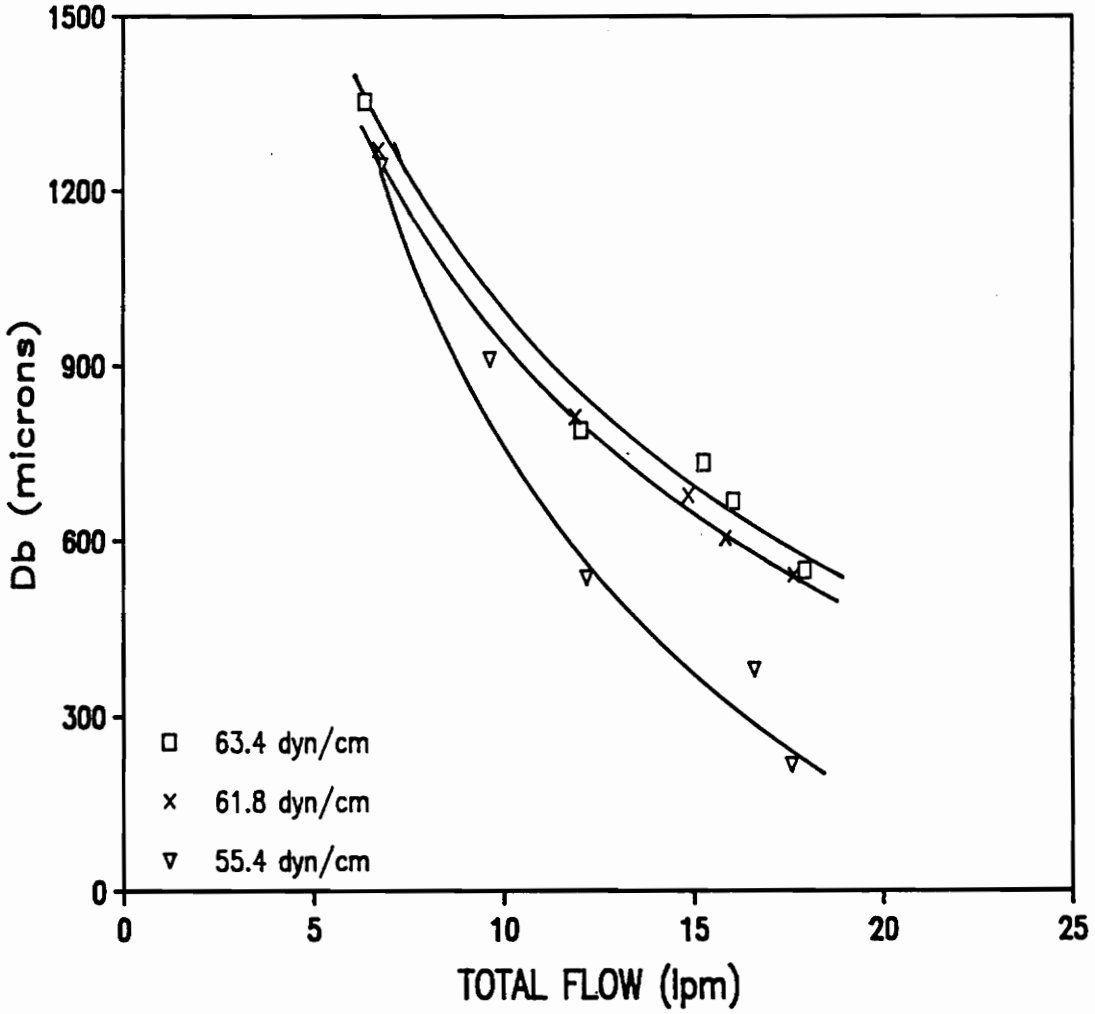

Figure 3.18 Effect of surface tension on volume mean bubble diameter for a 7-element Kenics mixer at 10% air.

diameter is shown in Figure 3.19. For a given flow rate, the higher air fraction produced a significantly larger bubble size. The larger bubble sizes may be due to an increase in bubble-bubble coalescence as the air fraction rises. However, preliminary experimental results suggest that the larger bubble sizes may be an artifact of the data collection procedure. At high air fractions, many of the smaller bubbles are hidden from view by the larger bubbles. Thus, the calculated mean bubble size is weighed in favor of the larger bubbles. The increased scatter in the data obtained at the higher air fractions also tends to support this possibility. Further test work is warranted in order to determine the significance of this problem in determining bubble sizes by photographic techniques.

3.3 Centrifugal Pump Performance Studies

The effects of entrained air on the performance of a centrifugal pump used for microbubble generation were studied using the equipment previously shown in Figure 2.6. The studies were conducted on a Teel centrifugal pump (model 1P797A) driven by a 3/4-horsepower variable speed Dayton electric motor. Information concerning the effects of entrained air on the performance of the centrifugal pump was collected at entrained air

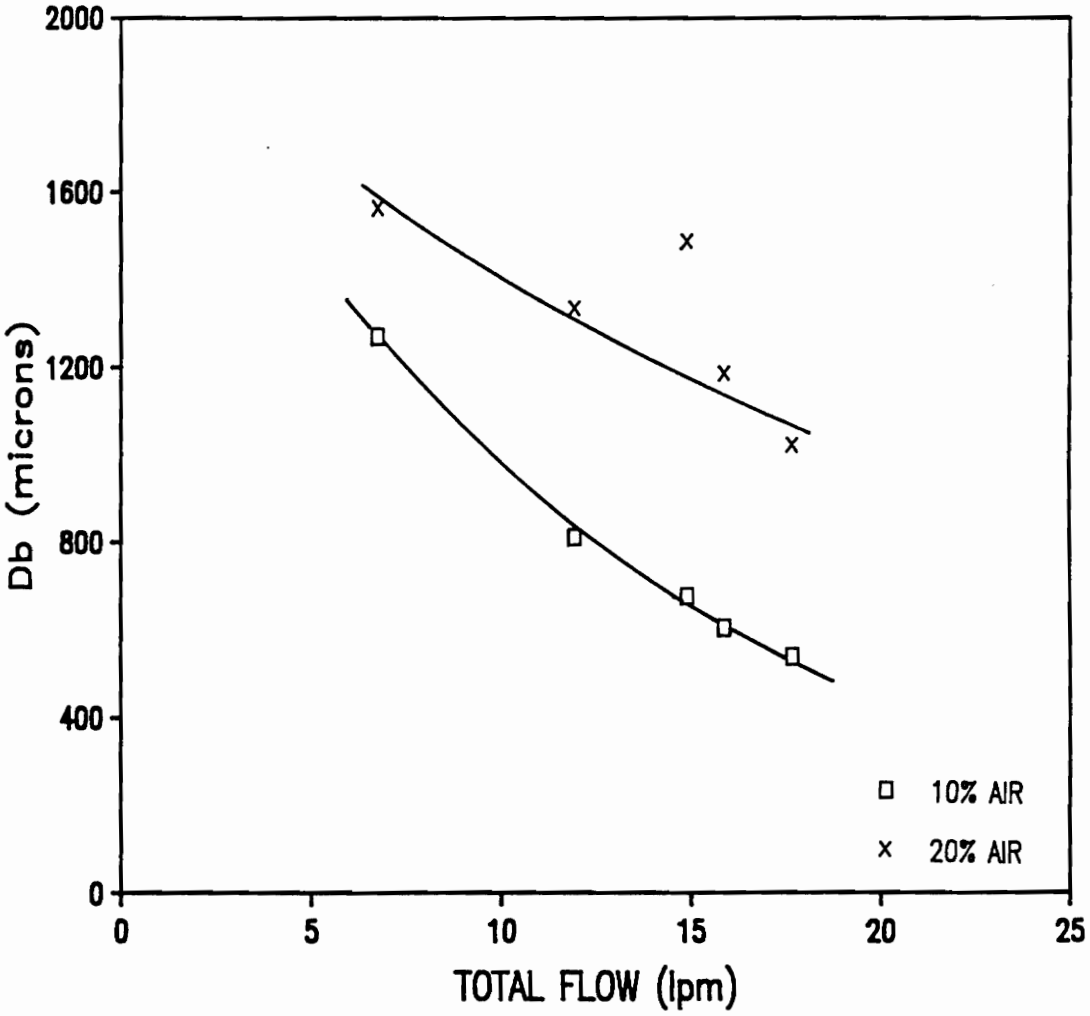

Figure 3.19 Effect of air fraction on volume mean bubble diameter for a 7-element Kenics mixer at various flow rates.

percentages varying from 5% to 21%. It was discovered that the pump generally lost prime at air contents greater than 20-25%.

The effects of entrained air on the pump performance curves are shown in Figure 3.20. It can be concluded that pump performance is not adversely affected by entrained air until the air content becomes greater than approximately 10%. It should be noted that total fluid flow of gas and liquid was used in the performance evaluations. The reason for using the combined liquid-gas flow rate is that the total flow rate has been shown to be more useful than the liquid flow rate for characterizing the behavior of the various in-line microbubble generators.

3.4 Microbubble Size Distributions

Figures 3.21, 3.22, and 3.23 are logarithmic plots of microbubble size distributions from three tests conducted on two Kenics- and one Koflo-type generators. The slopes of the linear portions of the distributions (i.e., the distribution modulli) vary slightly while volume weighted mean bubble diameters fall between 217 and 850 microns. From this, it is possible to conclude that the bubble size distributions vary only slightly in terms of spread. The data tend to suggest that the distributions shift which changes mean bubble diameter,

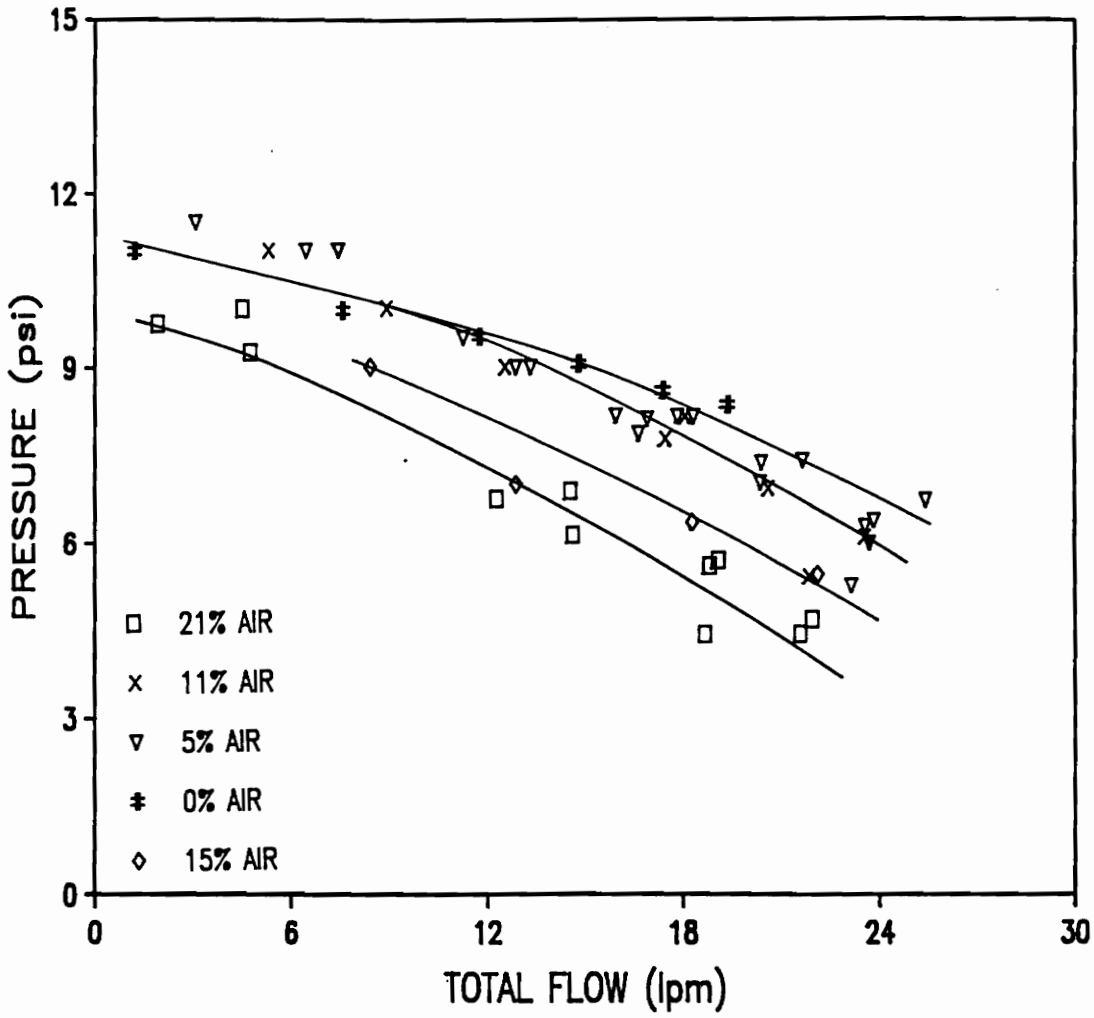

Figure 3.20 Effect of entrained air on the pressure versus total flow curve for an open face impeller centrifugal pump.

but that the spreads of the distributions remain essentially the same. This finding may be useful for future work related to the scale-up and design of microbubble column flotation.

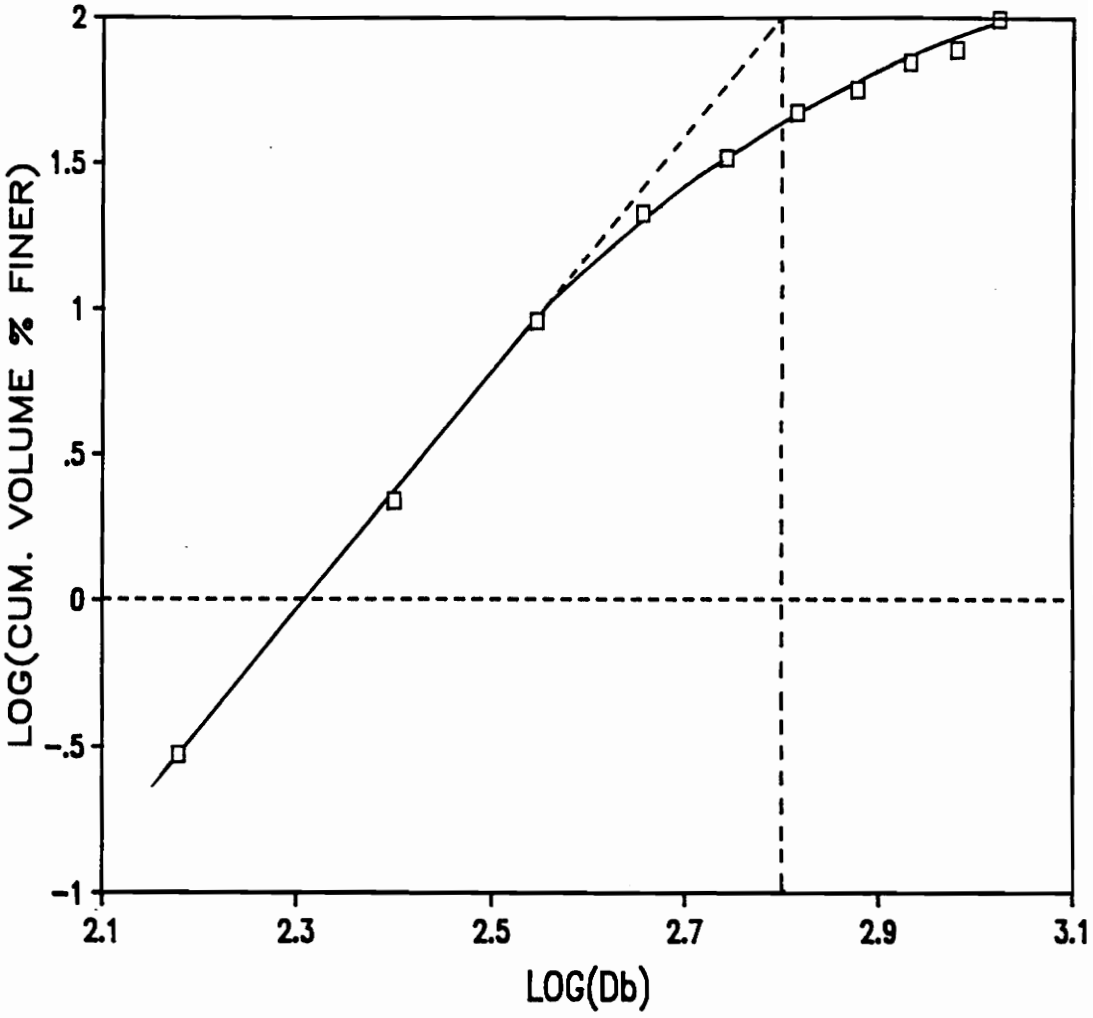

Figure 3.21 Microbubble size distribution produced by a Koflo mixer (0.62-inch diameter) at 10% air using 10^{-3}M Dowfroth 1012.

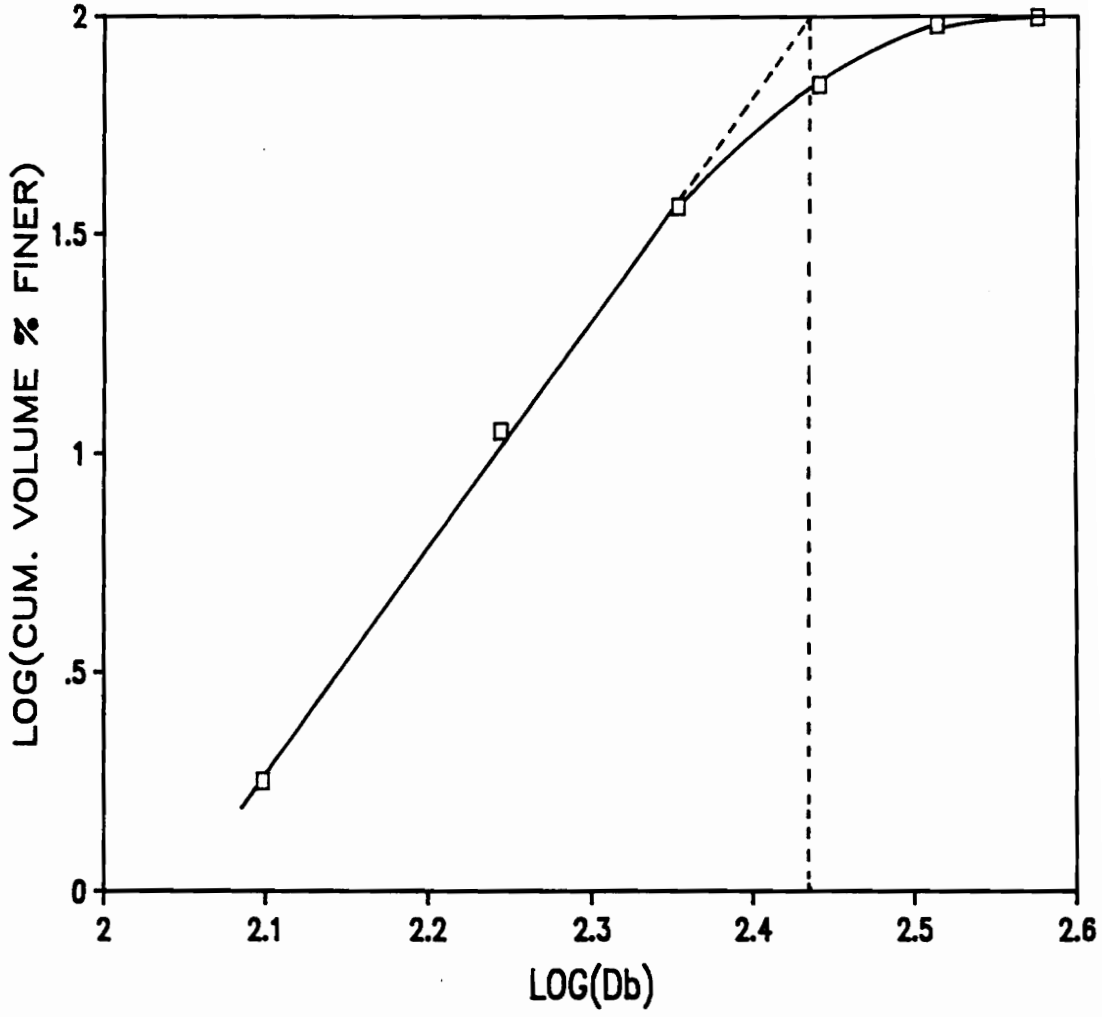

Figure 3.22 Microbubble size distribution produced by a 7-element Kenics mixer at 10% air using 10^{-3}M Dowfroth 1012.

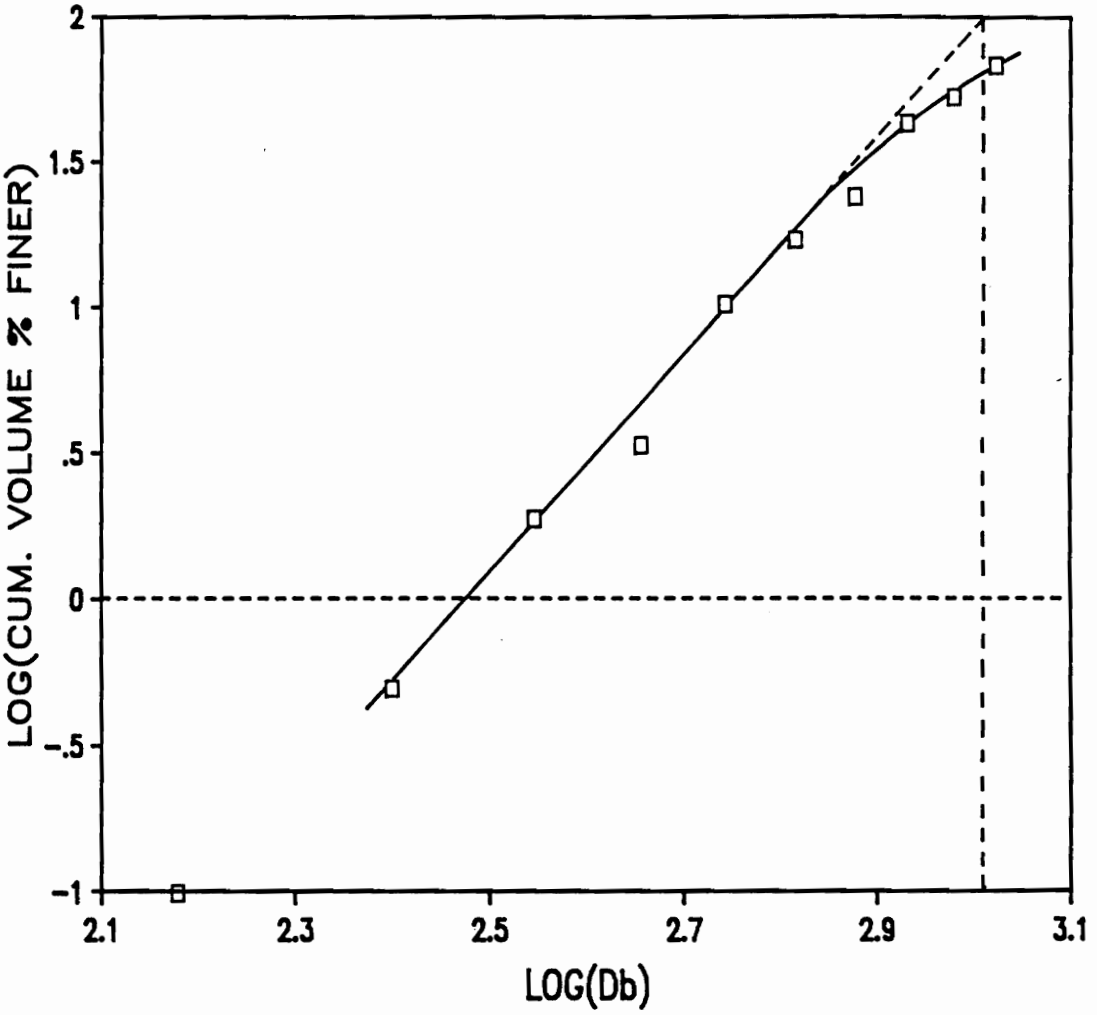

Figure 3.23 Microbubble size distribution produced by a 15-element Kenics mixer at 10% air using 10^{-3}M Dowfroth 1012.

CHAPTER 4

DISCUSSION

4.1 Microbubble Column Flotation

As has been shown in the present work, the microbubble column flotation process is capable of producing very good results for the upgrading of a wide variety of coal samples. Some of the most promising results were obtained with samples which could not be effectively upgraded using conventional flotation processes. The high combustible recoveries and low ash values obtained during the course of the flotation testing can be attributed to several of the novel features of the microbubble column process. These features are discussed in more detail in the following paragraphs.

The use of smaller than usual air bubbles is one characteristic of the microbubble column flotation process that results in enhanced flotation performance. The probability of collision between fine particles and microbubbles is higher than for the larger bubbles produced in conventional flotation columns. This enhanced collection rate can be explained by the fact that the streamlines around smaller bubbles do not diverge as greatly as those associated with larger bubbles (Luttrell, 1986). The reduced divergence of streamlines decreases the chance of small particles, which possess small

inertial forces, from being swept around the bubbles without making contact. Also, for a given volume of air, the surface area available for contact between air bubbles and fine particles is higher in the presence of small bubbles (Weber, 1988). Finally, the use of microbubbles improves selectivity in the column flotation process due to the absence of turbulent wakes behind the rising bubbles. The absence of this phenomenon results in a decrease in the amount of hydrophilic particles which may be recovered by an entrainment (Yoon, 1982; Yoon, et al., 1984).

Flotation performance is improved in part due to the geometry and configuration of column flotation cells. The countercurrent flow conditions and quiescent nature of column flotation cells allow for more efficient bubble-particle attachment and froth drainage (Weber, 1988). It should also be noted that the coalescence of air bubbles as they near the top of a column flotation cell aids in the production of cleaner products. This coalescence phenomenon results in a reduction of total air bubble surface area which in turn leads to the detachment of less hydrophobic particles, i.e., middlings.

The use of countercurrent wash water is another operating feature of column flotation that aids in enhanced flotation performance as compared to conventional

processes. The downward flow of clean wash water allows for the removal of undesirable materials that are not attached to air bubbles. Therefore, the majority of the water recovered in the froth product is not as likely to be contaminated by entrained material.

4.2 Scale-Up of In-Line Microbubble Generators

4.2.1 Pressure Drop

The prediction of pressure drop across an in-line microbubble generator is an important part of the scale-up procedure. Pressure drop must be quantified in order to properly size generator pumps and associated piping networks.

The effects of changing generator geometry and operating parameters on the pressure versus flow characteristic curves for various in-line microbubble generators were shown in Section 3.2.1. This behavior can be described using the same techniques employed to study the flow through an unrestricted open pipe.

For the case of flow through a smooth pipe, studies have shown that the resultant pressure drop (ΔP) can be described by:

$$\Delta P = f \frac{L}{D} \frac{\rho v^2}{2} \qquad [4.1]$$

in which f is the friction factor, L/D the length to diameter ratio, ρ the density of the continuous phase and V the superficial fluid velocity. The flow regime can be characterized by Reynolds number which is given by:

$$Re = \rho VD/\mu \qquad [4.2]$$

where D is the pipe diameter and μ the dynamic viscosity. It should be noted that the flow conditions for microbubble generation are transitional in nature, i.e., between pure turbulent and laminar flow conditions. Since the flow conditions are transitional, the friction factor (f) can be determined from:

$$f = \frac{0.316}{Re^{.25}}. \qquad [4.3]$$

Equation [4.3] is valid for Re values between 3,000 and 100,000. This range easily covers the typical values of Re commonly encountered in microbubble generation. By substituting Equation [4.3] into Equation [4.1], it can be shown that:

$$\Delta P = \frac{0.316}{Re^{.25}} \frac{L}{D} \frac{\rho V^2}{2}. \qquad [4.4]$$

Equation [4.4] can be used to calculate pressure drop across a smooth pipe having the same dimensions as a

static mixer used for microbubble generation.

Oldshue (1983) has outlined a method for predicting the pressure drop across a static mixer for liquid-liquid mixing using the following relation:

$$\Delta P^* = K \Delta P \qquad [4.5]$$

where ΔP^* is the pressure drop across the mixer, ΔP is the pressure drop across a smooth pipe of the same dimensions, and K is a constant dependent upon mixer design (type of elements and geometric dimensions).

In order to apply the technique outlined by Oldshue (1983) to the present work, values of K were calculated by dividing the pressure drop measured during the course of the experiments for each type of generator by the values calculated by Equation [4.4] for smooth pipes of equal size. Since bubble generation involves the passage of a two-phase gas-liquid suspension through a static mixing device, it was necessary to determine if K remained constant for varying air fractions.

A plot of K versus Reynolds number is shown in Figure 4.1. The data given in this figure show that K does remain constant for a given generator configuration for all of the air fractions tested. Reynolds number was chosen for the determination of the constancy of K, since it is a convenient means of representing the flow regime.

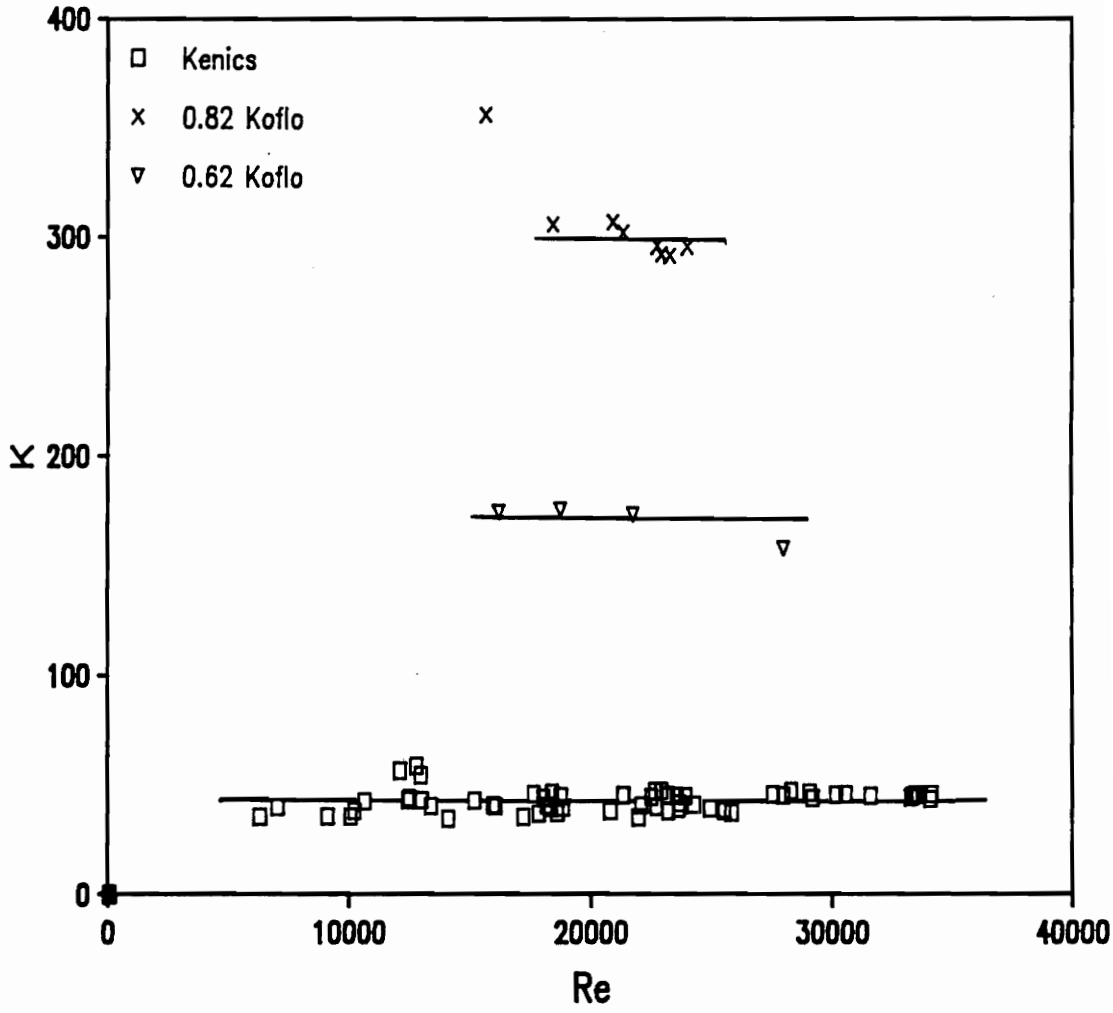

Figure 4.1 Mixer constant (K) versus Reynolds number (Re) for various element configurations, air fractions and frother dosages.

This data strongly supports the conclusion that K is a function of generator design and independent of the flow regime.

The shift in the pressure-flow characteristic curve after the introduction of air was initially thought to be related to an increase in apparent viscosity. It has been reported that the apparent viscosity of air-liquid emulsions is higher than for the liquid phase only (Wu, Sullivan, and Yee, 1984). However, estimated values of apparent viscosity do not appear to change sufficiently to produce the rather large shift in the pressure-flow curves. Therefore, it has been concluded that the normalization of the pressure-flow curve brought about by using total flow in place of liquid flow is due to a simple volumetric displacement of water by air.

Since two-phase pressure versus flow curves can be normalized with single-phase performance characteristics, the method outlined above can be used to predict the pressure drop across a static mixing device operating in two-phase conditions, i.e., for microbubble generation.

4.2.2 Volume Mean Bubble Diameter

The data collected from the microbubble generation tests were used to draw correlations between bubble diameter (volume weighted mean diameter) and various operating parameters. A successful attempt at developing

a relationship for bubble diameter prediction, regardless of generator geometry or element configuration, was made. The relationship was developed using forces derived from parameters such as velocity, surface tension, and geometry on the gas phase of the fluid passing through an in-line microbubble generator.

A relationship was defined by Oldshue (1983) for the scale-up of motionless mixing devices used for dispersive mixing operations. The method related droplet diameter to Weber number. The dimensionless Weber number group is defined as:

$$We = \frac{\rho V^2 L}{\sigma} \qquad [4.6]$$

where ρ is the continuous phase density, V is the fluid velocity, L is the characteristic length, and σ is the interfacial surface tension. Weber number, which is defined as the ratio of inertia forces to surface tension forces (Giles, 1962), is often used to aid in the quantification of atomization processes (Roberson and Crowe, 1985). The inertia forces act to deform the droplets and the surface tension forces tend to hold them together. Since Weber number is important in describing droplet formation, it was anticipated that Weber number would be useful in developing a expression for microbubble

generation.

In order to quantify the process of bubble generation, it was necessary to perform a dimensional analysis on all the factors that possibly influence the generation of bubbles from an in-line generator. It was determined that bubble diameter was most likely dependent upon the following parameters:

$$D_b = f(\sigma, \Delta P, V, L, D, \rho, \mu) \qquad [4.7]$$

where σ is the surface tension, ΔP the pressure drop across the generator, L the generator length, D the generator diameter, ρ the continuous phase density, and μ the apparent dynamic viscosity. In terms of its dimensional units, the function given by Equation [4.7] is equivalent to:

$$L = (M/T^2)^a(M/T^2L)^b(L/T)^c(L)^d(L)^e(M/L^3)^f(M/LT)^g \qquad [4.8]$$

where a-g are unknown constants and L, M and T represent units of length, mass and time. In order for Equation [4.8] to be dimensionally satisfied, then the following must hold true:

$$L: \quad 1 = -b + c + d + e - 3f - g \qquad [4.9]$$

$$M: \quad 0 = a + b + f + g \qquad [4.10]$$

$$T: \quad 0 = -2a - 2b - c - g \qquad [4.11]$$

Multiplying Equation [4.10] by 2 and adding it to [4.11] yields:

$$c = 2f + g \qquad [4.12]$$

Likewise, by combining Equations [4.9] and [4.12], it is possible to obtain:

$$b = d + e - f - 1 \qquad [4.13]$$

If we assume that one of the parameters that can be used to characterize microbubble generation is the Weber number (We), then additional restrictions can be placed on the values of the unknown exponents. Weber number, which includes ρ, V, L, and σ, dictates that:

$$f = d = -a = c/2. \qquad [4.14]$$

If we now substitute c/2 for f in Equation [4.12], it is possible to show that:

$$g = 0. \qquad [4.15]$$

By setting a = -f and g = 0 in Equation [4.10], we can also shown that:

$$b = 0. \qquad [4.16]$$

Finally, by substituting b = 0 into Equation [4.13], we find that:

$$e = 1. \qquad [4.17]$$

At this point, all of the unknown exponents have been defined in terms of a known integer value or in terms of one of the unknown exponents, i.e., a = -f, b = 0, c = 2f, d = f, e = 1, f = f and g = 0.

In a dimensional analysis, it is frequently assumed that the relationship between the parameters of interest (e.g., bubble size) and the operating variables (e.g., generator diameter, flow rate, etc.) is logarithmic in nature. In the present work, it has been assumed that a power function can be used to describe the process of bubble generation. From this it is possible to show that:

$$D_b = A\ [\sigma^a\ \Delta P^b\ V^c\ L^d\ D^e\ \rho^f\ \mu^g] \qquad [4.18]$$

where A is a proportionality constant. Substitution of the previously determined exponents from the dimensional analysis into Equation [4.18] yields:

$$D_b = A\ [\sigma^{-f}\ V^{2f}\ L^f\ D\ \rho^f] \qquad [4.19]$$

This expression can be rearranged to give:

$$D_b = A(\rho V^2 L/\sigma)^f D \qquad [4.20]$$

Equation [4.20] can be made dimensionless dividing each side of the expression by generator diameter, i.e.,

$$D_b/D = A(\rho V^2 L/\sigma)^f \qquad [4.21]$$

This dimensionless expression indicates that the ratio of bubble diameter to generator diameter is a direct function of the Weber number (We).

In order to further develop the equation for predicting bubble generator performance, it was necessary to examine plots of D_b/D versus We for the generators tested. Figure 4.2 illustrates the relationship between bubble diameter and Weber number. As shown, different curves exist for each type of generator. Equation [4.21] can also be plotted as a straight line in log-log form as shown in Figure 4.3. This allows for direct determination of the parameters A and f in Equation [4.21].

Since it is desirable to use one equation to predict microbubble diameter regardless of generator configuration, it was necessary to normalize the plots depicted in Figures 4.2 and 4.3. It was discovered that the resultant curves could be normalized by multiplying the dimensionless ratio of D_b/D by the mixer constant (K). The curve normalization is shown on a standard linear grid in Figure 4.4 and on a log-log grid in Figure 4.5.

Since the mixer constant (K) is also needed to predict bubble diameter in addition to predicting pressure drop across an in-line microbubble generator, it was

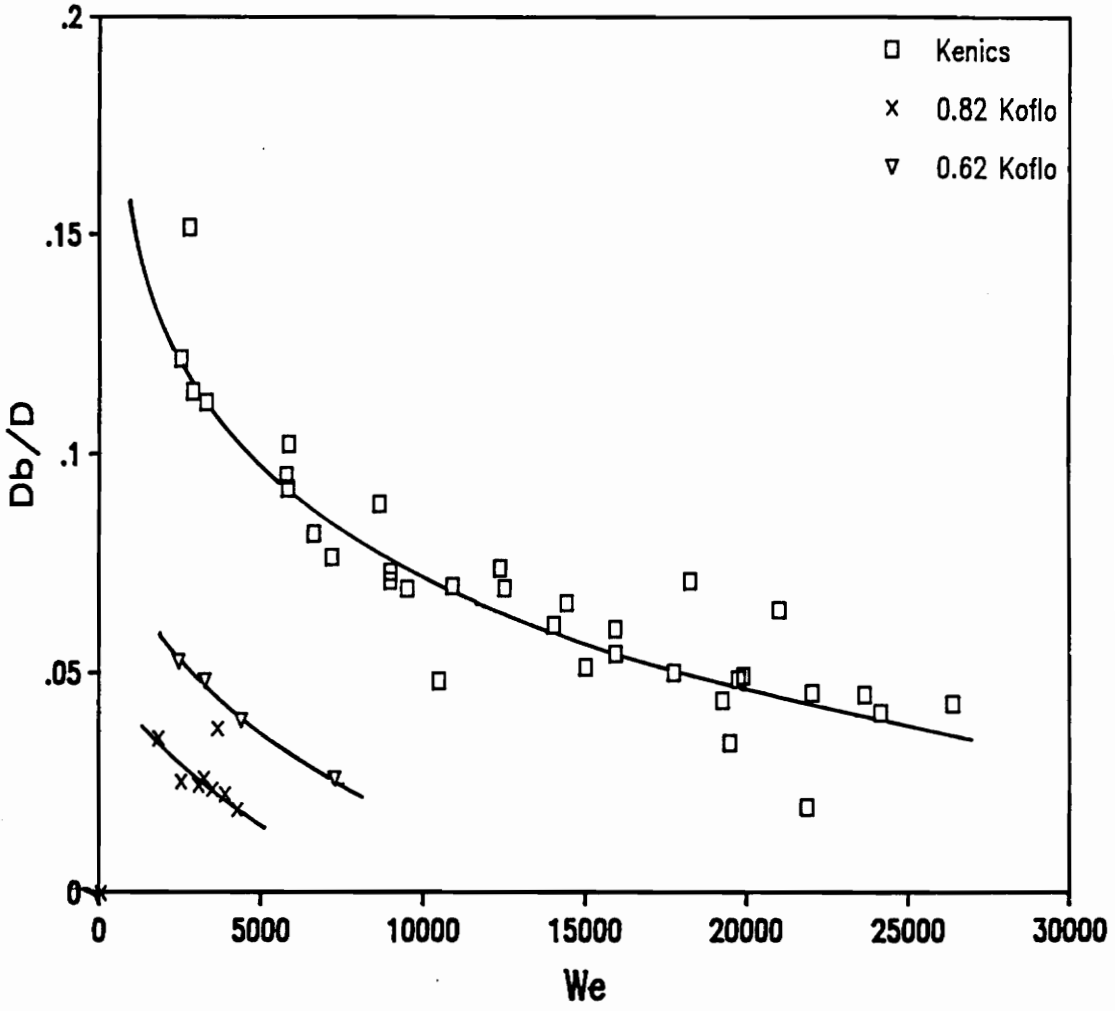

Figure 4.2 Normalized volume mean bubble diameter versus Weber number (We) for various element configurations at 10% air.

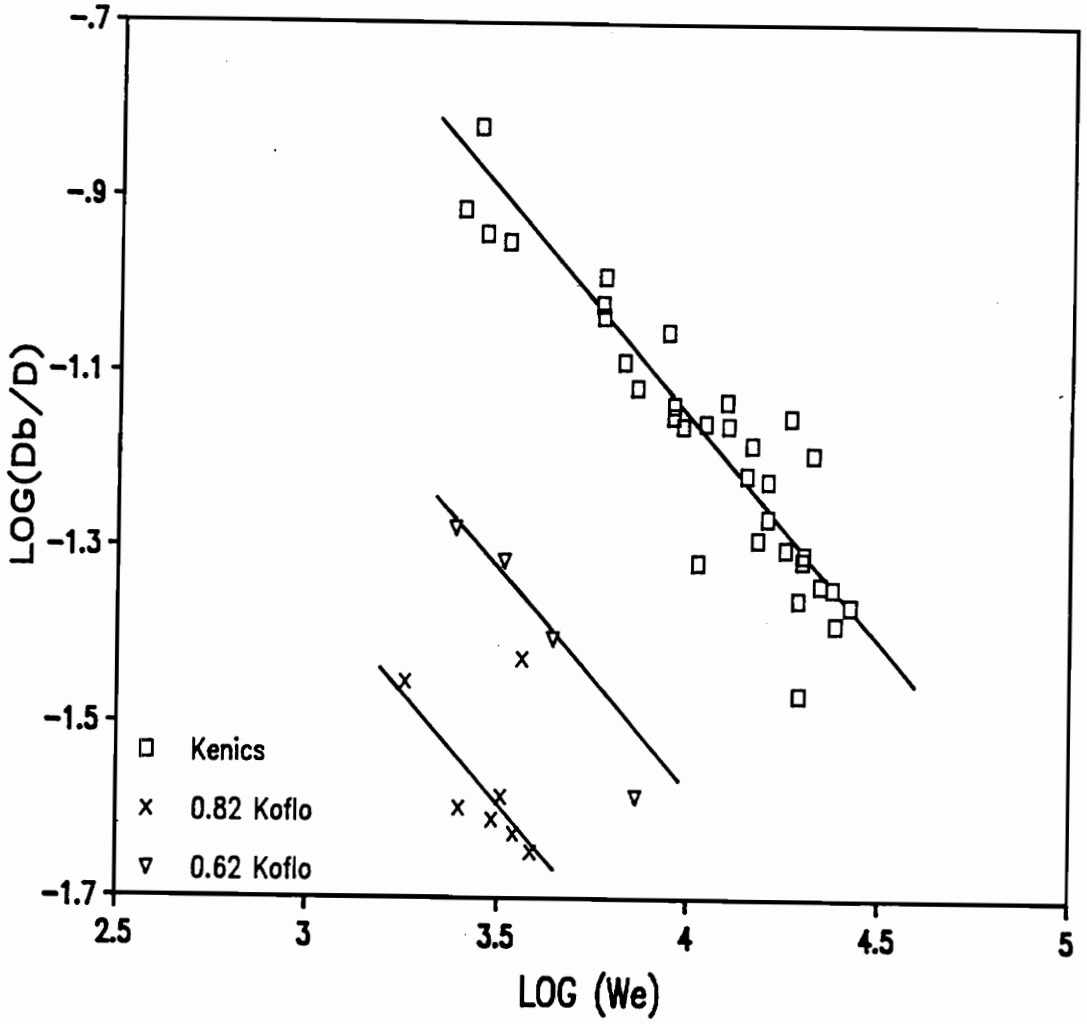

Figure 4.3 Normalized volume mean bubble diameter versus Weber number (We) for various element configurations at 10% air.

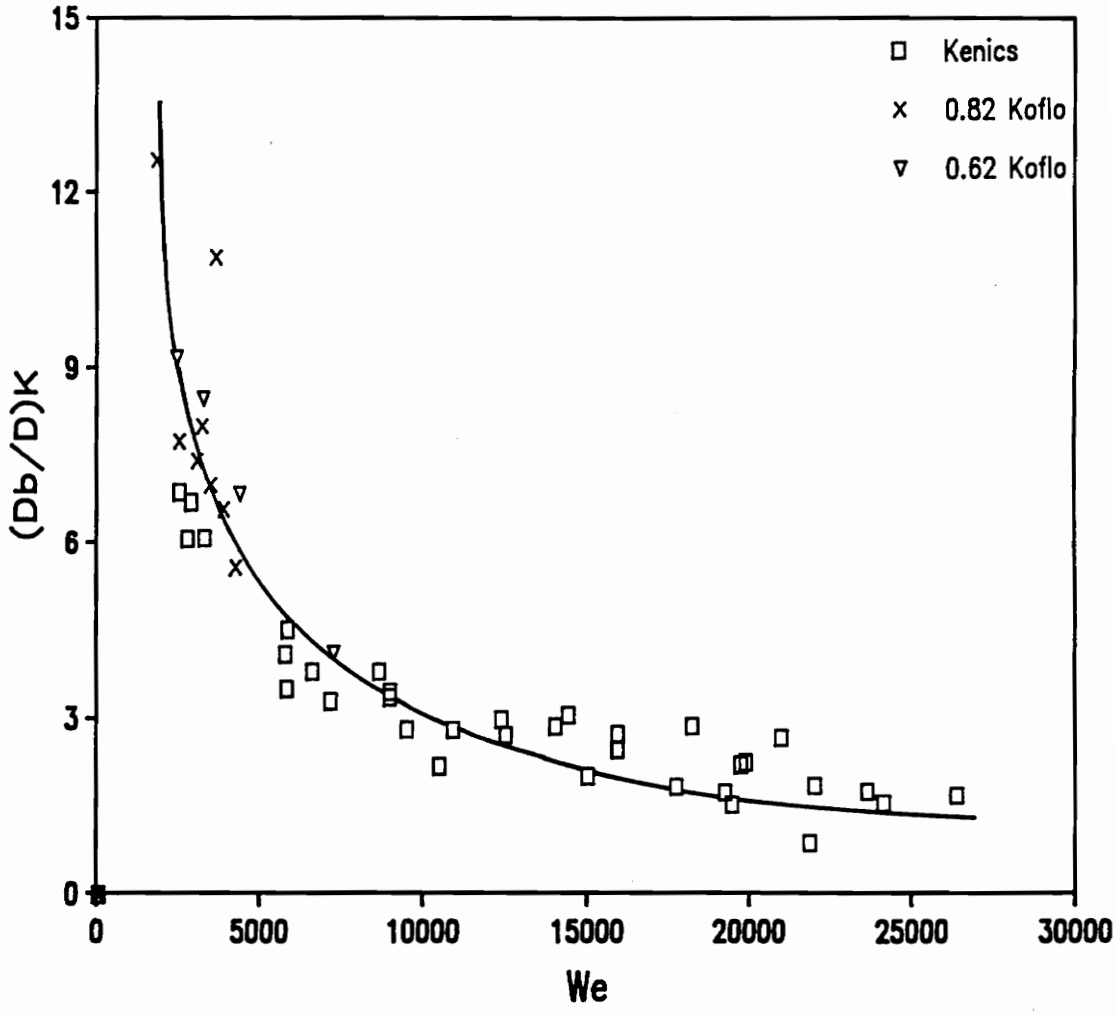

Figure 4.4 Normalized volume mean bubble diameter (corrected) versus Weber number (We) for various element configurations at 10% air.

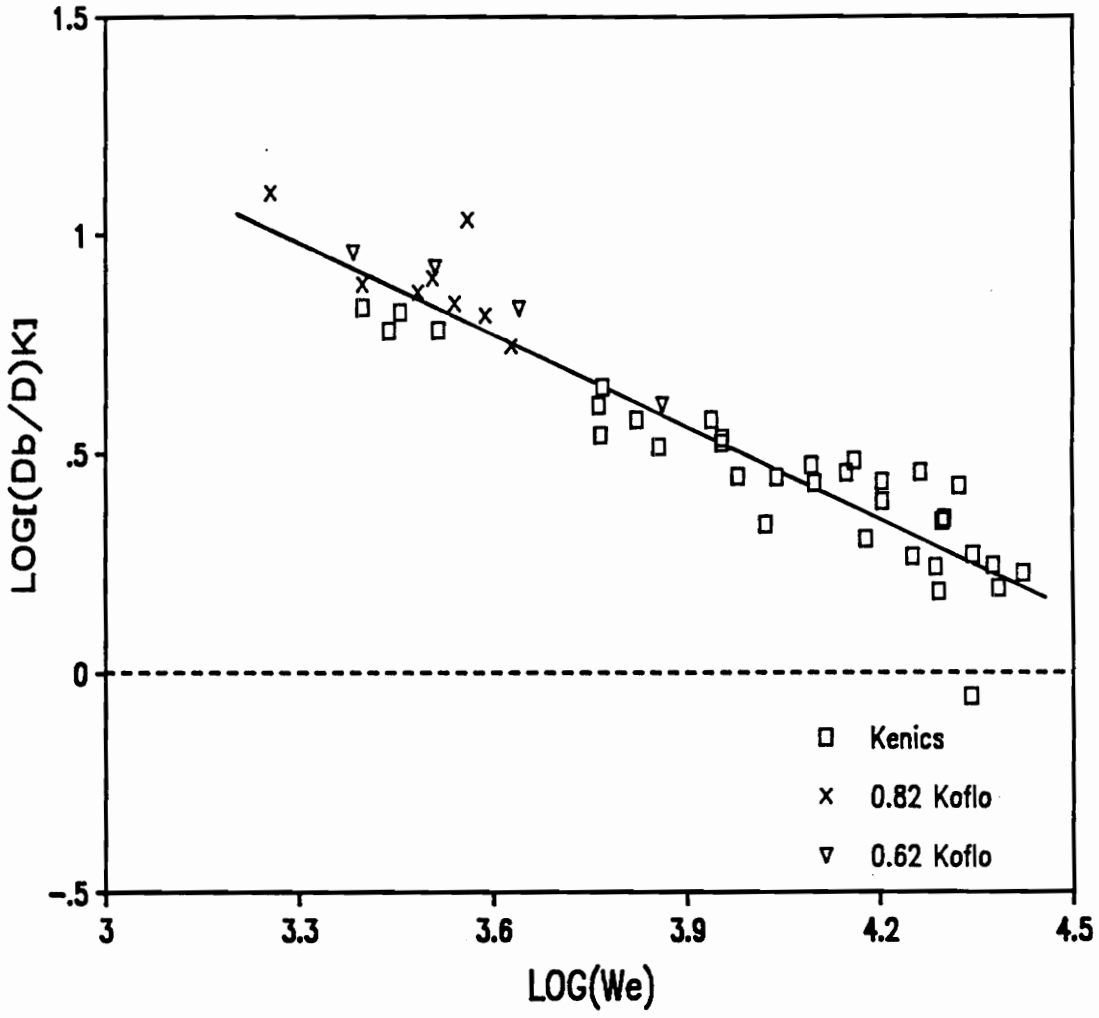

Figure 4.5 Normalized volume mean bubble diameter (corrected) versus Weber number (We) for various element configurations at 10% air.

necessary to determine if K remains constant when bubble diameter is changed. Examination of a plot of D_b/D versus K, shown in Figure 4.6, demonstrates that K does in fact remain constant when bubble diameter changes. Therefore, it was possible to develop an equation for bubble diameter prediction which utilizes the generator constant (K) as a normalization factor.

Using the expressions determined above, an equation for predicting the volume weighted mean bubble diameter was developed. The proportionality constant, A, and the power exponent, f, from Equation [4.21] was determined by performing a least squares fit on the data presented in Figure 4.5. This procedure yielded the following expression:

$$D_b = \frac{2190\ D}{K\ We^{.71}} \qquad [4.22]$$

in which all units are in the cgs system. Equation [4.22] should be useful for predicting the volume weighted mean bubble diameter produced by various types of in-line microbubble generators. In order to use this expression, the generator diameter (D), mixer constant (K) and Weber number (We) must be calculated. The value of K can be determined from experimental measurements or from pressure-flow data provided by the manufacturer of the in-

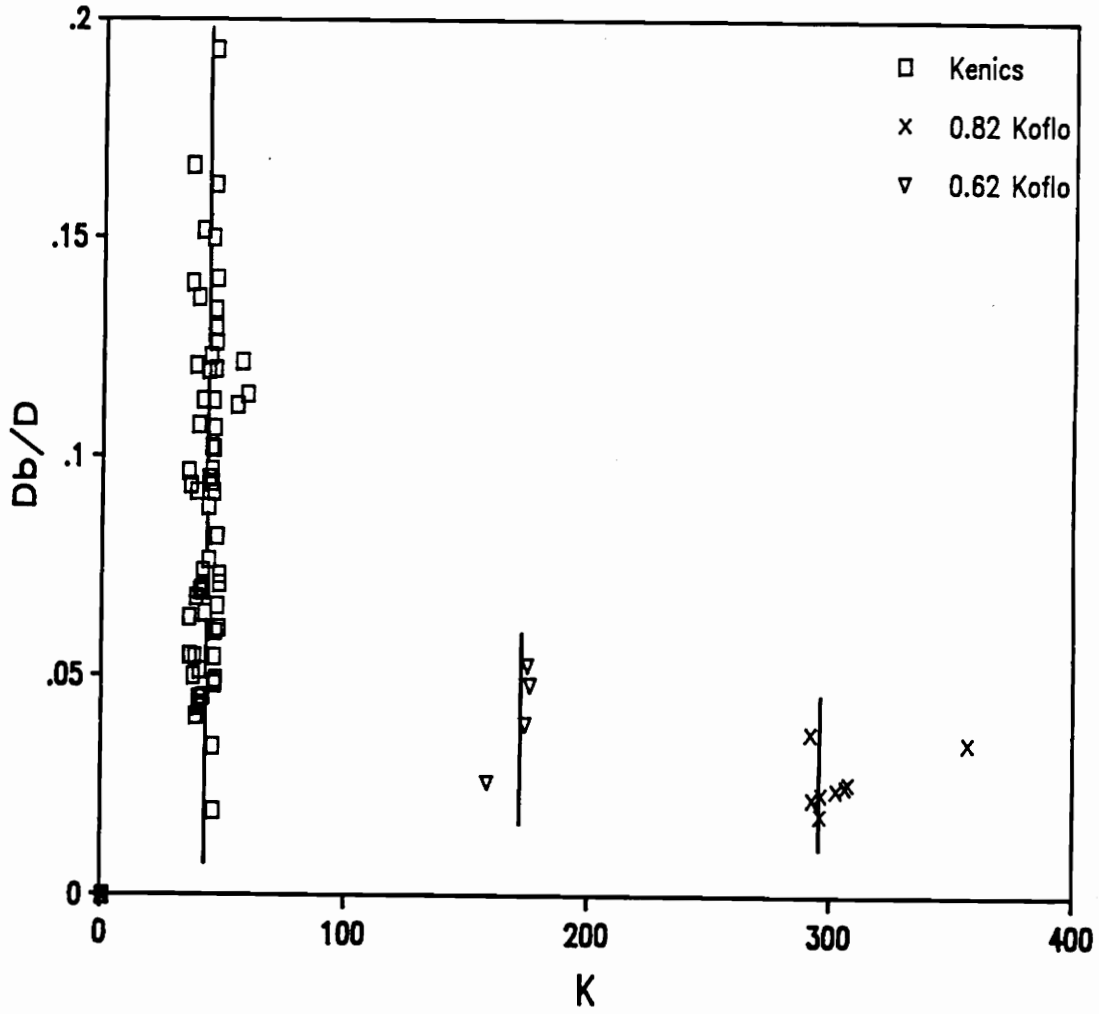

Figure 4.6 Normalized volume mean bubble diameter versus K for all mixers under various air fractions and operating conditions.

line mixer.

It should be noted that the equations derived for predicting microbubble diameter were produced from data collected with the units operating at an air content of 10% by volume. Test work conducted at higher air contents indicate that the data scatter becomes more pronounced as the air content is increased. This phenomenon is shown in Figures 4.7 and 4.8 for air contents of 10% and 20% air by volume. Also, many of the points fall above those generated for the tests conducted at 10% air. This phenomenon is probably due to data bias in favor of the larger bubbles generated at the higher air content. The bias in sizing is due to the fact that smaller bubbles are frequently hidden from view by the larger bubbles in the viewing cell. This tends to bias the mean bubble size in favor of the larger bubbles. As expected, this problem becomes more pronounced at the higher air fractions. Therefore, the data collected at 10% air were used to develop the equations for predicting bubble diameter.

4.3 Centrifugal Pump Performance Prediction

The final step required to quantify the behavior of the microbubble generation circuit was the prediction of centrifugal pump performance under air admitting conditions. As shown previously in Figure 3.20, entrained air adversely impacts the performance of a centrifugal

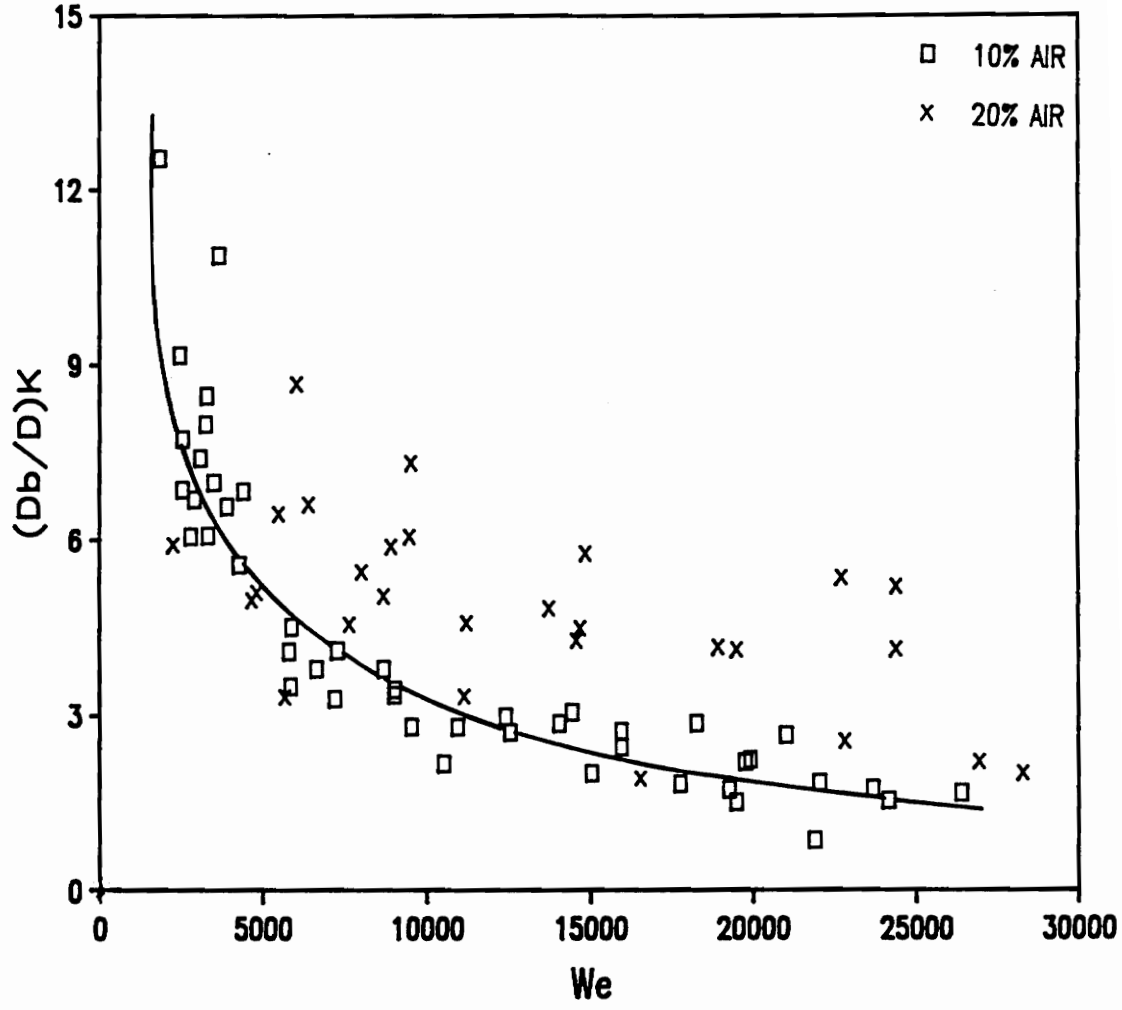

Figure 4.7 Normalized volume mean bubble diameter versus Weber number for all mixers under various air fractions and operating conditions.

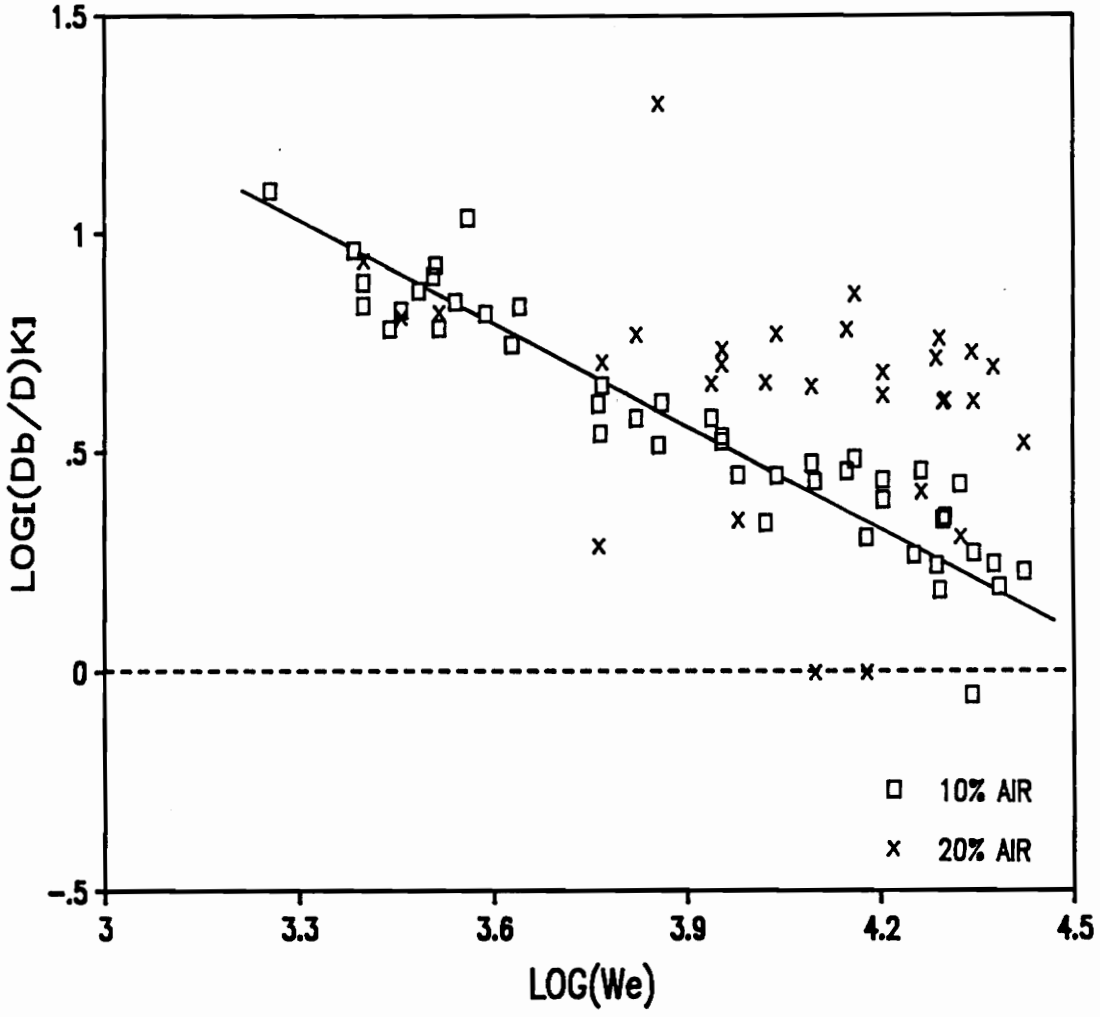

Figure 4.8 Normalized volume mean bubble diameter versus Weber number for all mixers under various air fractions and operating conditions.

pump. Therefore, an understanding of the degradation in pump performance due to the entrainment of air is necessary in order to properly select a pump for a given microbubble generation circuit.

In terms of pump performance and design, it is generally convenient to depict pressure-flow performance curves for pumps using normalized head and flow coefficients. These factors allow for the plotting of the performance characteristics of all pumps, regardless of sizes or capacities, relative to a theoretical or ideal performance curve. The normalized performance curves consist of a head coefficient, ψ, and a flow coefficient, ϕ. The definition of the normalized head coefficient is:

$$\psi = g\Delta H/u^2 \qquad [4.23]$$

where g is the acceleration due to gravity, ΔH the head loss across the pump, and u is the tangential velocity of the pump impeller. The definition of the normalized flow coefficient is:

$$\phi = C_m/u \qquad [4.24]$$

where C_m is the radial component of the fluid velocity.

Velocity triangles representing Equations [4.23] and [4.24] are shown graphically in Figure 4.9 (after Karassik et al., 1976). The velocity components at the

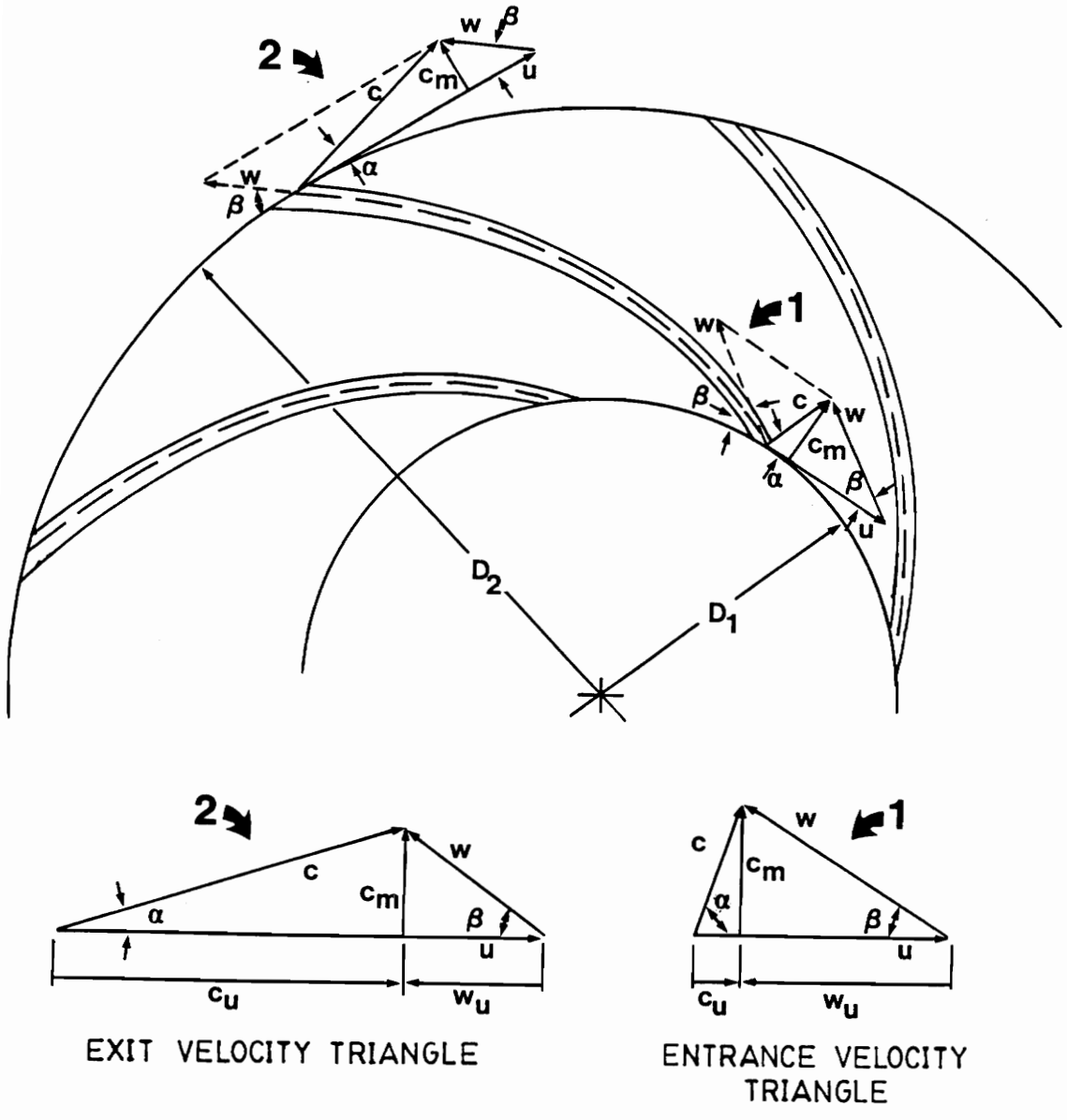

Figure 4.9 Entrance and exit velocity triangles relative to a centrifugal pump impeller as depicted by Karassik et al. (1976).

pump inlet are generally neglected, since they are of much smaller magnitude than those present at the pump outlet. Hypothetical pump performance curves are plotted in normalized form in Figure 4.10. The theoretical or ideal pump performance is denoted by the characteristic curve that forms a straight line from a value of 1 for head coefficient to a value of 1 for flow coefficient.

4.3.1 Performance Prediction Model

The two-phase pump performance model proposed by Mikielewicz, et al. (1978) utilizes the theoretical- and single-phase performance curves to predict two-phase pump performance. The model developed in this study was a slightly modified form of the one proposed by Mikielewicz et al. (1976) in which the angle of the fluid vector relative to the tangent to the impeller periphery was considered. However, this angle was not considered in the model used in this study since it was determined that theoretical performance could be defined without it.

For a given flow range, the two-phase head coefficient (ψ_{tp}) is determined by the theoretical (ψ_{th}) and single-phase (ψ_{sp}) head coefficients. These values are generally related through the use of a combined head loss ratio (H^*) which is given by:

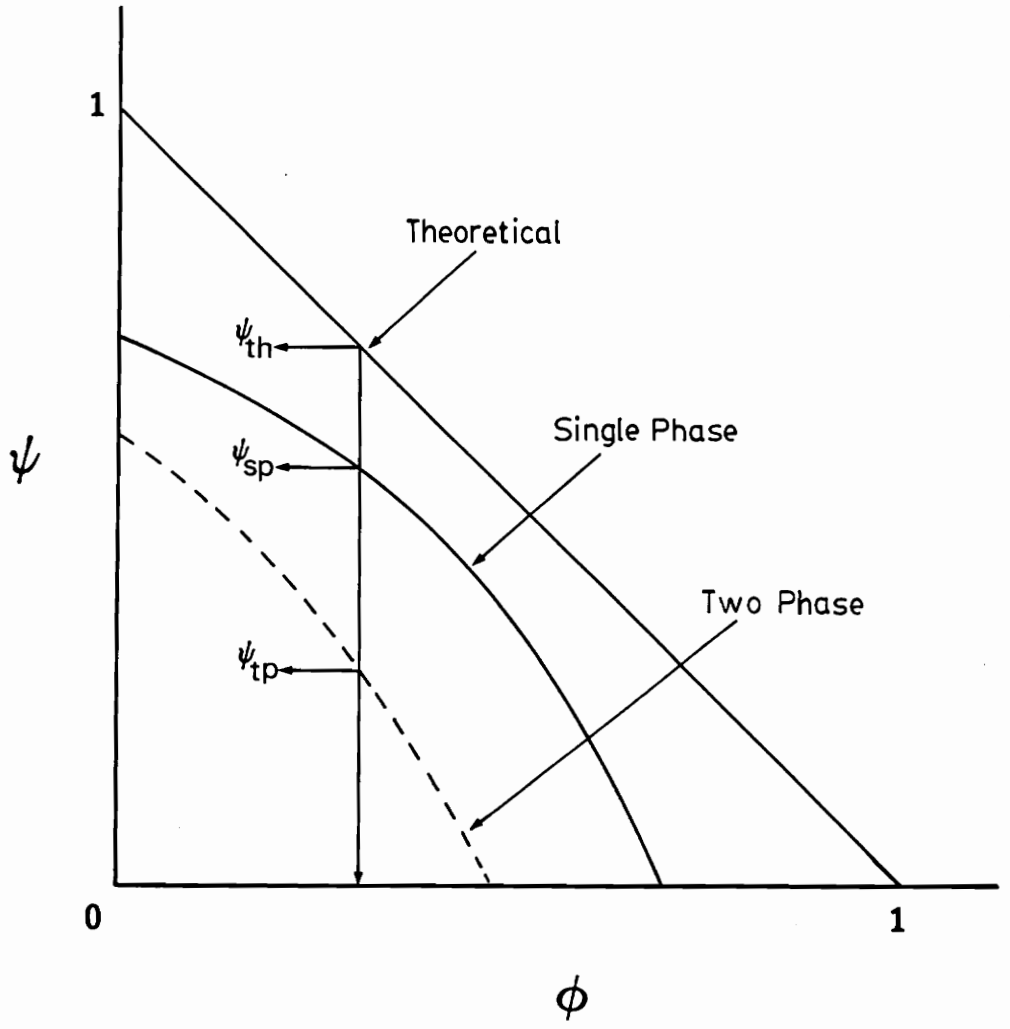

Figure 4.10 Normalized pump performance curves showing hypothetical single- and two-phase curves relative to the theoretical performance curve.

$$H^* = \frac{\psi_{th} - \psi_{tp}}{\psi_{th} - \psi_{sp}} \qquad [4.25]$$

where the subscripts denote:

th = theoretical
tp = two-phase, and
sp = single phase.

The head loss ratio is primarily a function of air fraction, but may also be dependent on flow coefficient values in some cases.

The head loss ratio was determined for a wide range of air fractions and flow coefficients. The data was collected by monitoring the two-phase performance a Teel Model 1P797A centrifugal pump driven by a variable-speed electric motor. The results of these calculations are shown in Figure 4.11. For low air fractions, H^* approached unity regardless of the flow rate. This indicates that for low air fractions the two- and single-phase performance curves are identical. As the air fraction increased, H^* increased in a corresponding fashion. The onset of this increase varied depending on the flow coefficient. In general, the degradation in pump performance under two-phase flow conditions occurred at a lower air fraction as the pump flow rate increased.

The values of H^* given in Figure 4.11 allow the pressure-flow curves to be predicted for other centrifugal

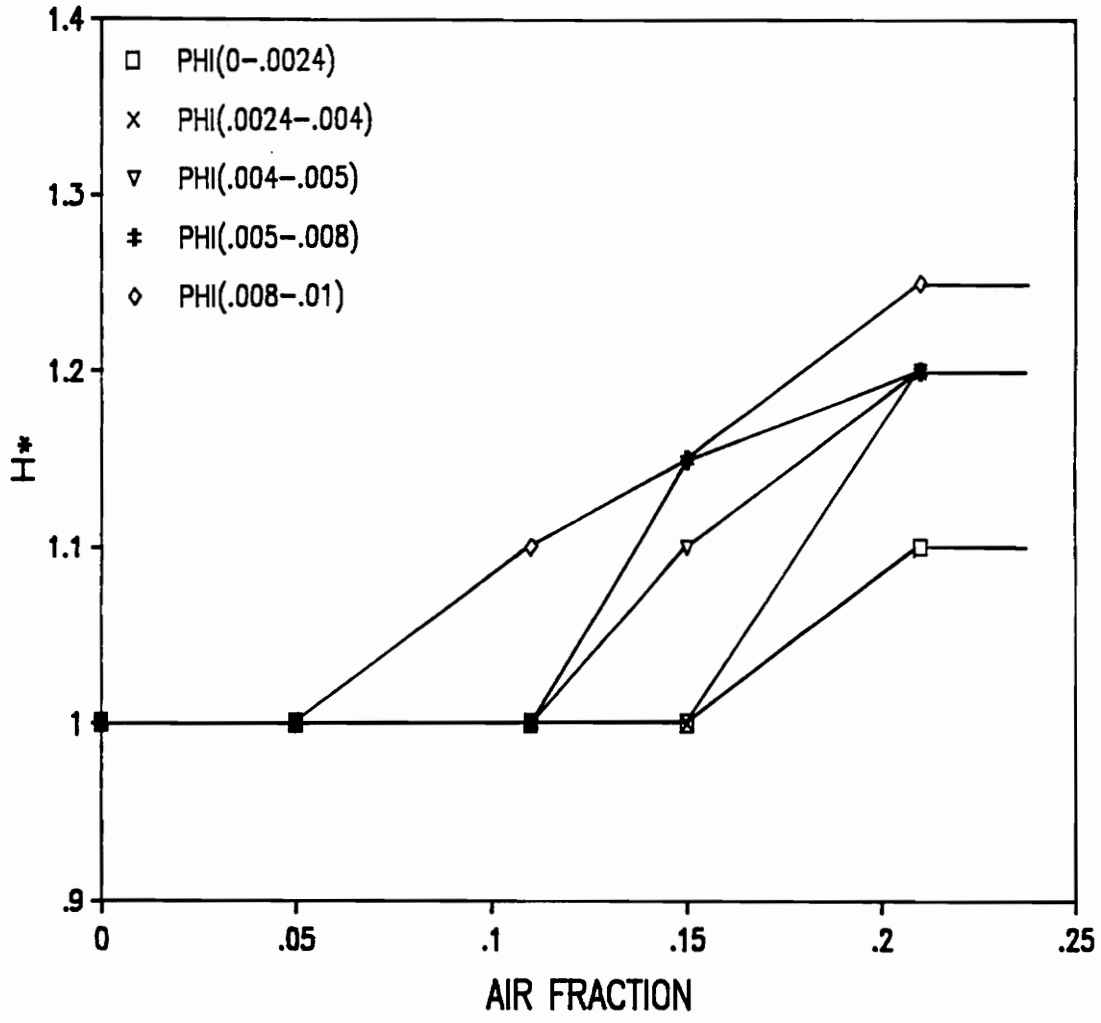

Figure 4.11 Head loss ratio versus air fraction for various flow coefficients (ϕ) for a Teel centrifugal pump (Model 1P797A).

pumps of similar configuration, but of differing size. This is accomplished by rearranging Equation [4.25] as follows:

$$\psi_{tp} = \psi_{th} - (\psi_{th} - \psi_{sp})H^* \qquad [4.26]$$

Thus, in order to predict two-phase flow performance, the theoretical performance curve is determined for the pump in question. The single-phase performance curve is determined experimentally or supplied by the pump manufacturer. These curves are then used to determine ψ_{th} and ψ_{sp} for a given flow coefficient. H^* can be be determined from Figure 4.11 if the appropriate air fraction and flow coefficient are known. Once these values have been determined, Equation [4.26] can then be used to predict the pump performance under two-phase conditions.

4.3.2 Model Validation

In order to determine the validity of the two-phase pump model, it was necessary to use it to predict performance characteristics of a pump of different size when it was operating under air admitting conditions. The pump used for model verification was a Teel model 1P796A centrifugal pump. This pump was similar in configuration to the model 1P797A, but smaller in size.

After the single-phase characteristic curve was determined for the pump used for model verification, head loss ratios were determined from Figure 4.11. These values were used to predict two-phase performance for various values of flow coefficient. The results of this comparison are illustrated in Figure 4.12. The theoretical, single-phase, actual two-phase, and predicted two-phase performance characteristic curves are shown. The two-phase curve depicts the performance of the pump operating at 15% air. As shown, the agreement between the predicted and measured two-phase performance curves is quite good.

It can be concluded that the model used in this study can be used to adequately approximate the performance degradation of a centrifugal pump operating under air admitting conditions from single-phase performance characteristics. Single-phase performance curves are supplied by pump manufacturers. It should be noted that the head curves for head loss ratio as a function of air fraction and flow coefficient must be developed from a pump of similar configuration (e.g., similar impeller and casing design) in order to obtain reasonable predictions.

4.4 Microbubble Circuit Scale-Up Procedure

The scale-up procedure for the microbubble generation circuit can be outlined as follows:

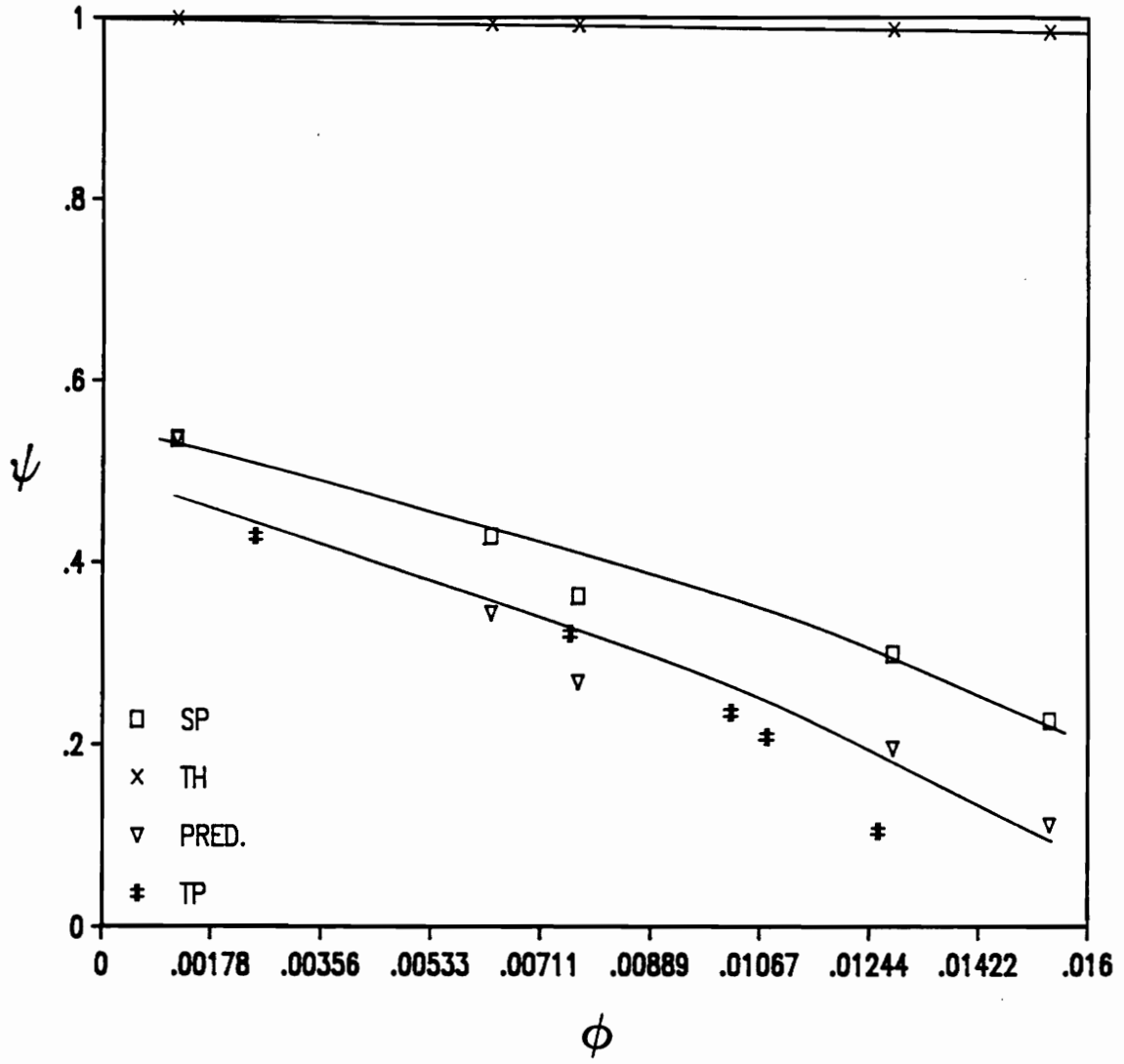

Figure 4.12 Normalized performance curves for a Teel centrifugal pump depicting theoretical single-, two- and predicted two-phase performances at 15% air.

1. The volume mean bubble diameter required for a particular situation is determined from laboratory testing.

2. The volumetric gas flow is determined from the required superficial gas velocity as determined in the flotation column scale-up procedure.

3. The density and surface tension of the continuous phase of the medium used for bubble generation is determined by laboratory testing.

4. The amount of air recirculated by the centrifugal pump used for bubble generation is determined by laboratory testing.

5. The type and size (length and diameter) of an in-line microbubble generator is selected and one unit is obtained for laboratory testing. The generator constant (K) is determined by dividing measured pressure drop by the pressure drop calculated for a smooth pipe of the same dimensions over a range of volumetric flow rates.

6. The total volumetric flow of gas and liquid required for bubble generation is determined. The gas content of the fluid passing through the generators

is kept below 15% in order to prevent "slugging".

7. The fluid velocity required through each generator is calculated using Equation [4.22].

8. The appropriate number of generators is selected such that the velocity through each is approximately the value calculated in step 7, since the generators will be installed in a parallel configuration.

9. If the number of generators is excessive, the entire procedure is repeated using generators of slightly larger size.

10. The procedure described in Section 4.3 is utilized to predict centrifugal pump performance so as to allow for the selection of a pump that can meet required pressure and flow values. The head losses that result from plumbing configuration as well as the generator pressure drop calculated in step 5 must be accounted for when selecting a pump. Laboratory testing of a smaller version of the pump to be used may be required in order to determine head loss ratios for performance prediction.

It should be noted that the scale-up procedure detailed in the present work is based on a two-phase (gas

and liquid) system only. In nearly all mineral systems, a three-phase (gas, liquid, and solid) situation exists. It was felt, however, that in the case of coal processing the two-phase basis will allow for sufficient scale-up for most industrial applications. This assumption is based on the low solids content of the material being circulated by the centrifugal pump used for bubble generation. The processing of extremely fine particles at high solids content will most likely require modifications to the procedure to allow for viscosity effects. These modifications should be quite easy to make with a minimum of additional laboratory work.

CHAPTER 5

SUMMARY AND CONCLUSIONS

The flotation tests conducted in the present work demonstrate that the microbubble column flotation process is an attractive method for the upgrading of fine particles. This capability has been verified for size classes ranging from a topsize of 28 mesh to below approximately 5 microns. The process has the capability to concentrate feed materials that can not be processed by conventional flotation machines. In the present work, this capability was best demonstrated for the upgrading of the refuse coal samples supplied by various industrial groups. These coals could not be effectively treated using conventional froth flotation due to the presence of disproportionate amounts of ultrafine clay minerals. Nevertheless, all of the refuse samples were successfully upgraded by the microbubble column flotation process.

The major contribution of the present work was the development of relationships which describe the behavior of the bubble generation circuit utilized by the microbubble column flotation process. The scale-up procedure for the microbubble generation circuit provides equations for determining the pressure drop across the generator as well as a means for predicting the volume mean bubble diameter. Expressions were also developed to

describe the operating behavior of a centrifugal pump under air admitting conditions. A step-by-step procedure has been outlined which describes how these expressions can be used to select the proper size, number and type of microbubble generators, as well as the appropriate centrifugal pump, for a given application. This procedure eliminates the need for trial-and-error experimental testing which was required prior to the completion of this work.

CHAPTER 6

RECOMMENDATIONS FOR FUTURE WORK

From the information gathered in the present study, further research into the following areas is recommended:

1. The scale-up procedure for the microbubble generation circuit should be tested on a pilot-scale before being applied to industrial situations. This test work could be used to validate the assumption that the scale-up can be applied on a two-phase flow basis.

2. A scale-up procedure allowing for the viscosity effects that would undoubtedly be present in systems containing unusually fine particle sizes and high solids contents should be developed. This would then allow the microbubble generation circuit scale-up procedure to be applied to mineral systems in which pulp solids contents are higher than for coal flotation systems.

3. The operating conditions in which "slugging" occurs in microbubble generators should be investigated in greater detail. "Slugs" of air exit the microbubble generators when operating conditions do not allow for proper dispersion of the gas phase. The

conditions under which the gas phase is not properly dispersed need further quantification.

4. Numerous types of static mixing devices are in existence and many may be suitable for use as microbubble generators. It is recommended that additional types of generators be tested in order to further evaluate the scale-up procedure outlined during this study.

REFERENCES

Bogdanov, O.S., Emelyanov, M.F., Maximov, I.I., and Otrozhdennova, L.A., "Influence of Some Factors on Fine Particle Flotation," Fine Particles Processing, Vol. 1 (P. Somasundaran, ed.), AIME, New York, 1980.

Bor, T., "The Static Mixer as a Chemical Reactor," British Chemical Engineering, July, 1971.

Boss, J. and Czastkiewicz, W., "Principles of Scale-Up for Laminar Mixing Processes of Newtonian Fluids in Static Mixers," International Chemical Engineering, Vol. 22, No.2, April, 1982.

Chemineer, Water/Wastewater Technical News, Vol. 2, No. 1, 1986.

Chen, S.J. and Macdonald, A.R., "Motionless Mixers for Viscous Polymers,"Chemical Engineering, March 19, 1973.

Chen, S.J., "Inline, Continuous Mixing and Processing - A New Approach," First European Conference on Mixing and Centrifugal Separation, Septermber, 1974.

Chen, S.J. and Gilbert, G.R., "Mass Transfer and Mixing in the Kenics Aeration System," Water - 1976: II. Biological Wastewater Treatment, AICHE Symposium Series, No. 167, Vol. 73, 1976.

Deister, Deister Flotaire Column Flotation Cells Information Brochure.

Federighi, R.P. and Federighi, F.F., U.S. Patent 4511258, April, 1985.

Furstenau, D.W., "Fine Particle Flotation," Fine Particles Processing, Vol. 1 (P. Somasundaran, ed.), AIME, New York, 1980.

Furuya, O., "On Performance of Two-Phase Flow Pumps," Cavitation and Multiphase Flow Forum - 1984, ASME, New York, 1984.

Gilbert, G.R. and Libby, D., "Field Testing for Oxygen Transfer and Mixing in Static Mixer Aeration Systems," Kenics Technical Report, Presented at the 32nd. Purdue Industrial Waste Conference, May 10, 1977.

Giles, R.V., Theory and Problems of Fluid Mechanics and Hydraulics, 2nd. Ed., Schaum's Outline Series, McGraw - Hill Book Co., New York, 1962.

Grosz-Roll, F., Battig, J., and Moser F., "Gas/Liquid Mass Transfer with Static Mixing Units," Fourth European Conference on Mixing, April 27 - 29, 1982.

Karassik, I.J., Krutzsch, W.C., Fraser, W.H., and Messina, J.P., Pump Handbook, McGraw - Hill Book Co., New York, 1976.

Killmeyer, R.P., Hucko, R.E., and Jacobsen, S., "Interlaboratory Comparison of Advanced Froth Flotation Processes," Presented at the AIME Annual Meeting, Las Vegas, Nevada, February 27 - March 2, 1989.

Kim, J.H., "Perspectives on Two-Phase Flow Pump Modeling for Nuclear Reactor Safety Analysis," Cavitation and Multiphase Flow Forum - 1983, ASME, New York, 1983.

Kim, J.H., "A Formulation for Two-Phase Flow Dynamics in Centrifugal Pump," Cavitation and Multiphase Flow Forum - 1984, ASME, New York, 1984.

Kim, J.H. and Duffey, R.B., "On Centrifugal Pump Head Degradation in Two-Phase Flow," Design Methods for Two-Phase Flow in Turbomachinery, FED - Vol. 26 (W.F. Wade and M.C. Roco, ed.), Presented at the ASCE/ASME Mechanics Conference, Albuquerque, NM, June 24 - 26, 1985.

Leja, J., Surface Chemistry of Froth Flotation, Plenum Press, New York, 1982.

Luttrell, G.H., PhD Dissertation, Dept. of Mining and Minerals Engineering, Virginia Polytechnic Institute and State University, Blacksburg, VA, 1986.

Luttrell, G.H., Weber, A.T., Adel, G.T., and Yoon, R.H., "Microbubble Flotation of Fine Coal," Presented at the Column Flotation Symposium during the AIME Annual Meeting, Phoenix, AZ, January 25 - 28, 1988.

Mathieu, G.I., "Comparison of Flotation Column with Conventional Flotation for Concentration of Molybdenum Ore," CIM Bulletin, 1972.

Mikielewicz, J., Wilson, D., Chan, T., and Goldfinch, A., "A Method for Correlating the Characteristics of Centrifugal Pumps in Two-Phase Flow," Journal of Fluids Engineering, Transactions of the ASME, Vol. 100, December, 1978.

Mutsakis, M., Streiff, F.A., and Schneider, G., "Advances in Static Mixing Technology," Chemical Engineering Progress, July, 1986.

Mutsakis, M. and Rader, R., "Static Mixers Bring Benefits to Water/Wastewater Operations," Water/Engineering and Management, November, 1986.

Oldshue, J.Y., Fluid Mixing Technology, Chemical Engineering, McGraw - Hill Publishing Co., New York, 1983.

Pahl, M.H. and Muschelknautz, E., "Static Mixers and their Applications," International Chemical Engineering, Vol. 22, No. 2, April, 1982.

Patel, B.R. and Rustadler, Jr., P.W., "Investigations Into the Two-Phase Flow Behavior of Centrifugal Pumps," Polyphase Flow in Turbomachinery, ASME, New York, 1978.

Roberson, J.A. and Crowe, C.T., Engineering Fluid Mechanics, 3rd. Ed., Houghton Mifflin Co., Boston, 1985.

Rohatgi, U.S., "Pump Model for Two-Phase Transient Flow," Polyphase Flow in Turbomachinery, ASME, New York, 1978.

Sebba, F., "Microfoams - An Unexploited Colloid System," Journal of Colloid and Interface Science, Vol. 35, No.4, April, 1971.

Streiff, F.A., "Adapted Motionless Mixer Design," Third European Conference on Mixing, April 4 - 6, 1979.

Suggs, J.A., M.S. Thesis, Dept. of Chemical Engineering, Virginia Polytechnic Institute and State University, Blacksburg, VA, 1987.

U.S.B.M., Column Flotation, U.S. Dept. of the Interior.

WE&M Reference Handbook, 1985.

Weber, A.T., M.S. Thesis, Dept. of Mining and Minerals Engineering, Virginia Polytechnic Institute and State University, Blacksburg, VA, 1988.

Weiss, N.L., ed., SME Mineral Processing Handbook, Vol. 1, AIME, New York, 1985.

Wilkinson, W.L. and Cliff, M.J., "An Investigation Into the Performance of a Static In-Line Mixer," Second European Conference on Mixing, March 30 - April 1, 1977.

Williams, G., "How to Buy a Static Mixer," The Chemical Engineer, October, 1984.

Wills, B.A., Mineral Processing Technology, 4th. Ed., Pergamon Press, Oxford, 1988.

Wu, M.S., Sullivan, M.E., and Yee, D.J., "The Viscosity of a Foam (Air in Water Emulsion)," Colloids and Surfaces, 12, 1984.

Yoon, R.H., "Flotation of Coal Using Microbubbles and Inorganic Salts," Mining Congress Journal, Vol. 68, No.12, 1982.

Yoon, R.H., Luttrell, G.H., Adel, G.T., and Trigg, R.D., "Cleaning of Ultrafine Coal by Microbubble Flotation," Proceedings, 1st. Annual Pittsburgh Coal Conference, Pittsburgh, PA, September, 1984.

Yoon, R.H. and Luttrell, G.H., "The Effect of Bubble Size on Fine Coal Flotation," Coal Preparation, Vol. 2, 1986.

Yoon, R.H., Adel, G.T., Luttrell, G.H., Mankosa, M.J., and Weber, A.T., "Microbubble Flotation of Fine Particles," Interfacial Phenomena in Biotechnology and Materials Processing, Elsevier Science Publishers B.V., Amsterdam, 1988.

APPENDIX I

Pressure-Flow Characteristic Curves for In-Line Microbubble Generators Used for Scale-Up and Characterization Studies

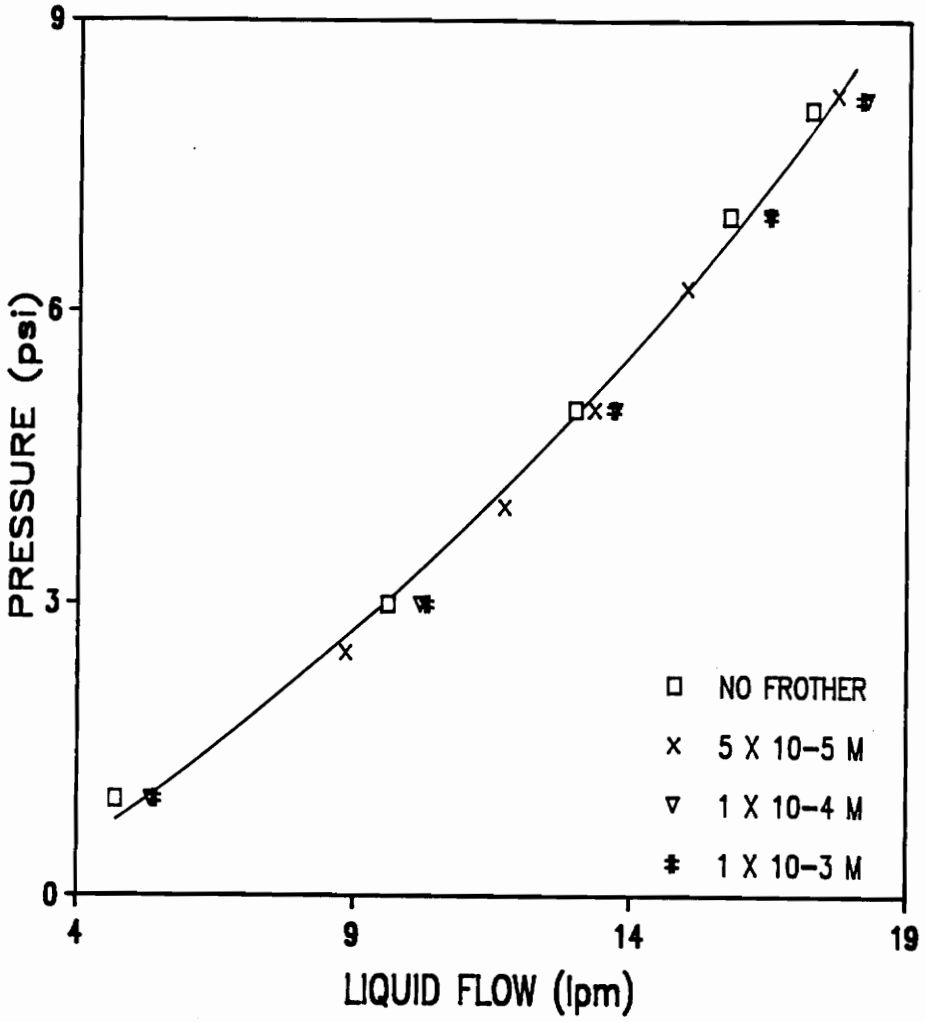

Figure A1 - Pressure versus volumetric liquid flow for a 7 element (5.25-inch length; 0.4375-inch I.D.) Kenics in-line microbubble generator at 0% air and various surfactant concentrations.

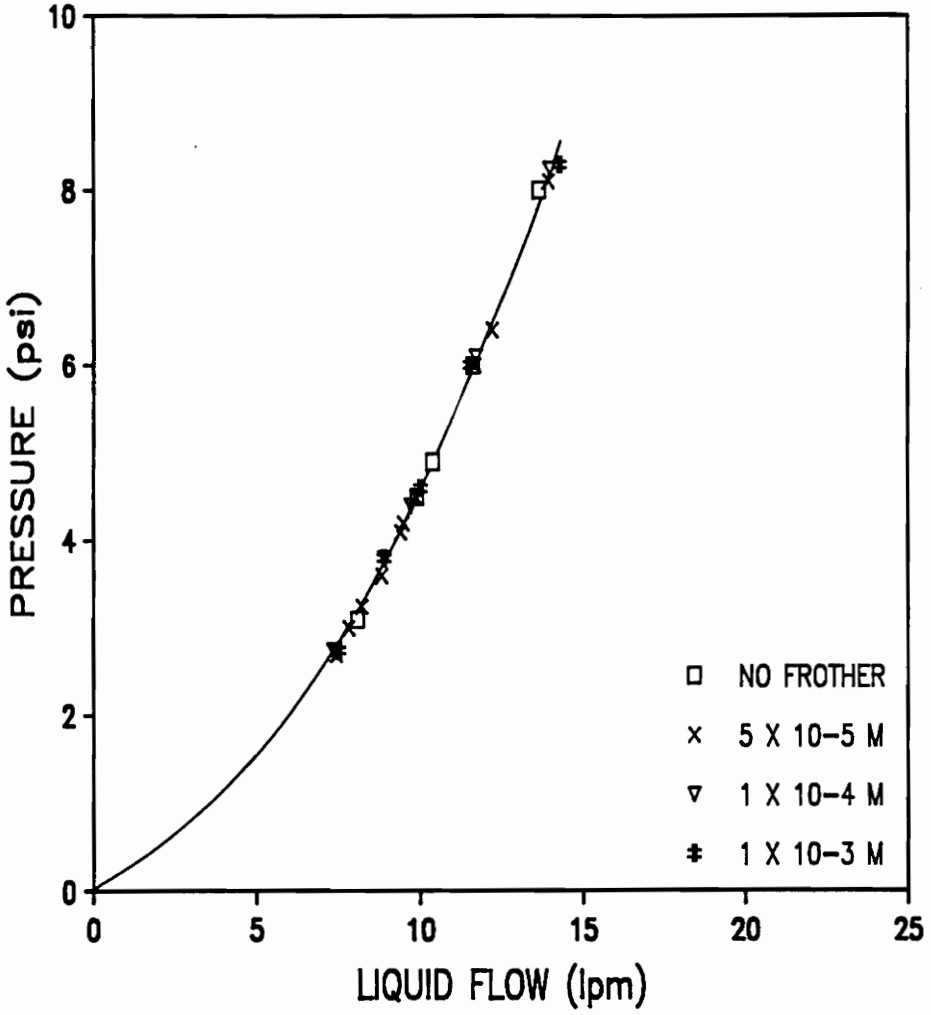

Figure A2 - Pressure versus volumetric liquid flow for a 7 element (5.25-inch length; 0.4375-inch I.D.) Kenics in-line microbubble generator at 20% air and various surfactant concentrations.

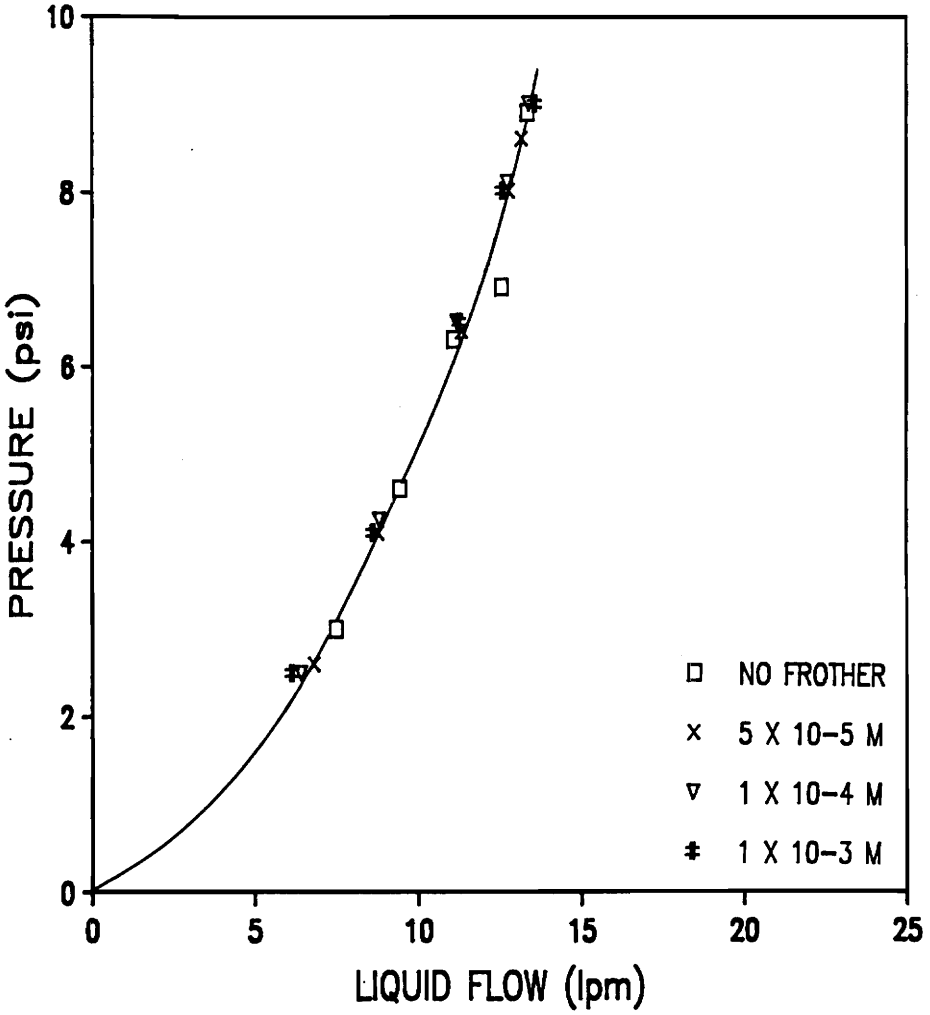

Figure A3 - Pressure versus volumetric liquid flow for a 7 element (5.25-inch length; 0.4375-inch I.D.) Kenics in-line microbubble generator at 30% air and various surfactant concentrations.

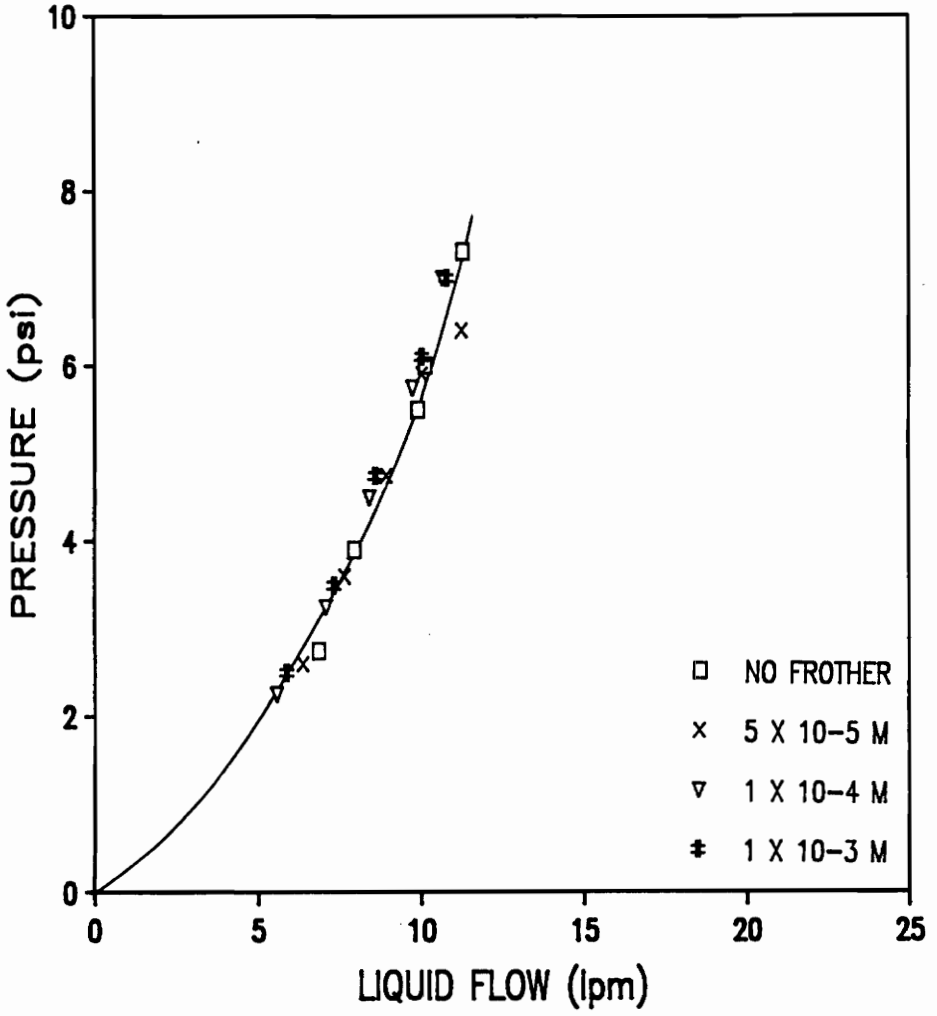

Figure A4 - Pressure versus volumetric liquid flow for a 7 element (5.25-inch length; 0.4375-inch I.D.) Kenics in-line microbubble generator at 40% air and various surfactant concentrations.

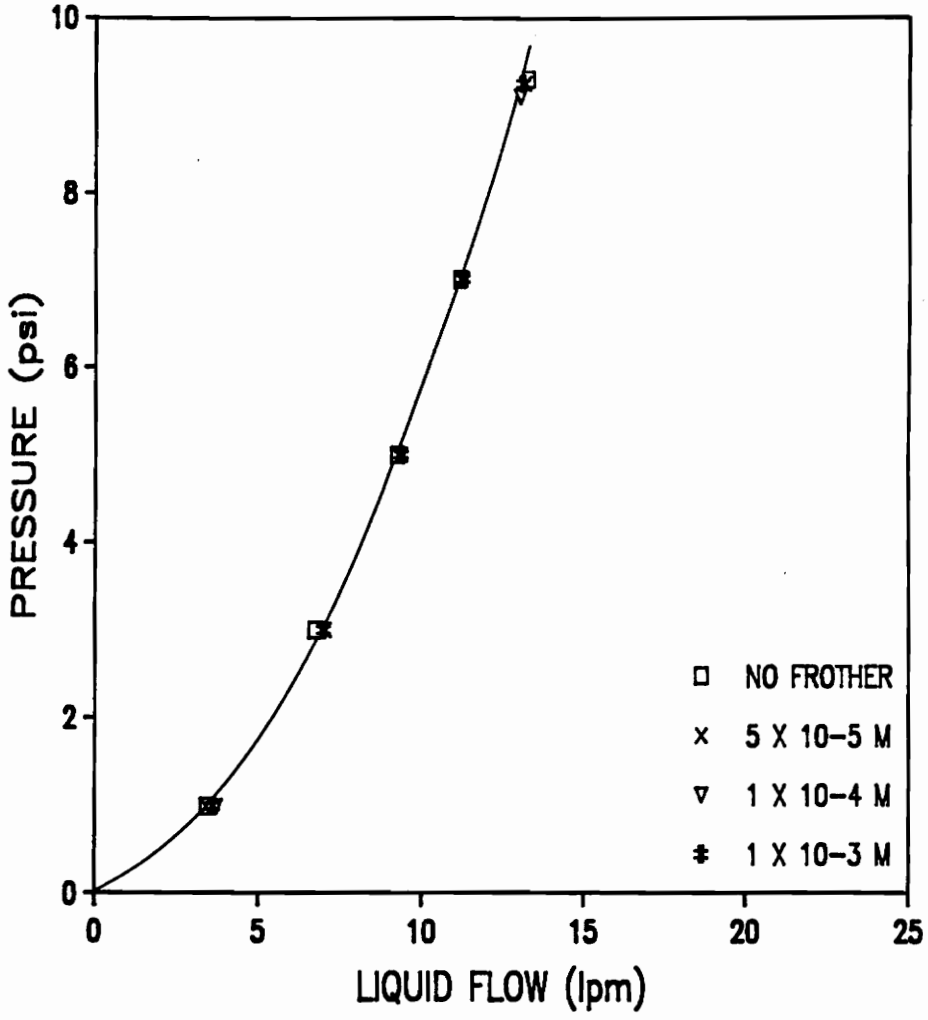

Figure A5 - Pressure versus volumetric liquid flow for a 15 element (11.25-inch length; 0.4375-inch I.D.) Kenics in-line microbubble generator at 0% air and various surfactant concentrations.

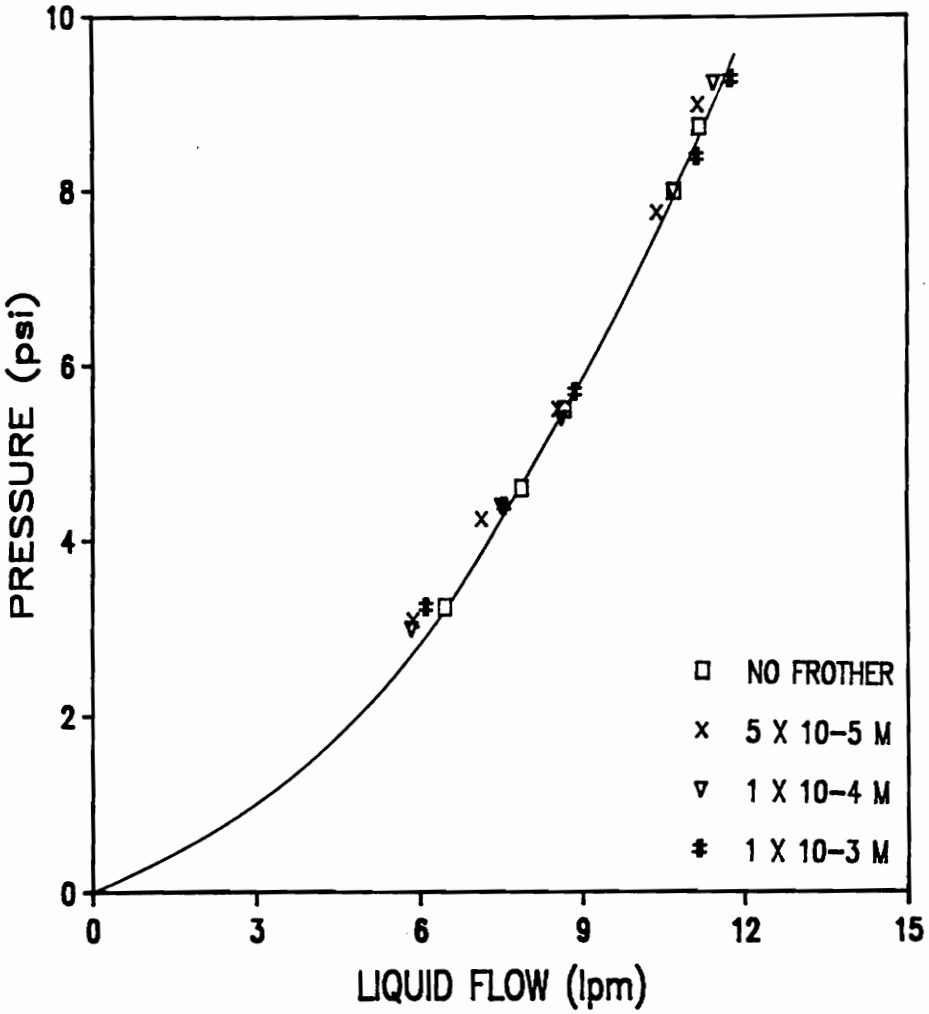

Figure A6 - Pressure versus volumetric liquid flow for a 15 element (11.25-inch length; 0.4375-inch I.D.) Kenics in-line microbubble generator at 10% air and various surfactant concentrations.

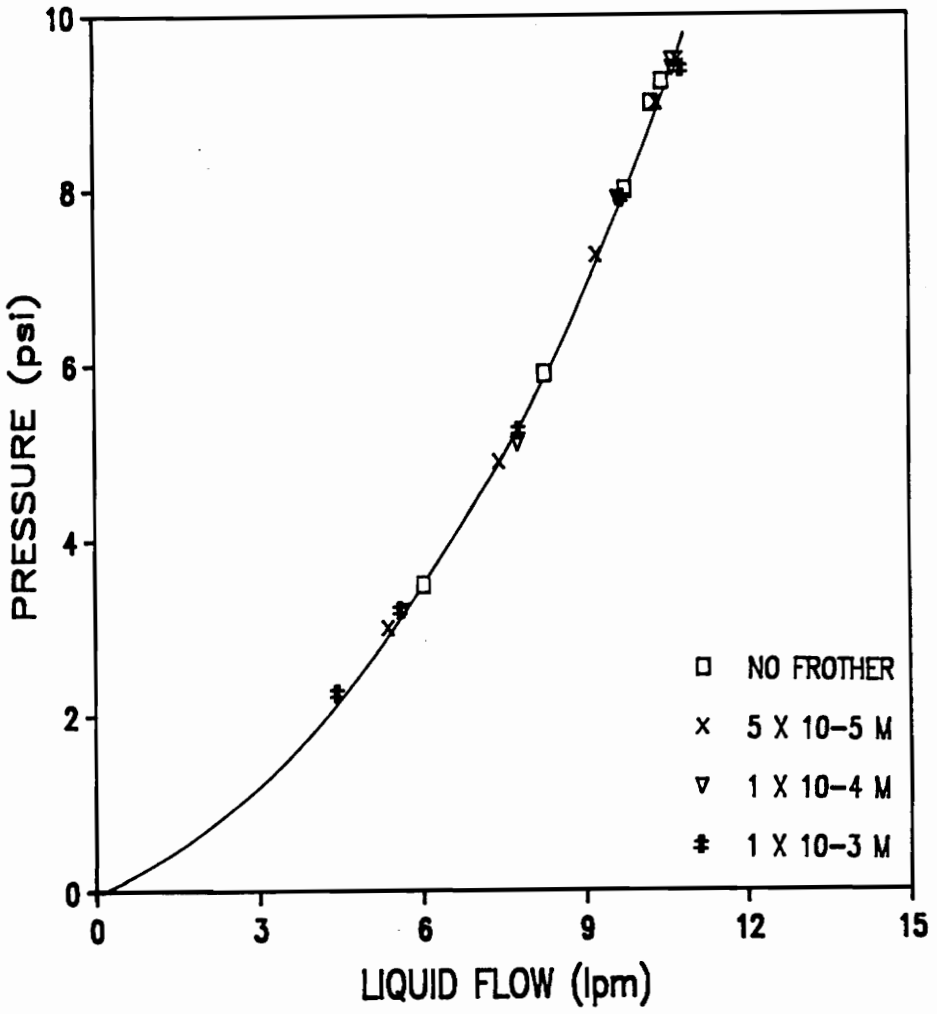

Figure A7 - Pressure versus volumetric liquid flow for a 15 element (11.25-inch length; 0.4375-inch I.D.) Kenics in-line microbubble generator at 20% air and various surfactant concentrations.

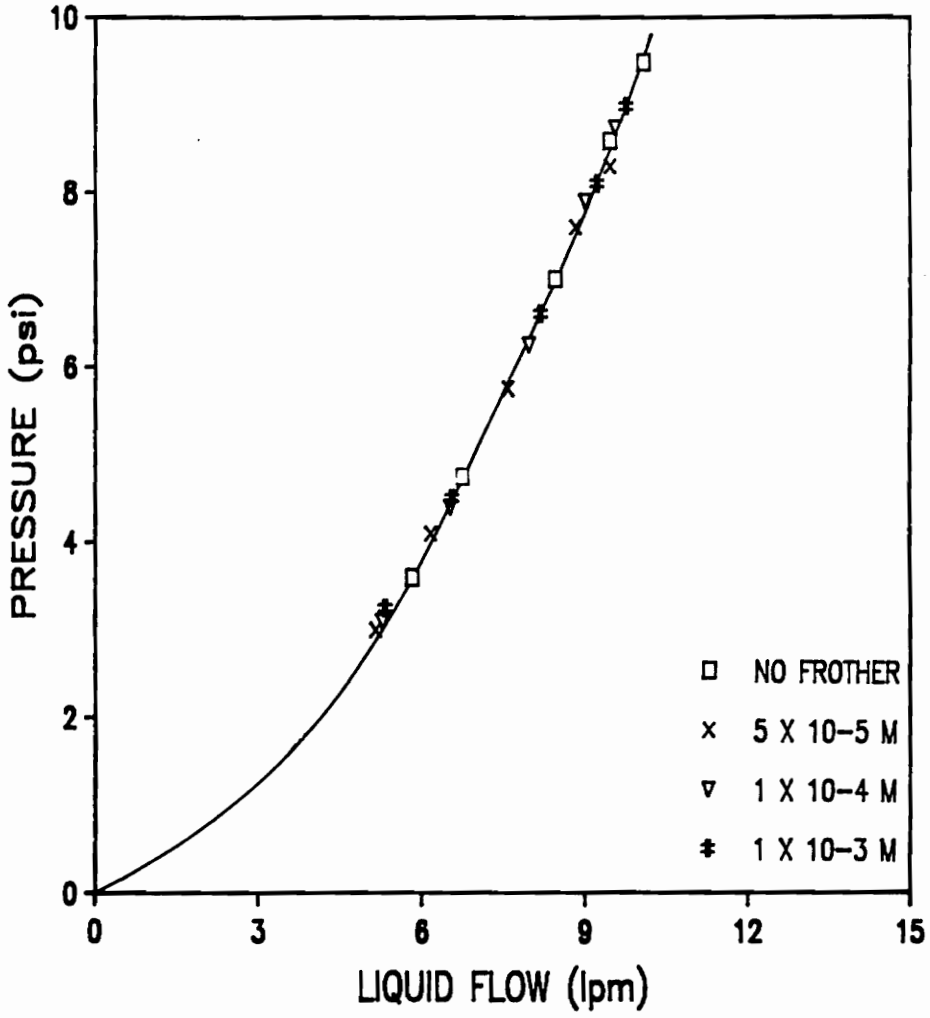

Figure A8 - Pressure versus volumetric liquid flow for a 15 element (11.25-inch length; 0.4375-inch I.D.) Kenics in-line microbubble generator at 30% air and various surfactant concentrations.

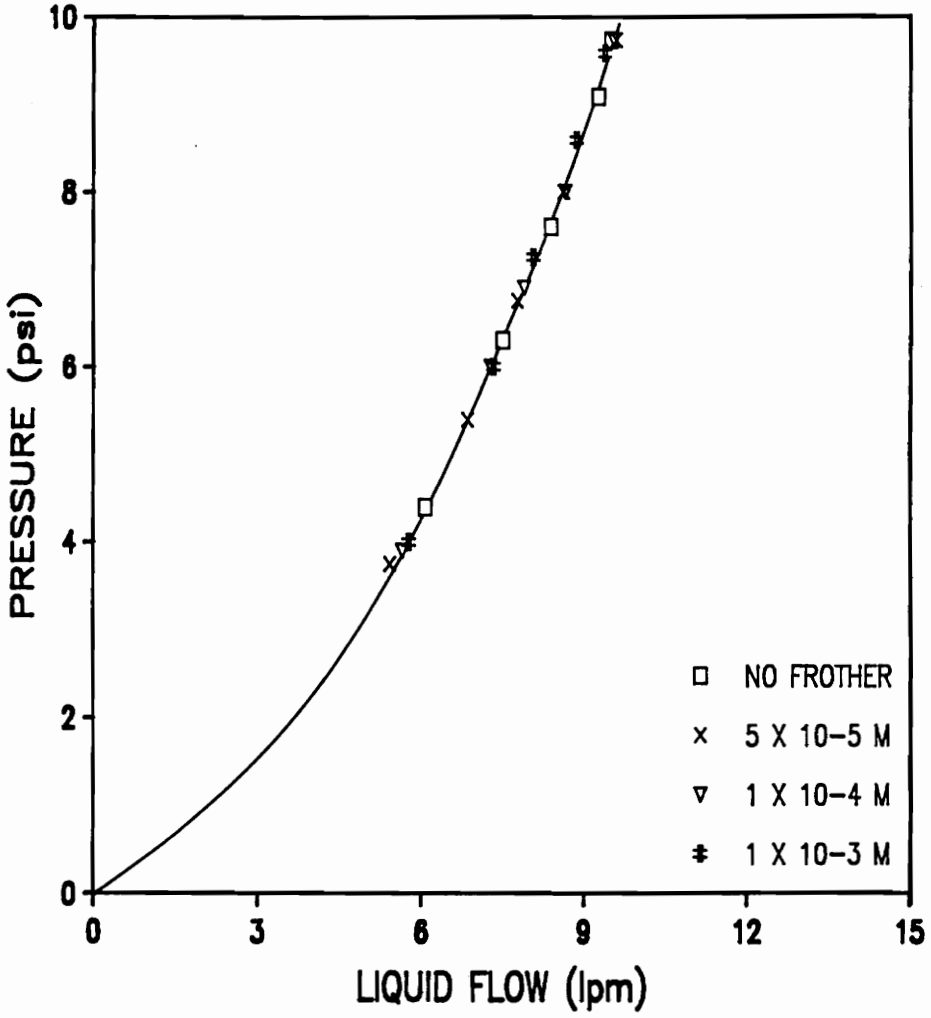

Figure A9 - Pressure versus volumetric liquid flow for a 15 element (11.25-inch length; 0.4375-inch I.D.) Kenics in-line microbubble generator at 40% air and various surfactant concentrations.

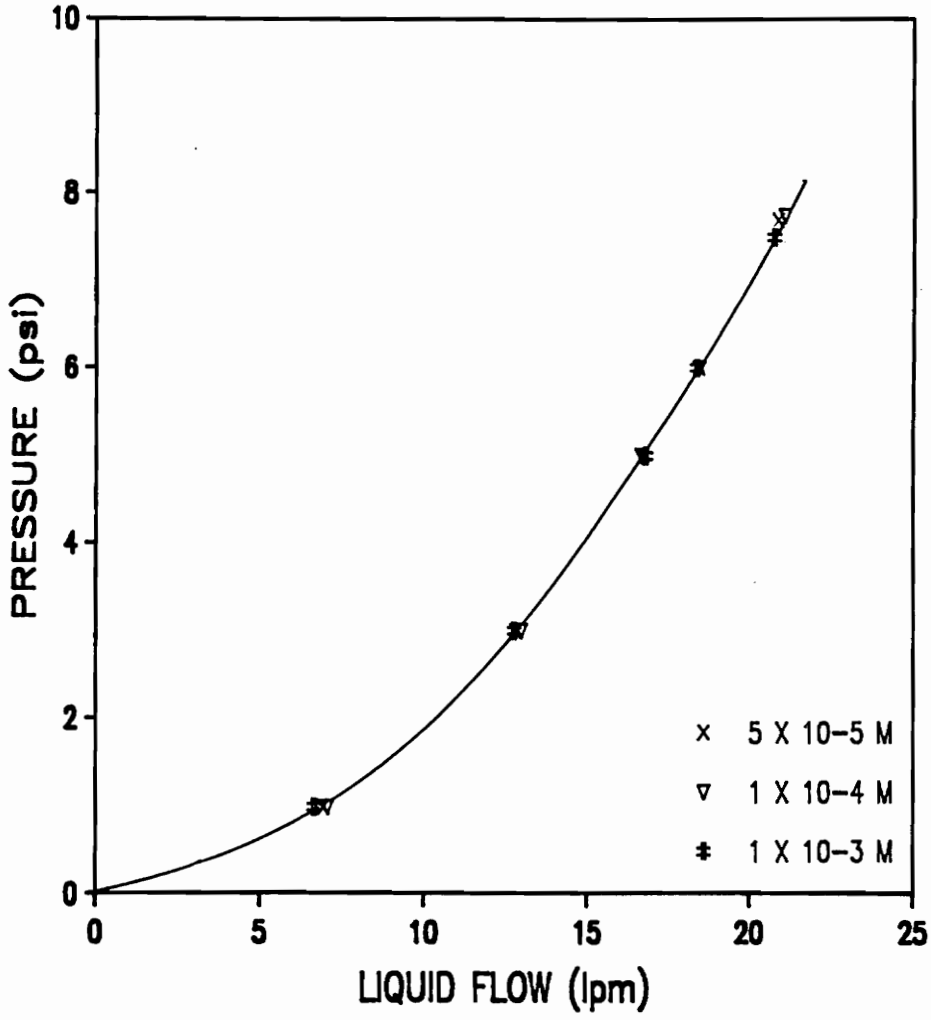

Figure A10 - Pressure versus volumetric liquid flow for a 0.62-inch I.D. (5-inch length) Koflo in-line microbubble generator at 0% air and various surfactant concentrations.

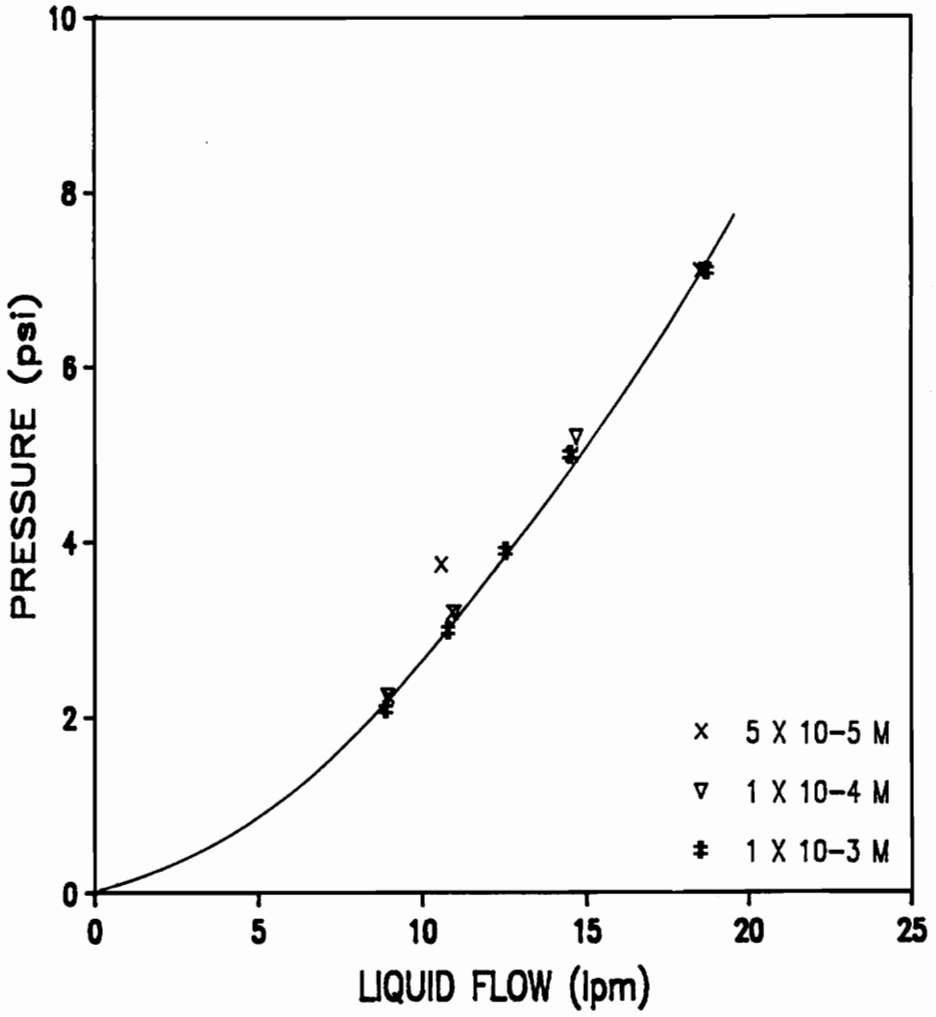

Figure A11 - Pressure versus volumetric liquid flow for a 0.62-inch I.D. (5-inch length) Koflo in-line microbubble generator at 10% air and various surfactant concentrations.

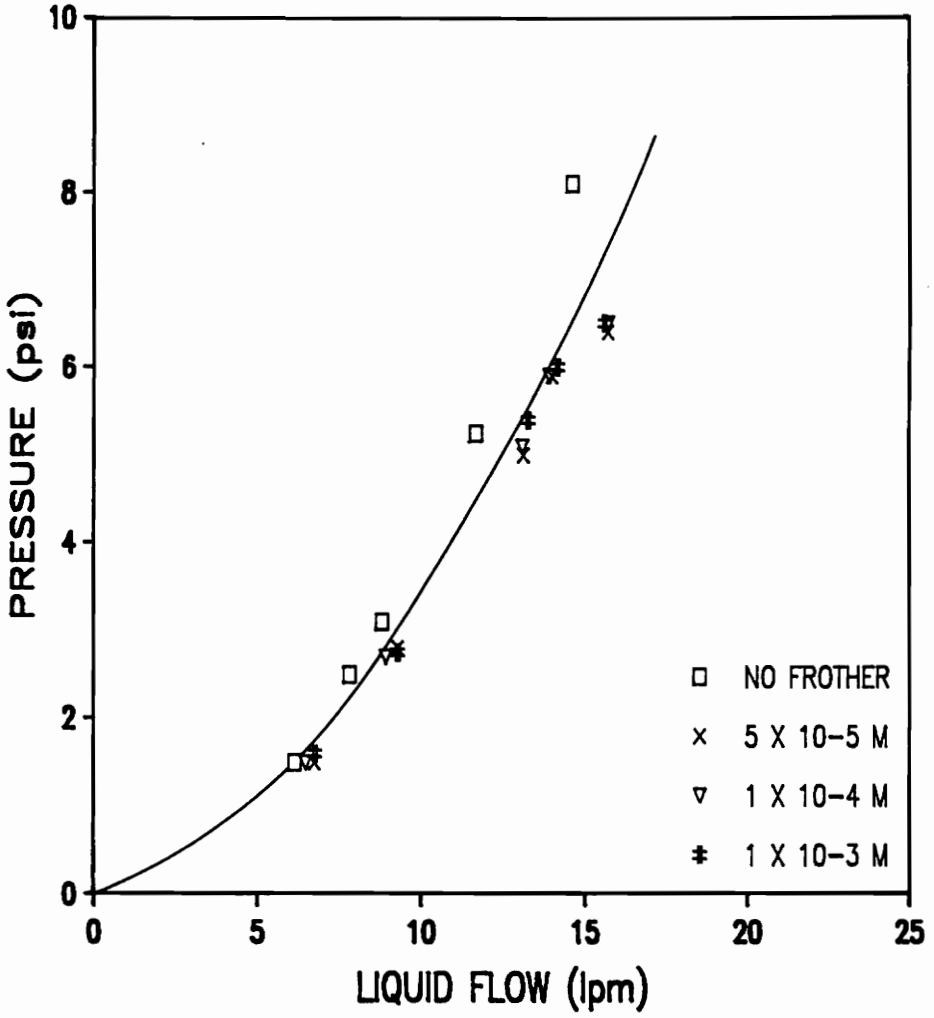

Figure A12 - Pressure versus volumetric liquid flow for a 0.62-inch I.D. (5-inch length) Koflo in-line microbubble generator at 30% air and various surfactant concentrations.

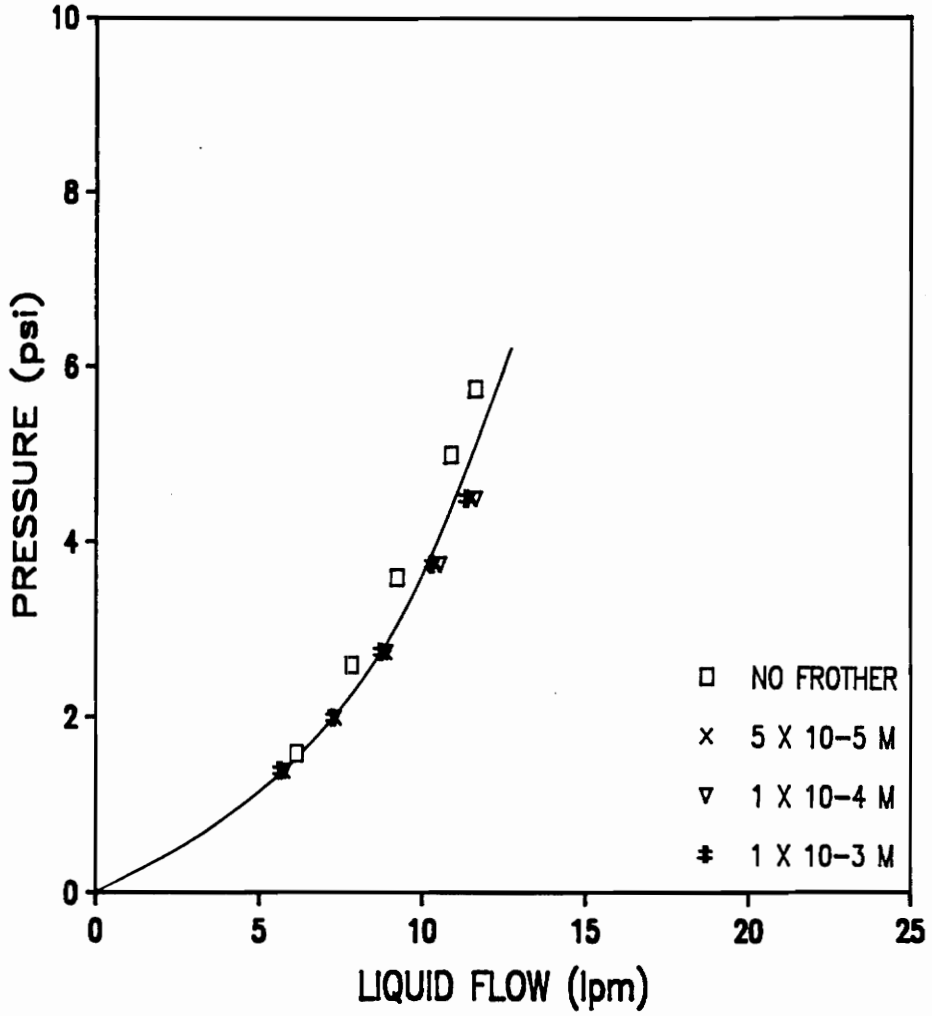

Figure A13 - Pressure versus volumetric liquid flow for a 0.62-inch I.D. (5-inch length) Koflo in-line microbubble generator at 40% air and various surfactant concentrations.

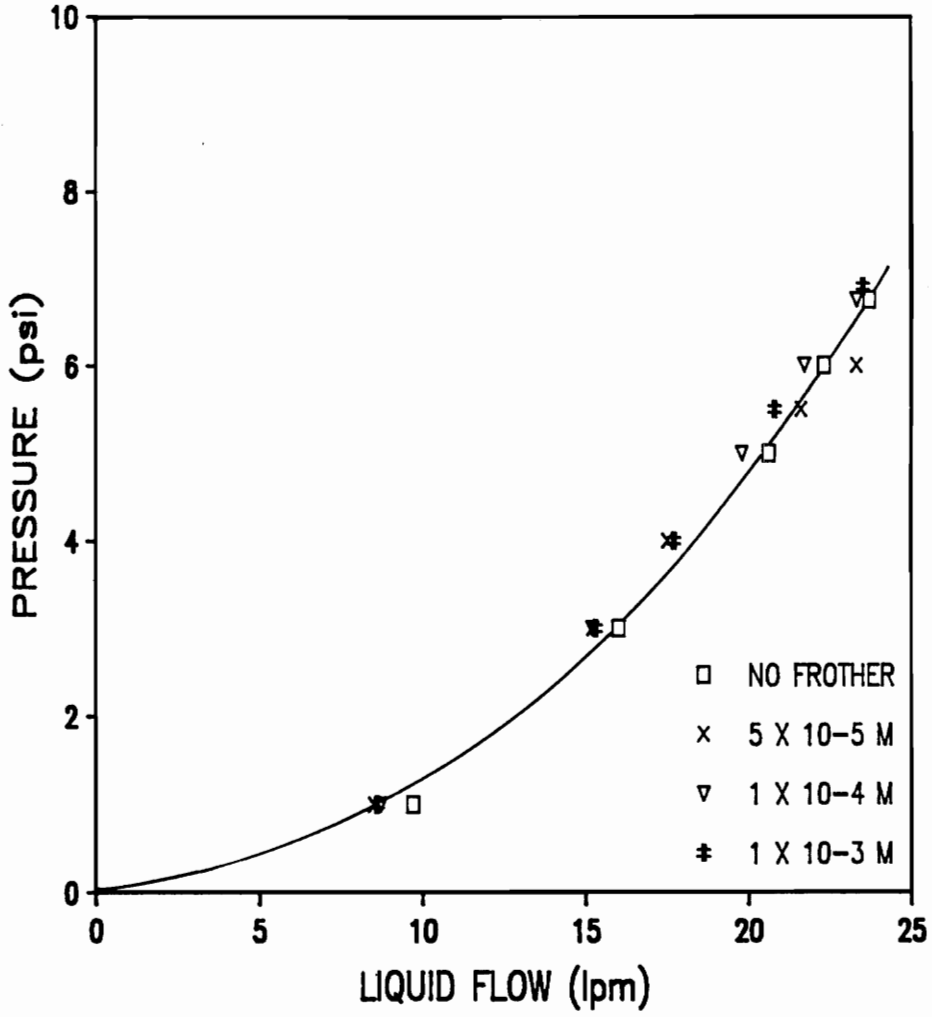

Figure A14 - Pressure versus volumetric liquid flow for a 0.82-inch I.D. (7-inch length) Koflo in-line microbubble generator at 0% air and various surfactant concentrations.

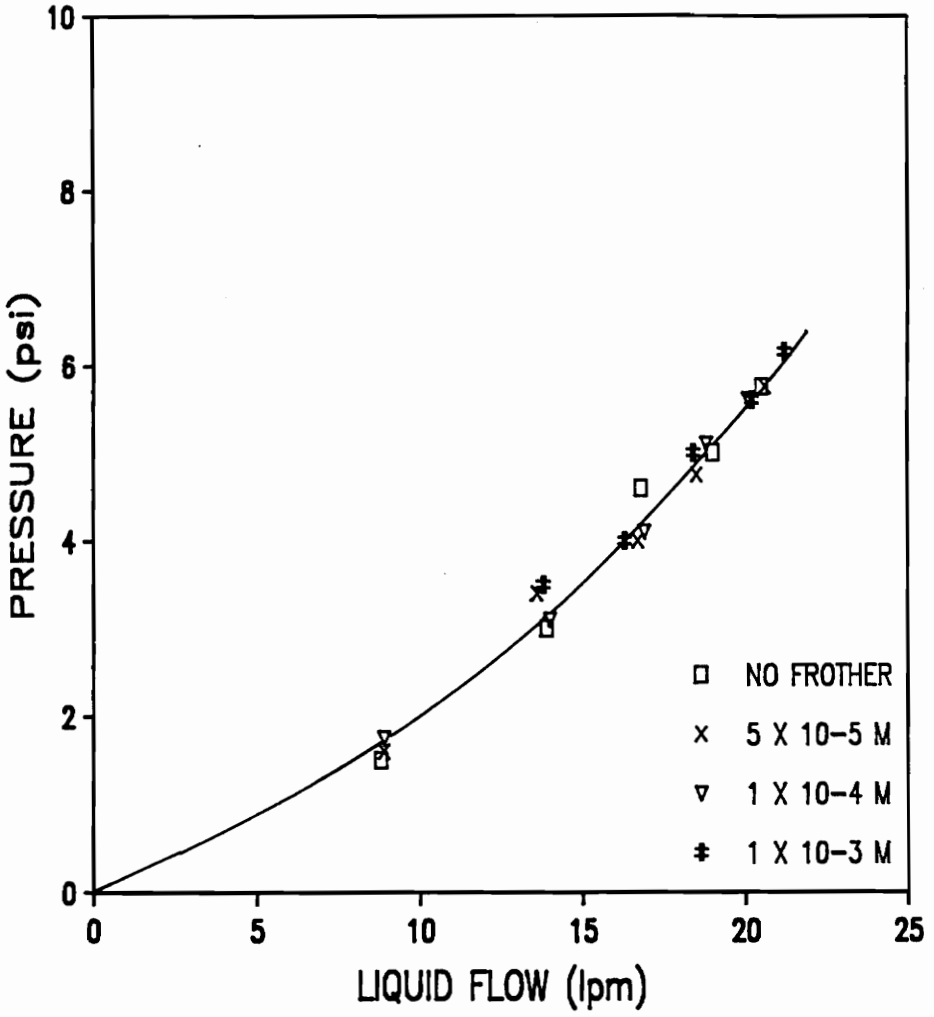

Figure A15 - Pressure versus volumetric liquid flow for a 0.82-inch I.D. (7-inch length) Koflo in-line microbubble generator at 10% air and various surfactant concentrations.

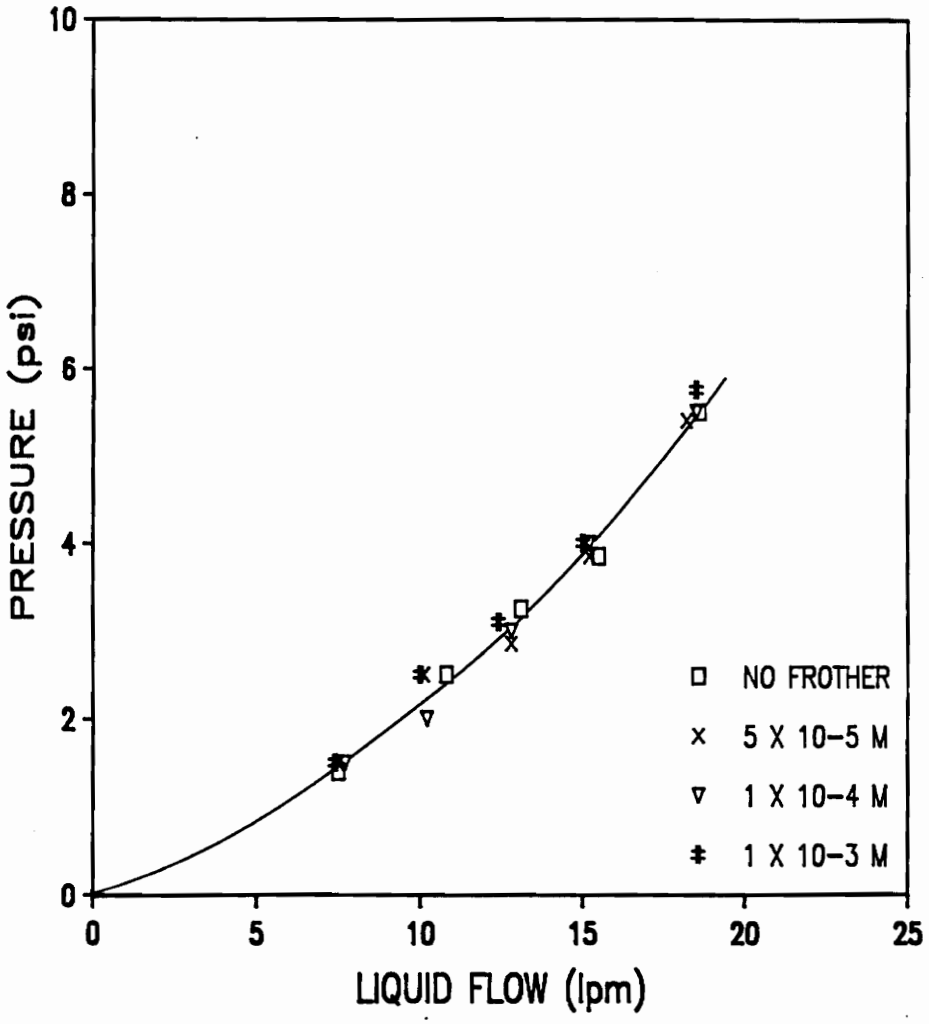

Figure A16 - Pressure versus volumetric liquid flow for a 0.82-inch I.D. (7-inch length) Koflo in-line microbubble generator at 30% air and various surfactant concentrations.

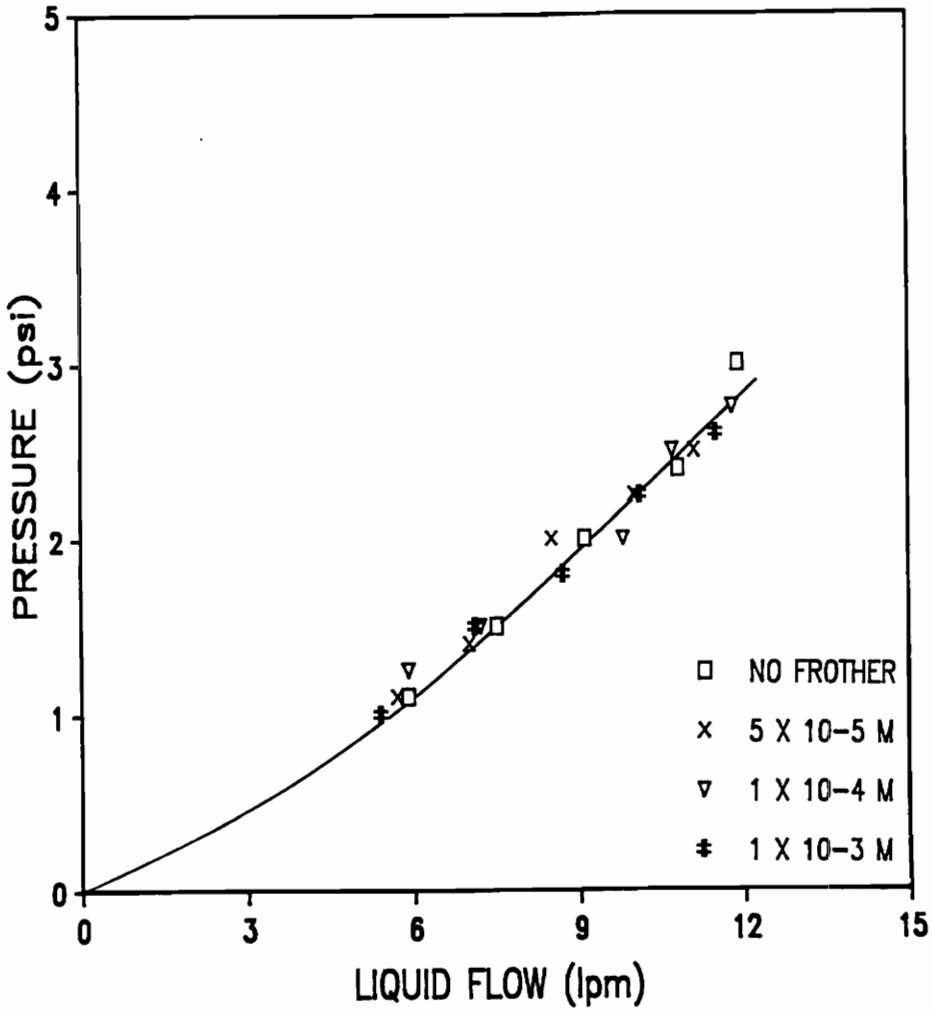

Figure A17 - Pressure versus volumetric liquid flow for a 0.82-inch I.D. (7-inch length) Koflo in-line microbubble generator at 40% air and various surfactant concentrations.

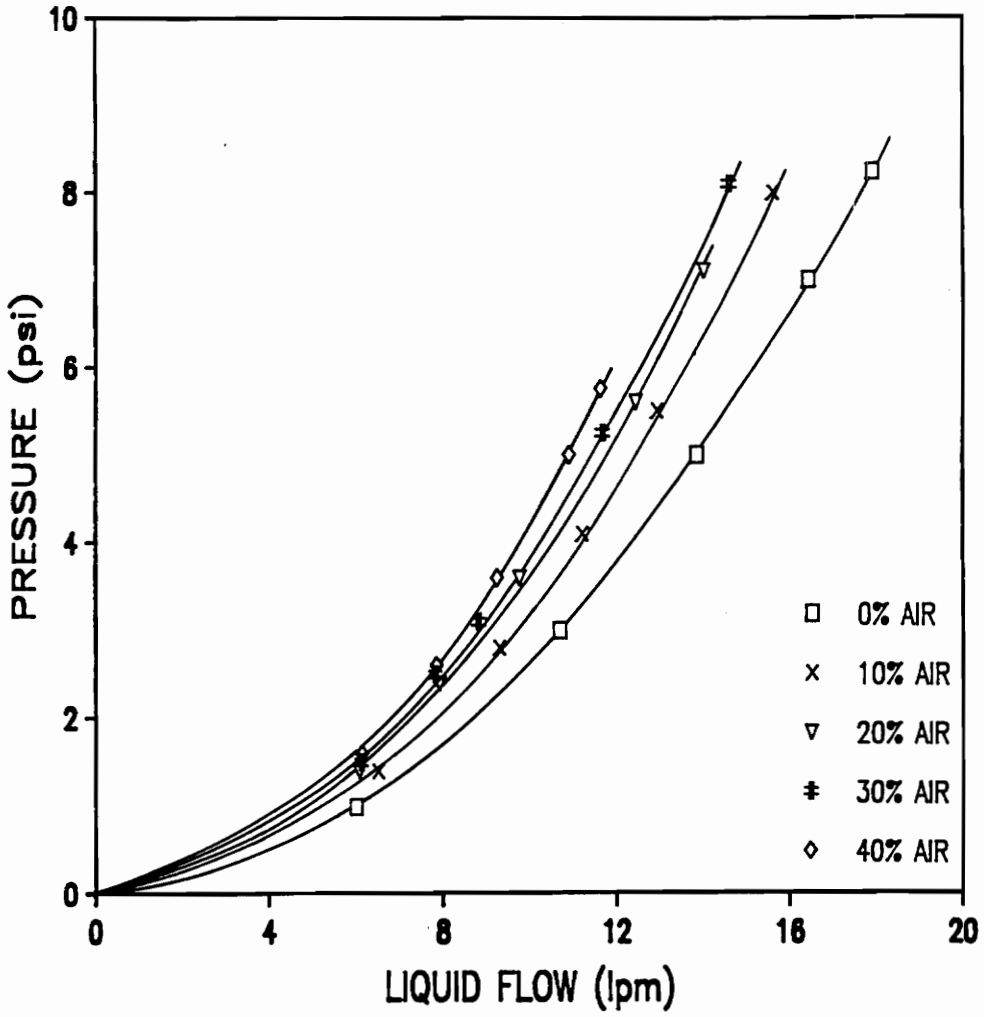

Figure A18 - Pressure versus volumetric liquid flow for a 0.62-inch I.D. (5-inch length) Koflo in-line microbubble generator with no surfactant at various air fractions.

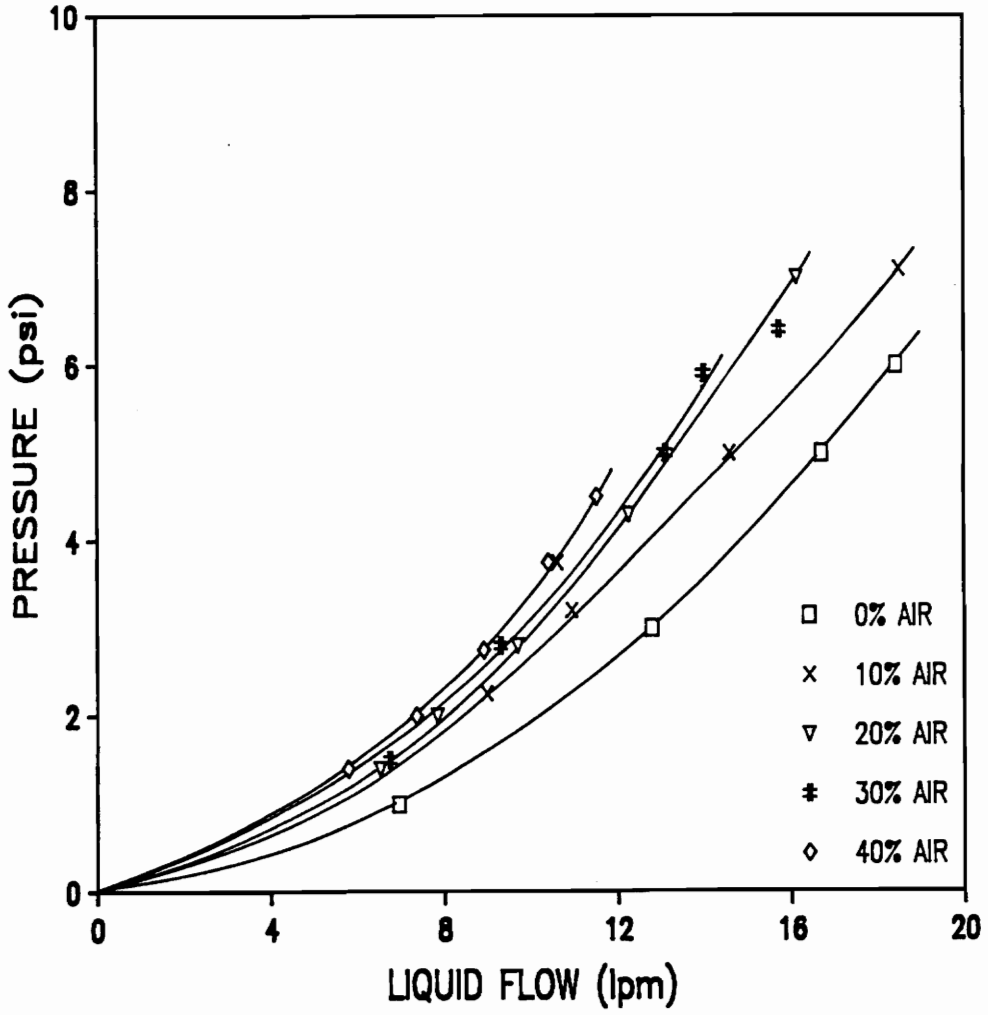

Figure A19 - Pressure versus volumetric liquid flow for a 0.62-inch I.D. (5-inch length) Koflo in-line microbubble generator at a Dowfroth M-1012 concentration of 5×10^{-5} M at various air fractions.

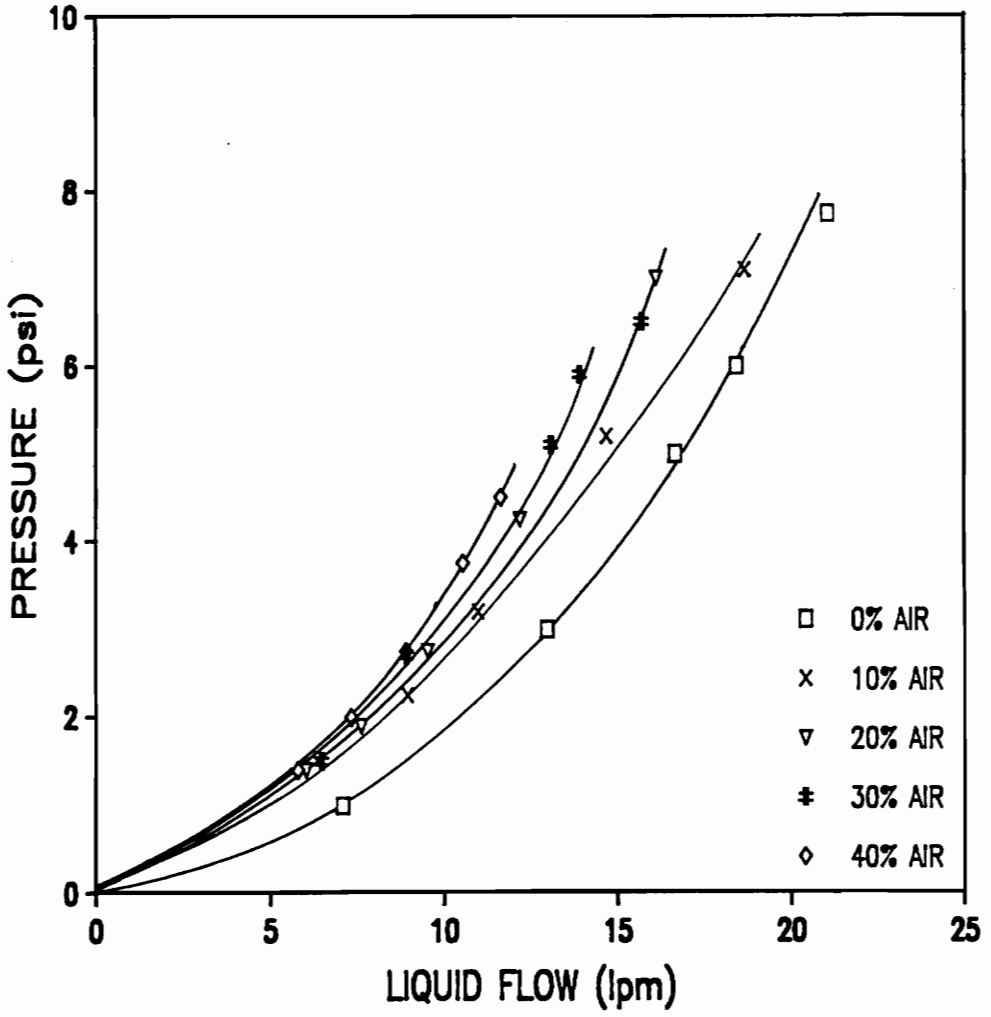

Figure A20 - Pressure versus volumetric liquid flow for a 0.62-inch I.D. (5-inch length) Koflo in-line microbubble generator at a Dowfroth M-1012 concentration of 1×10^{-4} M at various air fractions.

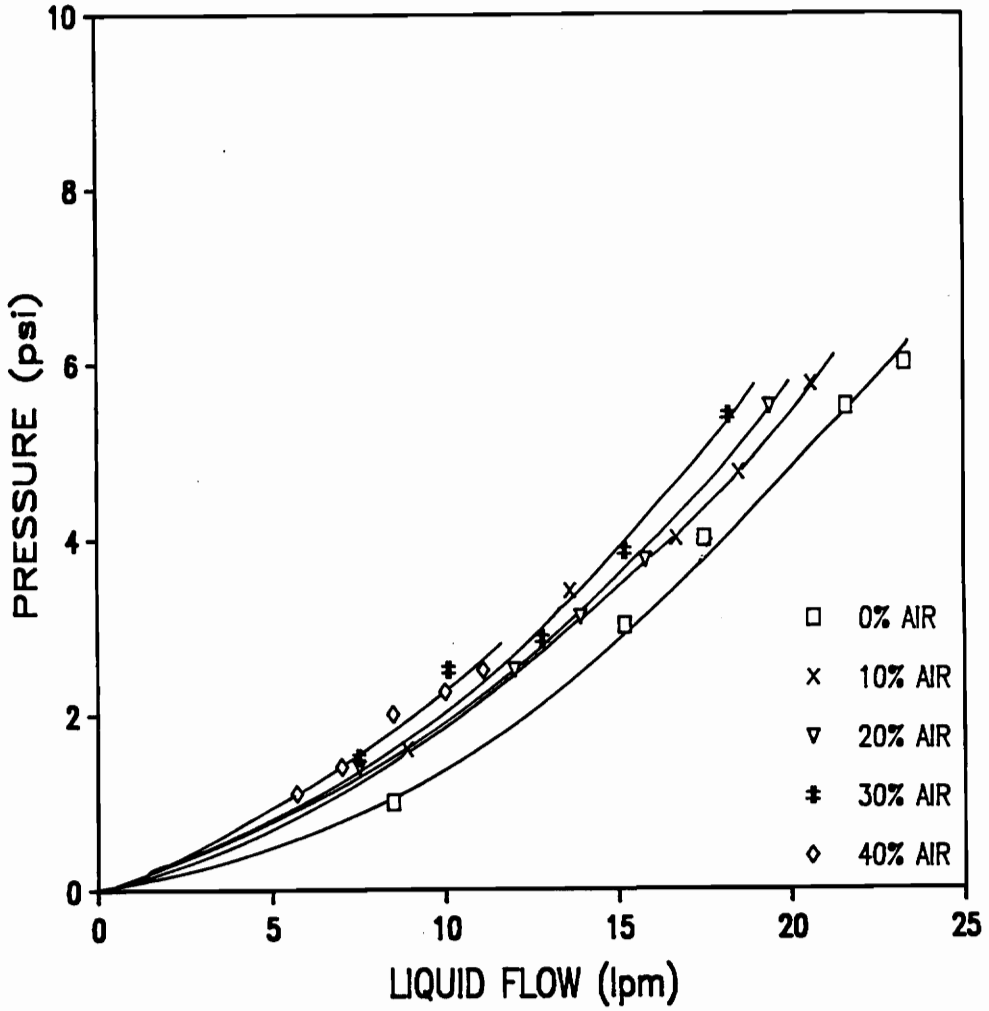

Figure A21 - Pressure versus volumetric liquid flow for a 0.82-inch I.D. (7-inch length) Koflo in-line microbubble generator at a Dowfroth M-1012 concentration of 5×10^{-5} M at various air fractions.

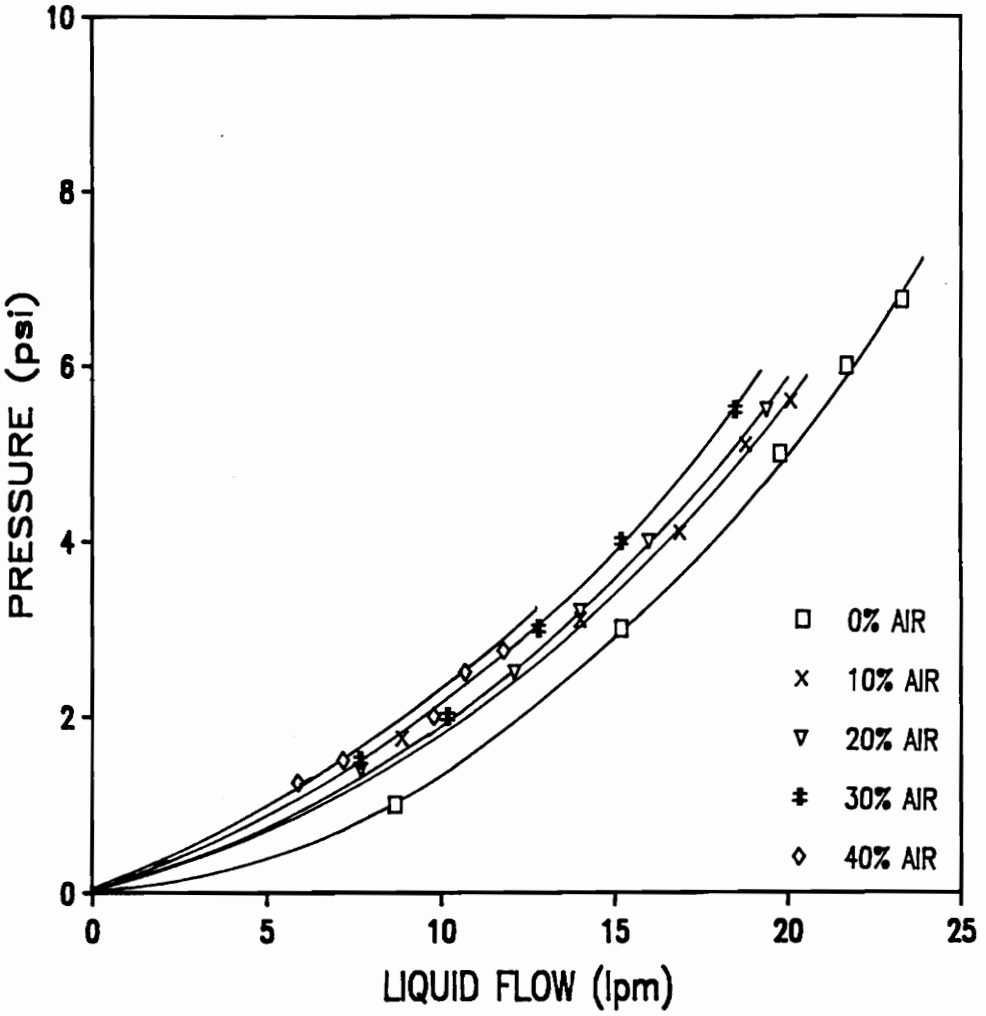

Figure A22 - Pressure versus volumetric liquid flow for a 0.82-inch I.D. (7-inch length) Koflo in-line microbubble generator at a Dowfroth M-1012 concentration of 1 x 10^{-4} M at various air fractions.

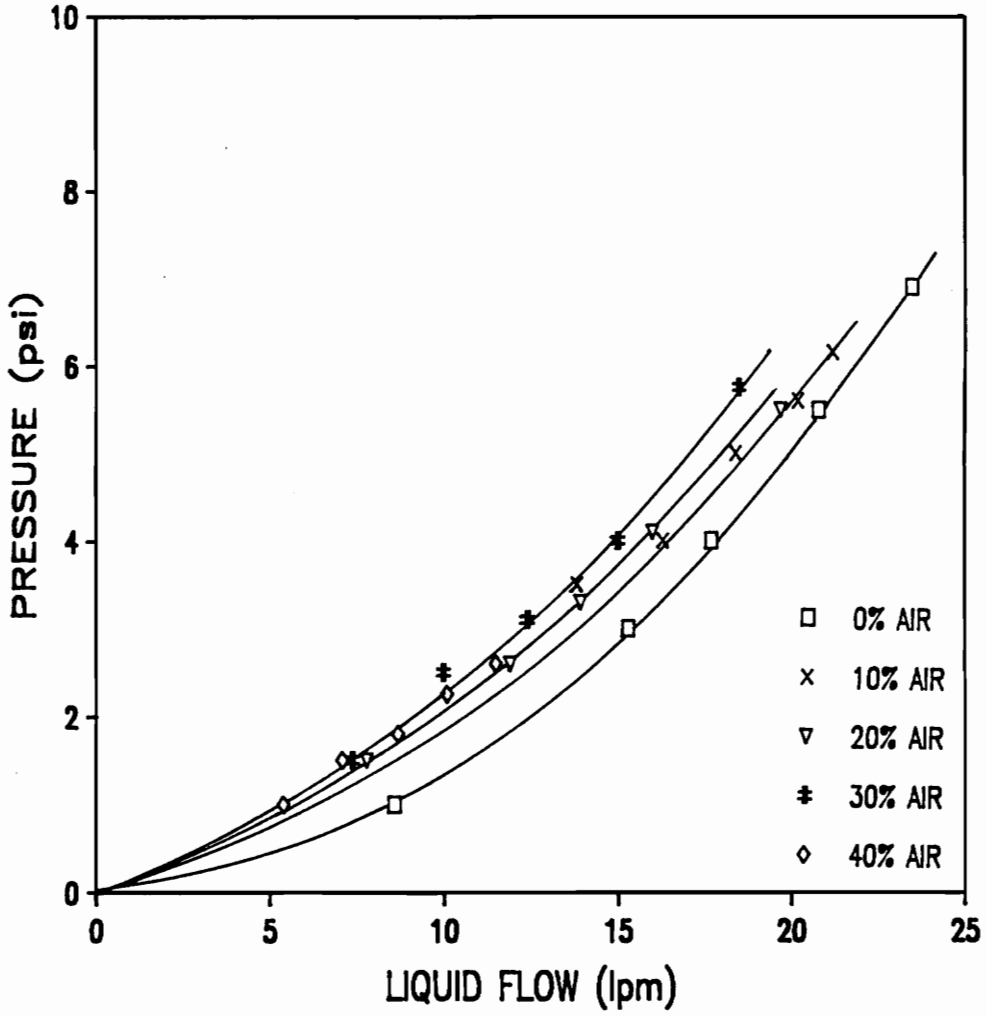

Figure A23 - Pressure versus volumetric liquid flow for a 0.82-inch I.D. (7-inch length) Koflo in-line microbubble generator at a Dowfroth M-1012 concentration of 1×10^{-3} M at various air fractions.

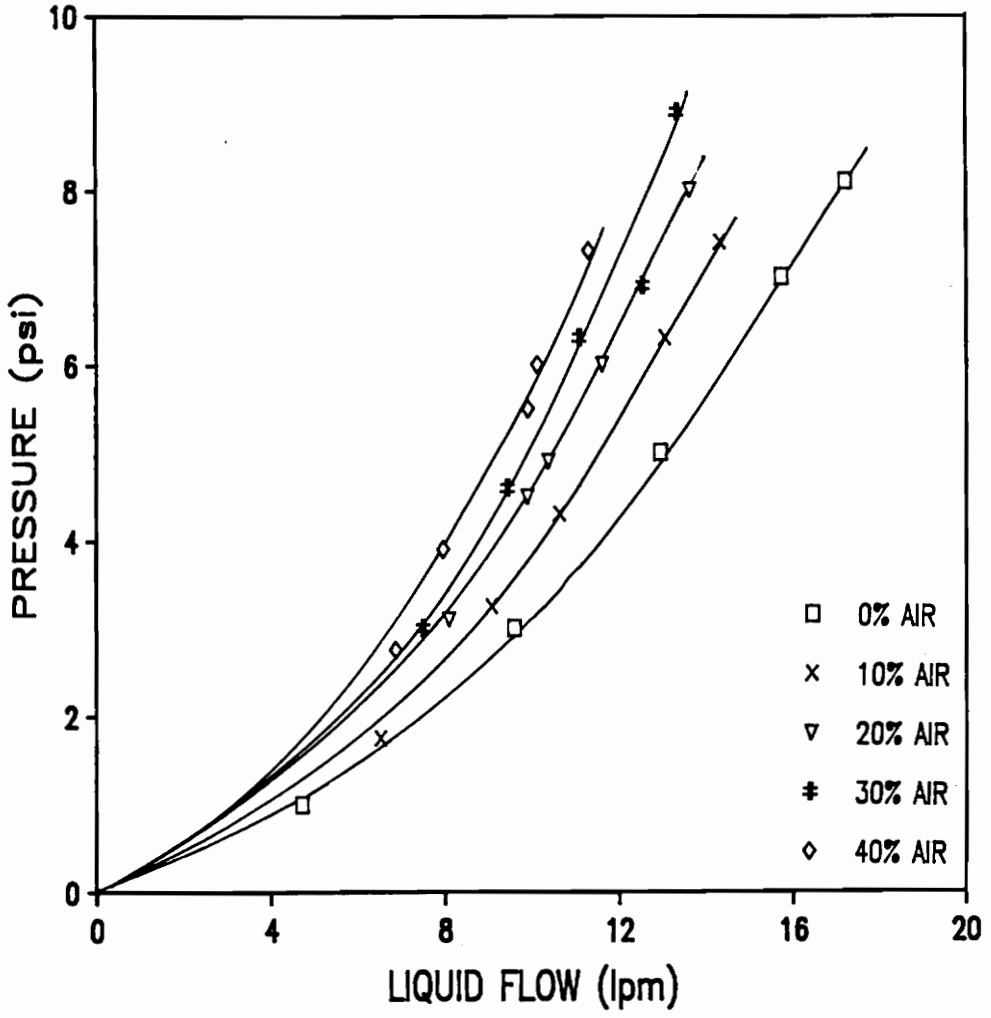

Figure A24 - Pressure versus volumetric liquid flow for a 7 element (5.25-inch length; 0.4375-inch I.D.) Kenics in-line microbubble generator with no surfactant at various air fractions.

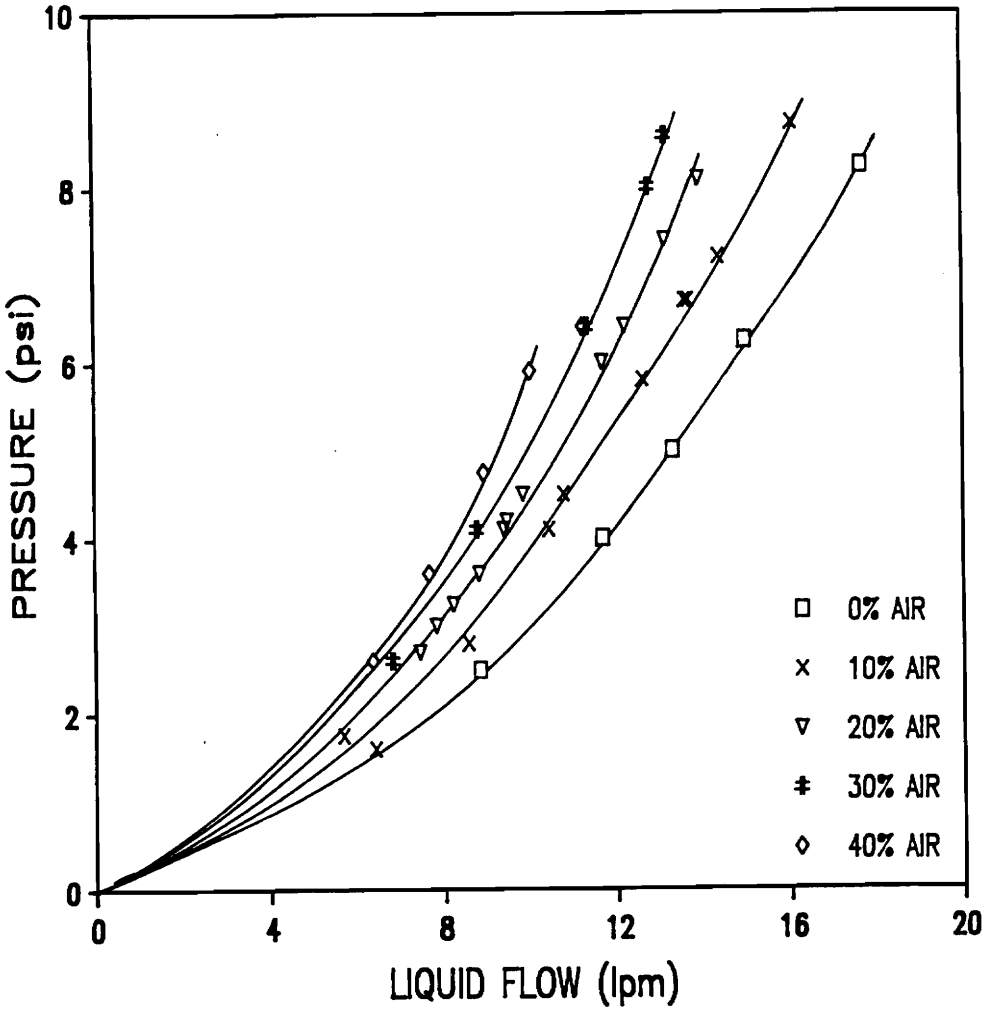

Figure A25 - Pressure versus volumetric liquid flow for a 7 element (5.25-inch length; 0.4375-inch I.D.) Kenics in-line microbubble generator at a Dowfroth M-1012 concentration of 5×10^{-5} M at various air fractions.

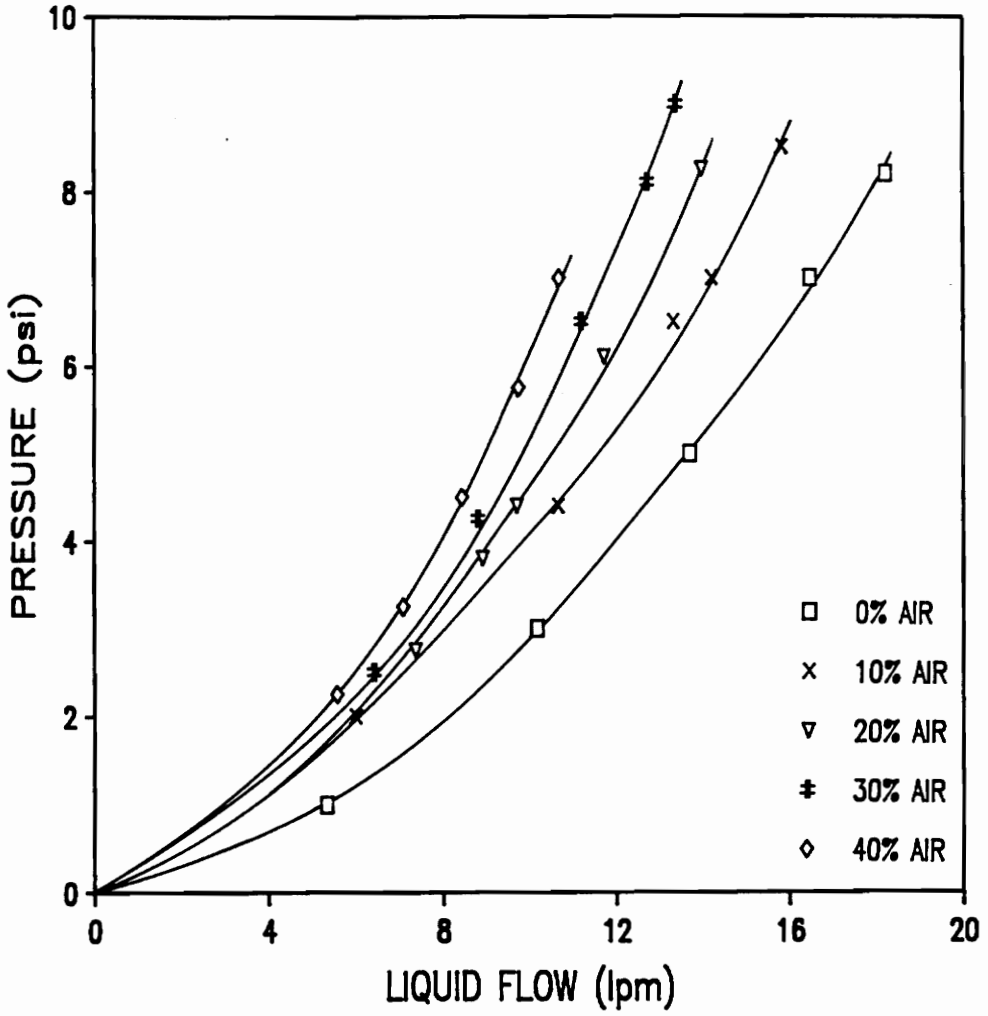

Figure A26 - Pressure versus volumetric liquid flow for a 7 element (5.25-inch length; 0.4375-inch I.D.) Kenics in-line microbubble generator at a Dowfroth M-1012 concentration of 1 x 10^{-4} M at various air fractions.

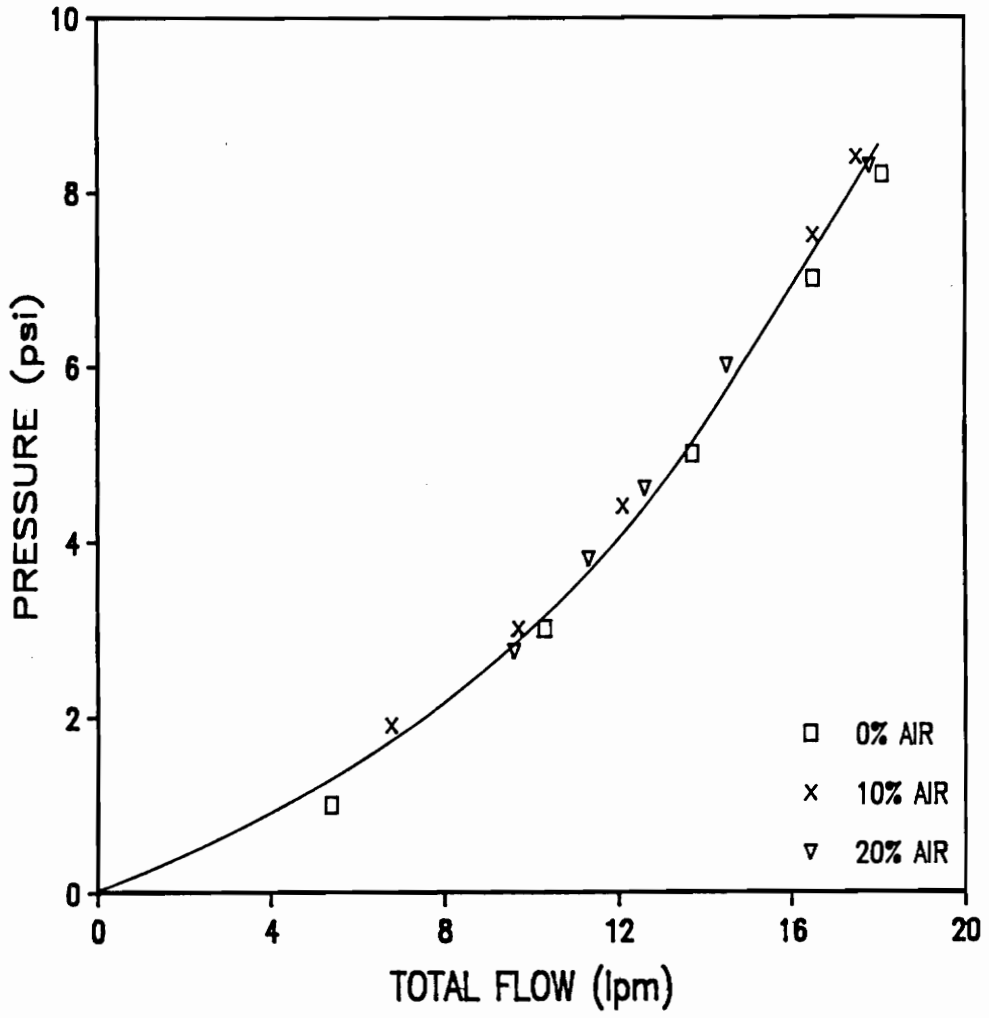

Figure A27 - Pressure versus volumetric liquid flow for a 7 element (5.25-inch length; 0.4375-inch I.D.) Kenics in-line microbubble generator at a Dowfroth M-1012 concentration of 1×10^{-3} M at various air fractions.

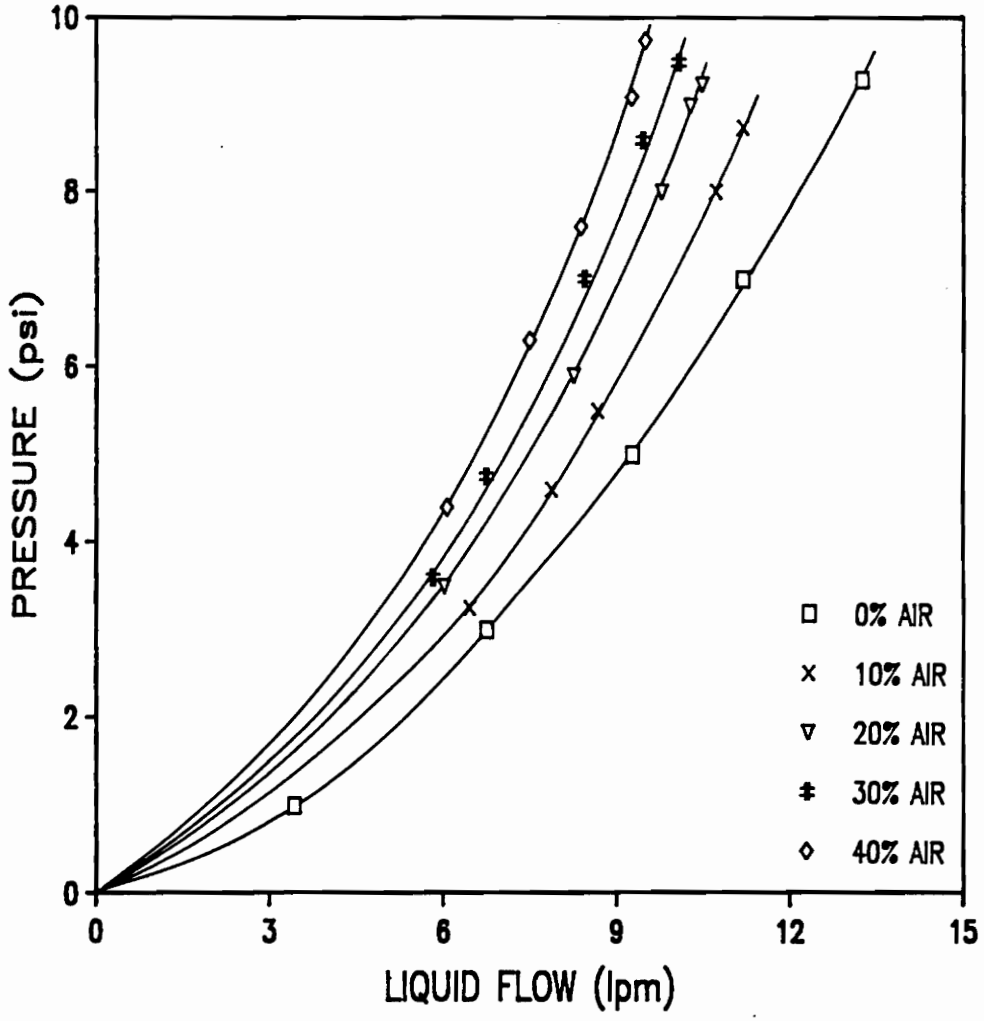

Figure A28 - Pressure versus volumetric liquid flow for a 15 element (11.25-inch length; 0.4375-inch I.D.) Kenics in-line microbubble generator with no surfactant at various air fractions.

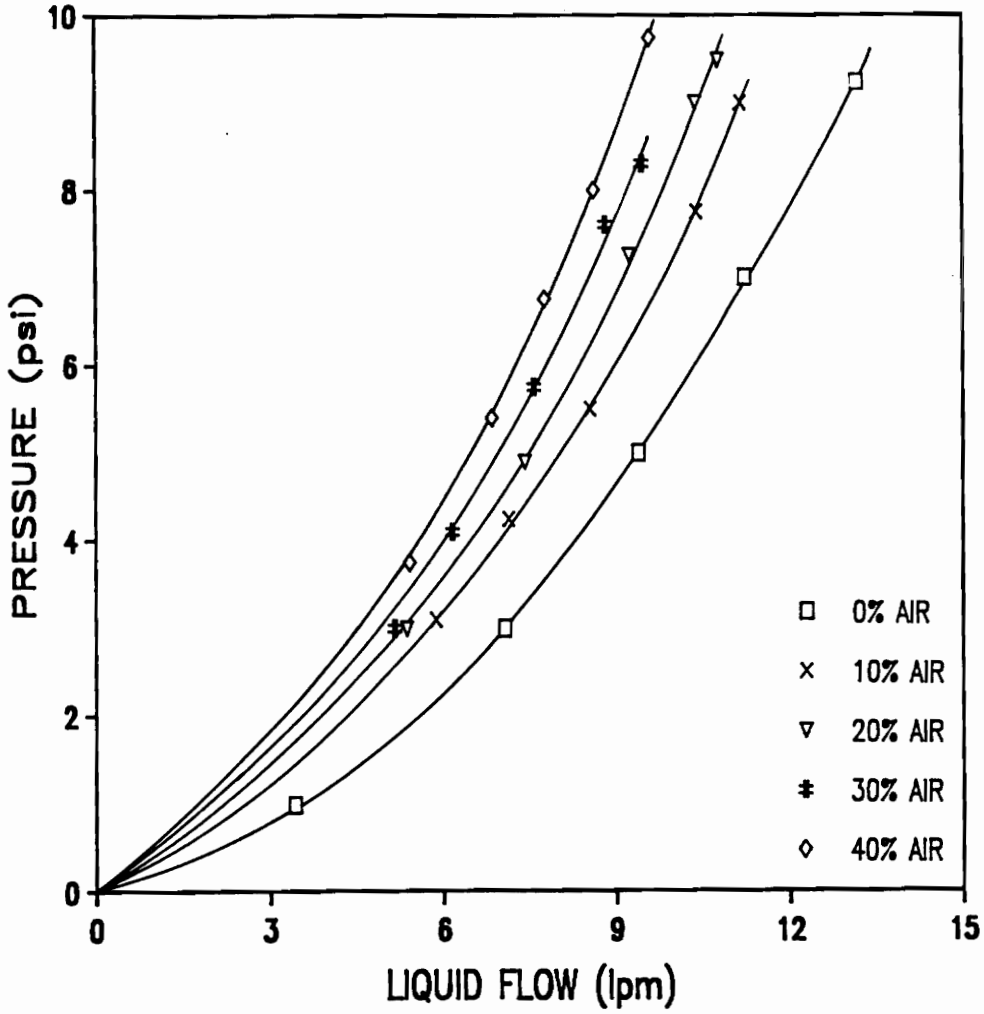

Figure A29 - Pressure versus volumetric liquid flow for a 15 element (11.25-inch length; 0.4375-inch I.D.) Kenics in-line microbubble generator at a Dowfroth M-1012 concentration of 5×10^{-5} M at various air fractions.

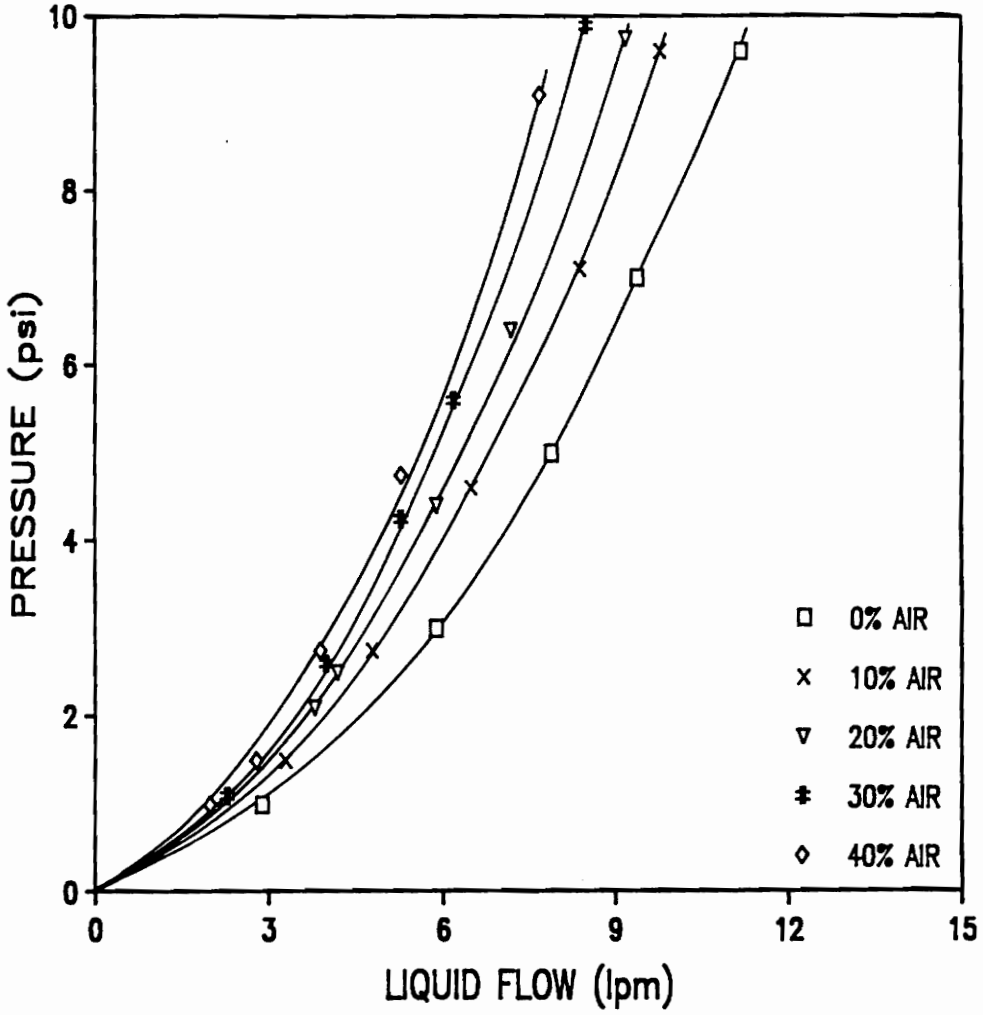

Figure A30 - Pressure versus volumetric liquid flow for a 22 element (16.5-inch length; 0.4375-inch I.D.) Kenics in-line microbubble generator at a Dowfroth M-1012 concentration of 1×10^{-4} M at various air fractions.

VITA

Van Leslie Davis, Jr. was born in Welch, West Virginia on March 13, 1959. He grew up in southwest Virginia and southern West Virginia and graduated from Iaeger High School in 1977.

After graduating from high school, Van worked in the coal industry as an underground miner for approximately six years. He held jobs as a machine operator as well as a salaried employee.

Van enrolled in the Engineering program at Southwest Virginia Community College in September, 1983 and transferred to Virginia Polytechnic Institute and State University in the fall of 1985. He graduated cum laude with a Bachelor of Science degree in Mining and Minerals Engineering in June, 1987. Van was an active member of the Burkhart Mining Society and served as the organization's president during his senior year. He was also an active member of the Society of Mining Engineers of the American Institute of Mining, Metallurgical, and Petroleum Engineers.

Van began work on a Master of Science degree in Mining and Minerals Engineering at Virginia Polytechnic Institute and State University during the summer of 1987.